U.S. Department of Transportation
Federal Railroad Administration

Small Scale Impact Simulation Tests

Office of Research and Development
Washington, D.C. 20590

M.A. Lishaa
J. Chen
J.C.S. Yang
R. Kao

Biotech Research Laboratories, Inc.
1600 East Gude Drive
Rockville, Maryland 20850

and

Advanced Technology and Research, Inc.
3933 Sandy Spring Road
Burtonsville, Maryland 20866

DOT/FRA/ORD-85/04

January 1985
Final Report

This document is available to the public through the National Technical Information Service, Springfield, Virginia 22161.

Technical Report Documentation Page

1. Report No.	2. Government Accession No.	3. Recipient's Catalog No.
DOT/FRA/ORD-85/04		

4. Title and Subtitle	5. Report Date
SMALL SCALE IMPACT SIMULATION TESTS	January 1985
	6. Performing Organization Code
7. Author(s): M. A. Lishaa, J. Chen, J. C. S. Yang, R. Kao	8. Performing Organization Report No.
9. Performing Organization Name and Address: Biotech Research Laboratories, Inc. 1600 East Gude Drive Rockville, Maryland 20850	10. Work Unit No. (TRAIS) 11. Contract or Grant No. DTFR53-82-C-00290
12. Sponsoring Agency Name and Address: U.S. Department of Transportation Federal Railroad Administration Office of Research and Development Washington, D.C. 20590	13. Type of Report and Period Covered: Final Report July 1982-December 1984 14. Sponsoring Agency Code: RRD-20

15. Supplementary Notes

16. Abstract

In derailments and switchyard operations, tank cars frequently experience impacts that result in tank car head puncture. From a cost effective viewpoint, it is not practical to conduct many full-scale testing to verify that a particular tank car design will perform satisfactorily in all possible impact situations. Therefore, there is a need for reliable small scale testing procedures to simulate the response of tank heads in impact situations. In this study some small scale model testing was performed: (1) to assess the effectiveness of mitigating materials on increasing the tank heads puncture resistance; (2) to evaluate the effect of low temperature on the threshold puncture energy of the model tank heads; (3) to test the validity of the scaling laws adopted; (4) to study the influence of lading on the vulnerability of the model tank head in the impact situations. A number of the 1/5 and 1/10 scale model tank heads with different head protective devices were tested under different impact, lading and temperature conditions. Besides using a stainless steel head shield as a protective device, a number of other shock mitigating materials, such as aluminum honeycomb materials, aluminum foams, corrugated steel plates, and TecsPak plates, were investigated. The test results indicate that both TecsPak and stainless steel provide good protection against head puncture even at low temperatures as compared with the bare tank heads; however, no substantial difference is found in terms of protection capability between TecsPak and stainless steel plates. An examination of the threshold puncture velocities between the two scaled models showed a difference of less than 10%. This concluded that the scaling laws adopted provide good accuracy in scaling the model tank heads.

17. Key Words	18. Distribution Statement
scale model, tank head, impact, puncture, mitigating material, low temperature, lading	Document is available to the U.S. public through the National Technical Information Service, Springfield, Virginia 22161

19. Security Classif. (of this report)	20. Security Classif. (of this page)	21. No. of Pages	22. Price
Unclassified	Unclassified	90	

Form DOT F 1700.7 (8-72) Reproduction of completed page authorized

METRIC CONVERSION FACTORS

Approximate Conversions to Metric Measures

Symbol	When You Know	Multiply by	To Find	Symbol
		LENGTH		
in	inches	*2.5	centimeters	cm
ft	feet	30	centimeters	cm
yd	yards	0.9	meters	m
mi	miles	1.6	kilometers	km
		AREA		
in²	square inches	6.5	square centimeters	cm²
ft²	square feet	0.09	square meters	m²
yd²	square yards	0.8	square meters	m²
mi²	square miles	2.6	square kilometers	km²
	acres	0.4	hectares	ha
		MASS (weight)		
oz	ounces	28	grams	g
lb	pounds	0.45	kilograms	kg
	short tons (2000 lb)	0.9	tonnes	t
		VOLUME		
tsp	teaspoons	5	milliliters	ml
Tbsp	tablespoons	15	milliliters	ml
fl oz	fluid ounces	30	milliliters	ml
c	cups	0.24	liters	l
pt	pints	0.47	liters	l
qt	quarts	0.95	liters	l
gal	gallons	3.8	liters	l
ft³	cubic feet	0.03	cubic meters	m³
yd³	cubic yards	0.76	cubic meters	m³
		TEMPERATURE (exact)		
°F	Fahrenheit temperature	5/9 (after subtracting 32)	Celsius temperature	°C

*1 in. = 2.54 cm (exactly). For other exact conversions and more detail tables see NBS Misc. Publ. 286. Units of Weight and Measures. Price $2.25 SD Catalog No. C13 10 286.

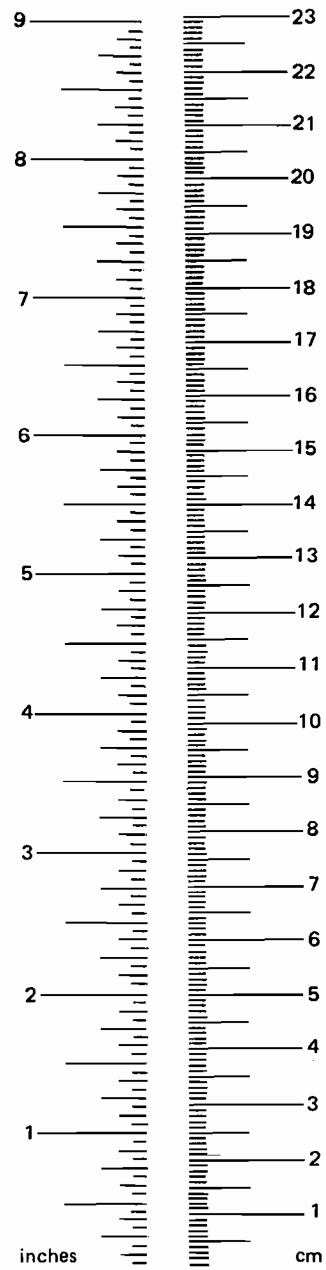

Approximate Conversions from Metric Measures

Symbol	When You Know	Multiply by	To Find	Symbol
		LENGTH		
mm	millimeters	0.04	inches	in
cm	centimeters	0.4	inches	in
m	meters	3.3	feet	ft
m	meters	1.1	yards	yd
km	kilometers	0.6	miles	mi
		AREA		
cm²	square centimeters	0.16	square inches	in²
m²	square meters	1.2	square yards	yd²
km²	square kilometers	0.4	square miles	mi²
ha	hectares (10,000 m²)	2.5	acres	
		MASS (weight)		
g	grams	0.035	ounces	oz
kg	kilograms	2.2	pounds	lb
t	tonnes (1000 kg)	1.1	short tons	
		VOLUME		
ml	milliliters	0.03	fluid ounces	fl oz
l	liters	2.1	pints	pt
l	liters	1.06	quarts	qt
l	liters	0.26	gallons	gal
m³	cubic meters	36	cubic feet	ft³
m³	cubic meters	1.3	cubic yards	yd³
		TEMPERATURE (exact)		
°C	Celsius temperature	9/5 (then add 32)	Fahrenheit temperature	°F

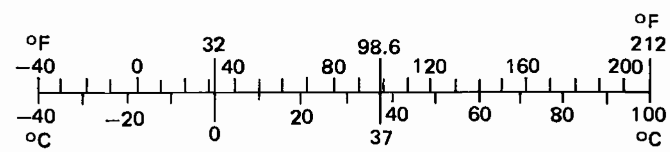

Table of Contents

LIST OF ILLUSTRATIONS

LIST OF TABLES

SUMMARY

In the study of the coupler-tank head impact phenomena in derailment and switchyard operations, many different test conditions have to be considered. In order to correlate the threshold puncture velocity with the conditions, many tests need to be performed to provide the necessary information. For these studies, small scale model testing is certainly desirable over full-scale testing as far as cost is concerned. It is imperative, however, that the scale model testing provides reliable information as to the real impact phenomena.

In this study, an attempt was made with small scale testing: (1) to assess the effectiveness of mitigating materials on protecting the model tank heads from puncture in the impact situations; (2) to evaluate the effect of low temperature on the threshold puncture energy of the model tank heads; (3) to test the validity of the scaling laws adopted; (4) to study the influence of lading on the vulnerability of the model tank heads in the impact situations.

A number of the 1/5 and 1/10 scale model tank heads with different head protective devices and with different materials backing up the tank heads were tested in this study. Besides using a stainless steel head shield as a protective device, a number of other shock mitigating materials, such as, aluminum honeycomb materials, aluminum foams, corrugated steel plates, and TecsPak plates, were investigated. From the results of some preliminary static and dynamic tests, a mitigating material "TecsPak" based on DuPont Hytrel polyester elastomer has been selected and used in the impact tests.

The test results indicate that both TecsPak and stainless steel plates provide good protection against head puncture as compared with the bare tank heads; however, no substantial difference is found in terms of protection capability between TecsPak and stainless steel plates. The test results also indicate no significant effect of low temperature on the vulnerability of the stainless steel model tank heads.

An examination of the scaling laws adopted reveals that the effect of strain rate is of very minor importance on the accuracy of these laws, when applied to the 1/5 and 1/10 scale model tank heads.

The test results also show a difference of less than 10% in the threshold puncture velocities between these two reduced scale models. This may be attributed to the various errors involved in the tests. Therefore, it is concluded that the scalnig laws adopted provide good accuracy in scaling the model tank heads used in this study.

The test results also show that an empty model tank head is susceptible to deeper dents, and less susceptible to puncture than one backed up with water or sand. However, no significant difference between water and sand is obtained in terms of model tank heads puncture.

1. INTRODUCTION

In derailments and switchyard operations, tank cars carrying hazardous materials frequently experience impacts that result in tank car head puncture by the coupler or any other projectile. Because of the catastrophic consequences involved in such accidents, which may cause the evacuation of cities, personal deaths and injuries, and property losses totalling millions of dollars, tank car head puncture phenomena have been widely studied (Ref. 1 - 4). In view of the complicated nature at the point of incipient puncture, no rigorous relationships among all variables involved have yet been established, thereby making a full-scale analytical investigation extremely difficult. In addition, because there are large combinations of tank car configurations and impact scenarios, it is not practical from a cost effective viewpoint to conduct full-scale testing to verify that a particular tank car design will perform satisfactorily in all possible impact situations. Therefore, there is a need for reliable small scale testing procedures to simulate the response of tank heads in impact situations.

In order to increase the resistance of a tank car head against puncture (when a coupler or an adjacent car rams into it), head shields are required on all D.O.T. specification 112/114 tank cars and certain newly built D.O.T. specification 105 tank cars. The steel head shield is not a particularly good energy absorber, but it spreads the load and blunts the striking edge of the impacting object. However, there are other D.O.T. specification tank cars (e.g., specification 103, 104, 106, 109, 110 and 111) that also carry hazardous materials. For many of these cars, the additional dead weight of the thick steel head shields would substantially increase fuel cost. To remedy this shortcoming, Advanced Technology & Research, Inc., proposed that a deformable shock mitigating material be placed between a thin head shield and tank car head. This report is to evaluate from test results the effectiveness of mitigating materials on reducing the vulnerability of tank car head puncture. This report is also to address the effect of low temperature on tank car impact performance, and to assess the degree of protection against head puncture rendered by mitigating materials at low temperature.

As already pointed out, since the cost of performing tests with full size tank cars to evaluate tank head protection would be prohibitively high, there is a need for reliable small scale testing procedures to simulate the response of tank cars in impact situations. Reliability of relating small scale model and prototype test results depends on the validity of scale laws employed. In order to establish the correct scaling laws, it was proposed that tests with models of two different scale factors under the same conditions be conducted. An analysis of the test results of the two different scale models should help establish the scaling laws, which are to be used for the prediction of the prototype performance.

The major catastrophy involved in the tank car head puncture following a derailment or switchyard collision is the spillage of lading contained in the tank. The ensuing spillage can lead to wide dispersion of highly toxic fumes for nonflammable cargo, or to quick ignition and conflagration for flammable cargo. Therefore, it is included in this study to determine the influence of lading on the threshold puncture velocity and puncture energy.

An outline of four objectives as described above is given in the next section. This is followed by a general description of testing procedures for four test series associated with the aforementioned objectives. Test results of a number of the 1/5 and 1/10 scale model tank heads obtained in drop weight tests and pendulum impact tests are presented and discussed in detail in Section 4. Conclusions based on the test results obtained and recommendations for the future research are given in the final sections.

2. OBJECTIVES

The objectives of this project are:

a. To assess the effectiveness of proposed mitigating materials on protecting model tank heads from puncture in impact situations.

b. To evaluate the effect of low temperature on the energy required to puncture a model tank head.

c. To test the validity of scaling laws adopted.

d. To study the influence of lading on the threshold puncture velocity in model tank car head impact situations.

3. DESCRIPTION OF SMALL SCALE TEST PROGRAM

In order to achieve the objectives as outlined in the previous section, a total of four series of tests were run on reduced scale models, with an ultimate goal of obtaining more insight into the tank car head impact phenomena, and thereby developing more efficient schemes to reduce the probability of tank car head puncture caused by impact during collision in derailment, accidents, switchyard operation and other emergency situations.

These tests involved two major testing schemes: drop weight test (vertical impact) and pendulum test (horizontal impact). In the drop weight test setup, scale model tank car heads, fastened to their holders and fixed on a wooden platform at the drop tower base were tested. The tests were performed on either bare heads or protected by stainless steel head shields or by other mitigating materials.

The first series of drop weight tests were performed on 1/10 scale model tank heads. The purpose of this test series was to evaluate the effectivenss of mitigating materials on protecting the model tank car heads from impact puncture as compared with the situation when steel head shields were used. A second series of drop weight tests were also performed on 1/10 scale model tank car heads at low temperature of -60 F, with the intent of investigating the effect of low temperature on the model behavior under impact conditions.

For the purpose of developing, establishing and testing the scaling laws, a third series of drop weight tests were performed on 1/5 scale model tank car heads. The results were compared with those of 1/10 scale model tests. Drop weight, head shields, and mitigating materials were scaled as close as possible to meet the ratio of 1/10 and 1/5 scales. The next series of tests were horizontal impact tests, conducted on 1/5 scale model tank car heads. A 1/5 scale tank car, with removable tank head identical with those used in the 1/5 scale drop weight tests, was used. An impact pendulum with an appropriate head weight and scaled coupler was used to deliver the impact blow at the apex of the tank head model. Tests in this series were performed for the purpose of measuring the effect of lading.

3.1 Test Facility

The test facility employed includes a drop/pendulum tower 46 feet high with a 40-feet drop range, 34 miles per hour drop velocity, 30 miles per hour swing velocity, and lift of 3000 pounds. A compact railroad track, a small size tank car, and an instrumentation room were also employed.

The tower is a four-legged free-standing structure made of wide flanged I-beams. Figure 1 (a and b), shows photo pictures of the front and rear views, respectively, of the tower, including the tank car, the track, and the instrumentation room. Figure 2 shows a 1/10 scale model tank car head in a drop impact setup. At the top of the tower, there are safety rails surrounding a platform which is used to service the hoist and to adjust the drop weight guide cables. Steel rungs are attached to the tower for access to the platform.

A 60-feet portable track laid on a gravel bed extends from the base of the tower. The track can be used to guide the tank car or any other object being impacted by the pendulum head. The pendulum arm can be adjusted by 1.5 inches increments between 17.5 to 19.0 feet in length. A variable head weight up to 3000 pounds, and a swing range up to 30 degrees above the horizontal level can be used. The pendulum pivot rotates into two special duty flange bearings fastened to two large brackets and fixed at 20 feet high on the pendulum tower.

An instrumentation room is situated near the tower to house the transient data acquisition equipment such as the tape recorder, the computer, the oscilloscope and other instruments. An electrical power source (115AC) is available in this room for operating the hoist and the instruments. A wide window faces the tower for the observation of the on-going experiments.

3.2 General Procedures

The threshold puncture velocity will be determined approximately by progressively narrowing the gap of the velocities that cause puncture and non-puncture. The impact velocity in each test will be determined based on the previous test results. In general, puncture failure can be determined with visual inspection.

Figure 1a

Figure 1b

Figure 1 - Drop/Pendulum Tower

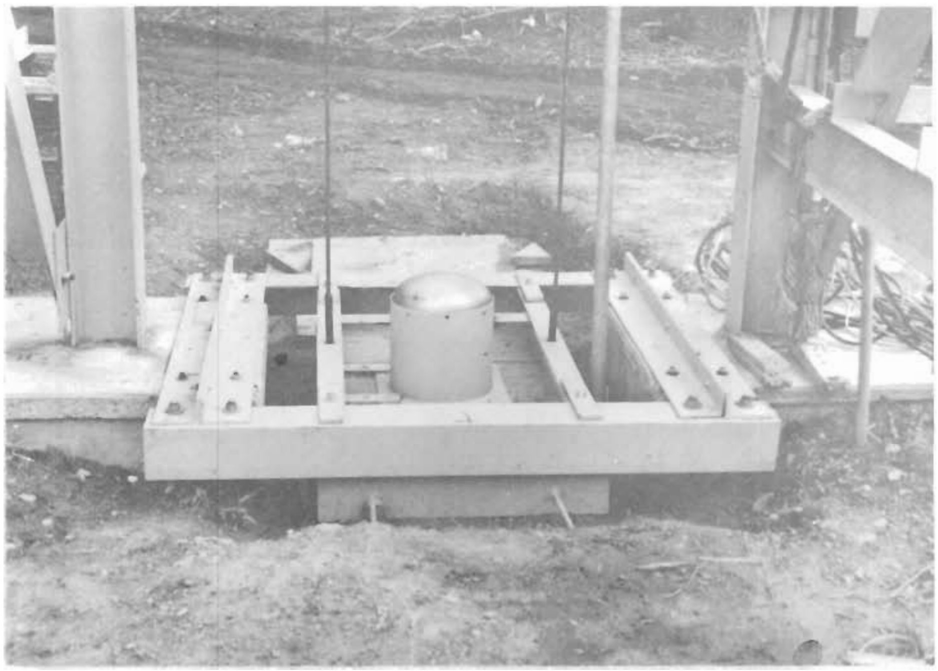

Figure 2 - 1/10 Scale Model Tank Car Head in
Drop Weight Impact Setup

Drop Weight

A drop weight of 247 pounds was used in the 1/10 scale drop tests. This weight has been selected as close as possible to the scale weight of the ram car described in DOT Docket No. HM-144 Sec. 179.105-5. A drop weight of 1,985 pounds was used in 1/5 scale drop tests.

Drop Height

The initial drop height for the drop weight in 1/10 scale drop tests was determined by equating the total kinetic energy available at impact and the approximated energy absorbing capacity before crack occurs.

3.3 Test Series

The following symbol definition is implied in the test series description.

H : Tank head

SI : S refers to stainless steel head shield, I to classification of thickness. For example, S1, S2 are head shields of thickness t_1, and t_2, respectively ($t_2 < t_1$).

MIJ: M refers to mitigator, I to classification of mitigating materials, J to type of thickness. For example, M21 indicates second type of mitigating material with thickness $T_1 (T_1 > T_2)$.

For example, H, S2, M21 indicate a case where tank head with stainless steel head shield of thickness t_2 and mitigator of material no. 2 and thickness T_1 is used in the test.

Following are four series of tests conducted in this program which are related to the four objectives listed in Section 2:

Series 1 - Effect of Mitigators (Drop weight tests on 1/10 scale tank car heads).

1/10 scale model tank car heads were used with the drop tower facility at temperatures above the transition temperature of model material. Cases chosen include (a) H, (b) H, S1, (c) H, S2, (d) H, M11, (e) H, M21, (f) H, M22, (g) H, M12. About six specimens were needed in each case to determine its corresponding threshold velocity.

Series 2 - Effect of Low Temperature (Drop weight tests on 1/10 scale tank car head at low temperature).

1/10 scale model tank car heads cooled below transition temperature of model material were used with the drop tower facility. Cases chosen included (a) H, (b) H, S1, (c) H, M11, (d) H, M22. About six specimens were needed in each case to determine threshold puncture velocity.

Series 3 - Scaling Laws (Drop weight tests on 1/5 scale tank car heads).

1/5 scale model tank car heads were used with the drop tower facility at temperatures above transition temperature of model material. Cases chosen were (a) H, (b) H, S3, (c) H, M23. About three specimens were needed in each case to determine the threshold puncture velocity.

Series 4 - Effect of Lading (Pendulum impact tests on 1/5 scale tank car heads).

1/5 scale model tank car heads were used with the pendulum facility at temperatures above the transition temperature of model material. Cases chosen were (a) target car with mass added to provide total weight, W, (b) target car filled with water to provide total weight, W. About five specimens were needed in each case to determine the threshold puncture velocity.

3.4 Materials and Geometry

3.4.1 Tank Heads

A great deal of efforts were spent to obtain the same materials used in manufacturing the railroad tank car heads as specified in A.A.R. Manual of Standard and Recommended Practices, Section C, Part III. Based on this manual, several materials can be used in manufacturing the tank car heads. These materials are listed in Table M1 in the manual under "Approved Materials For Tanks Fabricated By Welding". One of these materials is listed in Table M1-C in the manual and identified as "High-Alloy Steel Plate - ASTM A240, Type 304". This material was used to manufacture the 1/10 and 1/5 scale tank car heads in our tests.

The physical properties of this material are:

Yield Strength	37000 psi
Tensile Strength	94000 psi
Elongation in 2 inches	62%

These properties are within the range of the recommended physical properties given in the manual. On the other hand, the geometry of the heads is the same as recommended in ACF's Shipper Car Line Division, under Tank Car Anatomy, 15e Rev., Service Bulletin/May 1972. The tank heads have inner diameter of 118.75 inches and have an elliptical shape with the ratio of major to minor axes equal to 2:1. Also, in Part 179, "Specifications for Tank Cars", in DOT Docket No. HM-144, Table 179.101, it is recommended that the minimum plate thickness of the steel shell and heads is 9/16 inch. The dimensions of the 1/5 and 1/10 scale models were selected as follows:

Scale	1/5	1/10
Shape	2:1 elliptical	2:1 elliptical
Major Diameter	24 inches	12 inches
Minor Diameter	6 inches	3 inches
Plate Thickness (Tank Head)	11 gage	16 gage

Figure 3 shows detail drawings of the 1/5 and 1/10 scale model tank car heads.

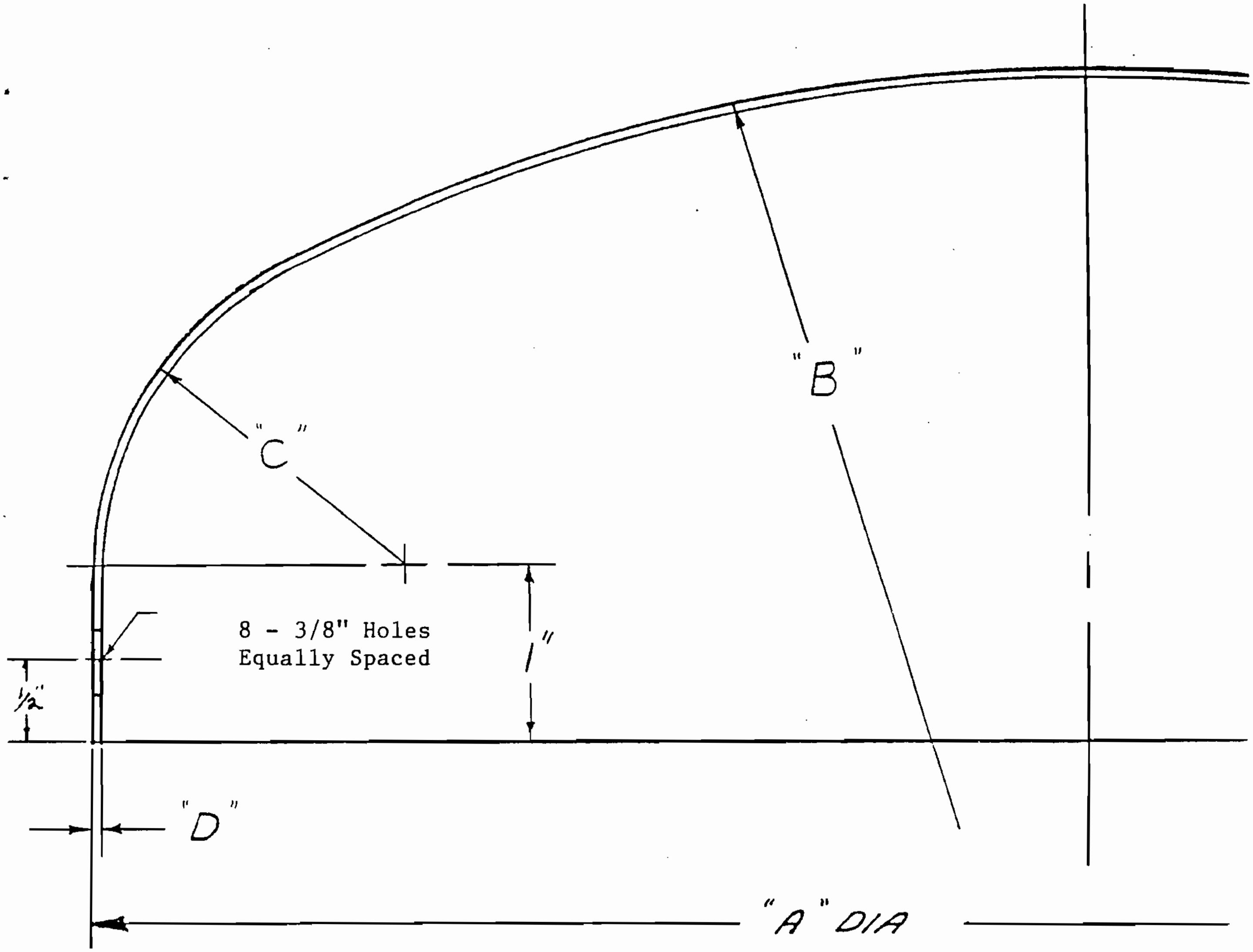

A	B	C	D
12"	10.8"	2.06"	16 GA
24"	21.6"	4.15	11 GA

Figure 3 - Detail Drawings of Model Tank Car Heads
Of 1/10 And 1/5 Scales

3.4.2 Head Shield

The head shield material was selected to be the same as the head material, ASME 240, Type 304 Steel. Different thicknesses of the head shield material were used in the tests. Head shields dimensions were selected as follows: (i) 8" x 8" x 13 gage, (ii) 6" x 6" x 16 gage, (iii) 8" x 8" x 18 gage, and (iv) 8" x 8" x 24 gage.

3.4.3 Mitigating Material

The mitigating material used in the 1/5 and 1/10 scale model impact tests was TecsPak material. This material is based on DU PONT Hytrel Polyester Elastomer. The energy absorption static calibration curves, and the peakload change vs. temperature relation, are given in Figure 4 (a and b) respectively. The dimensions of the TecsPak plates used in the impact tests were as follows: 5.5" in diameter, 3/8", 1/4", and 3/16" in thickness.

3.4.4 Couplers

1/5 and 1/10 scale couplers are made of 1045-CD carbon steel with 90,000 psi yield strength. Figure 5 shows the geometry and the dimensions of the 1/5 scale coupler.

3.5 Test Procedure

3.5.1 Drop Weight Test

1. Secure the weight by raising the drop weight above the ground just enough to put a special stand below the weight.

2. Place the tank head specimen and specimen holder assembly on the base, adjust its position so that the coupler will be exactly above a marked center of the specimen and then fix the specimen holder on the base.

3. Prepare the specimen according to the test schedule with head shield, mitigating material, etc.

4. Control the hoist and lift the drop weight to the desired height by measuring the exact distance between the coupler tip and the model tank head surface center.

5. Activate all tests instruments and carefully check all of them.

6. Run the tape recorder to start recording.

7. Control the fast release hook and release the drop weight to impact the specimen at the tower base.

8. Deactivate all the test instruments.

9. Secure the drop weight with the stand.

10. Remove the specimen for inspection.

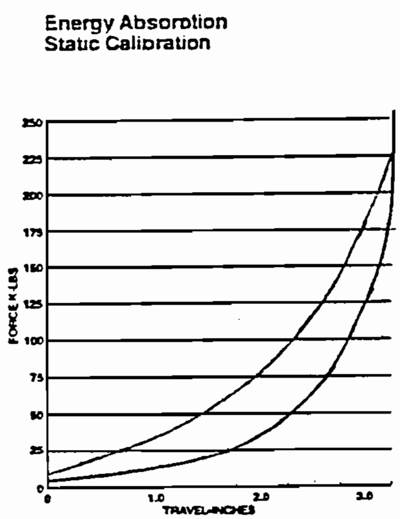

Figure 4a

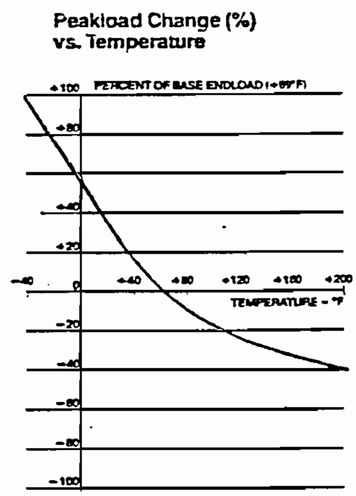

Figure 4b

Figure 4 - Energy Absorption Static Calibration Test And
Peak load Change (%) Vs. Temperature Curves
(TecsPak Material Used As Compression Springs)

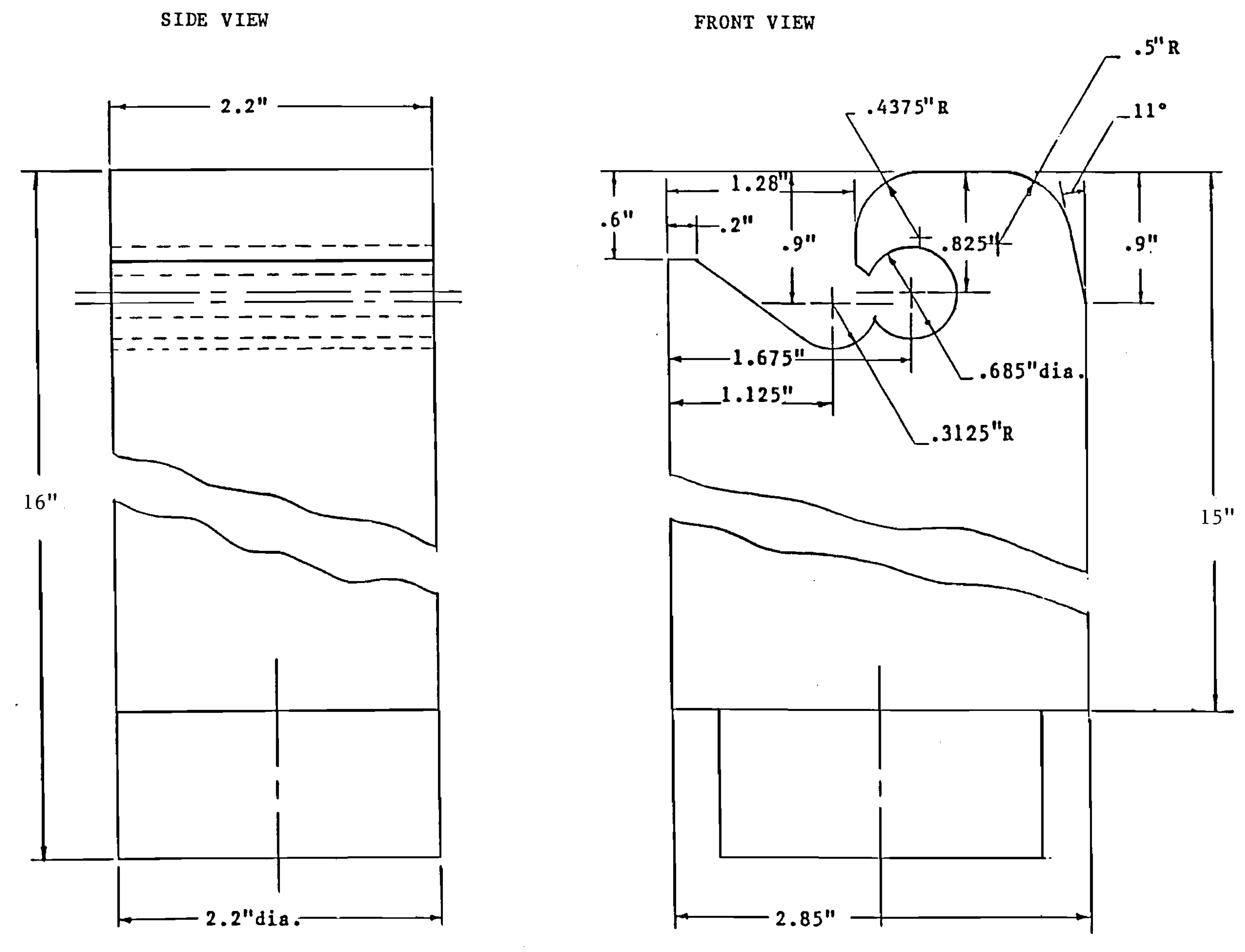

Figure 5 1/5 Scale Model Coupler

Figures 6a, 6b, and 6c show, respectively, the drop weight test setups for the bare model tank head, for the model tank head protected with stainless steel head shield, and for the model tank head protected with mitigating material plate.

3.5.2 Pendulum Test

1. Place a new tank head specimen on the special specimen holder, adjust and fix it.

2. Place the holder/specimen unit in position on the tank car, adjust and fasten it.

3. Move the tank car toward the pendulum until the coupler is next to the tank head.

4. Adjust the length of the pendulum arm so that the coupler points to the center of the head.

5. Prepare the tank car, according to the test schedule, by either loading the car with weights or by filling it with water.

6. Control the hoist and lift the pendulum to the desired height, making sure that no obstacle is in the swinging plane of the pendulum.

7. Activate all test instruments and carefully check all of them.

8. Run the tape recorder and start recording.

9. Control the fast release hook and release the pendulum to swing down and impact the specimen.

10. Deactivate all the test instruments.

11. After the pendulum completely stops remove the specimen for inspection.

Figure 7 shows a sketch drawing and a picture of the pendulum impact test setup.

The procedures for specimen preparations and weight preparation are listed in Appendices A and B, respectively.

3.6 Instrumentation

Following are a list of instruments employed for measuring and monitoring the various quantities and signals involved during the test:

a. Accelerometer - The impact deceleration is monitored with an accelerometer mounted on the back of the impact mass. The output will give a direct measure of deceleration during the impact. The maximum deceleration is selected to compute the maximum impact force.

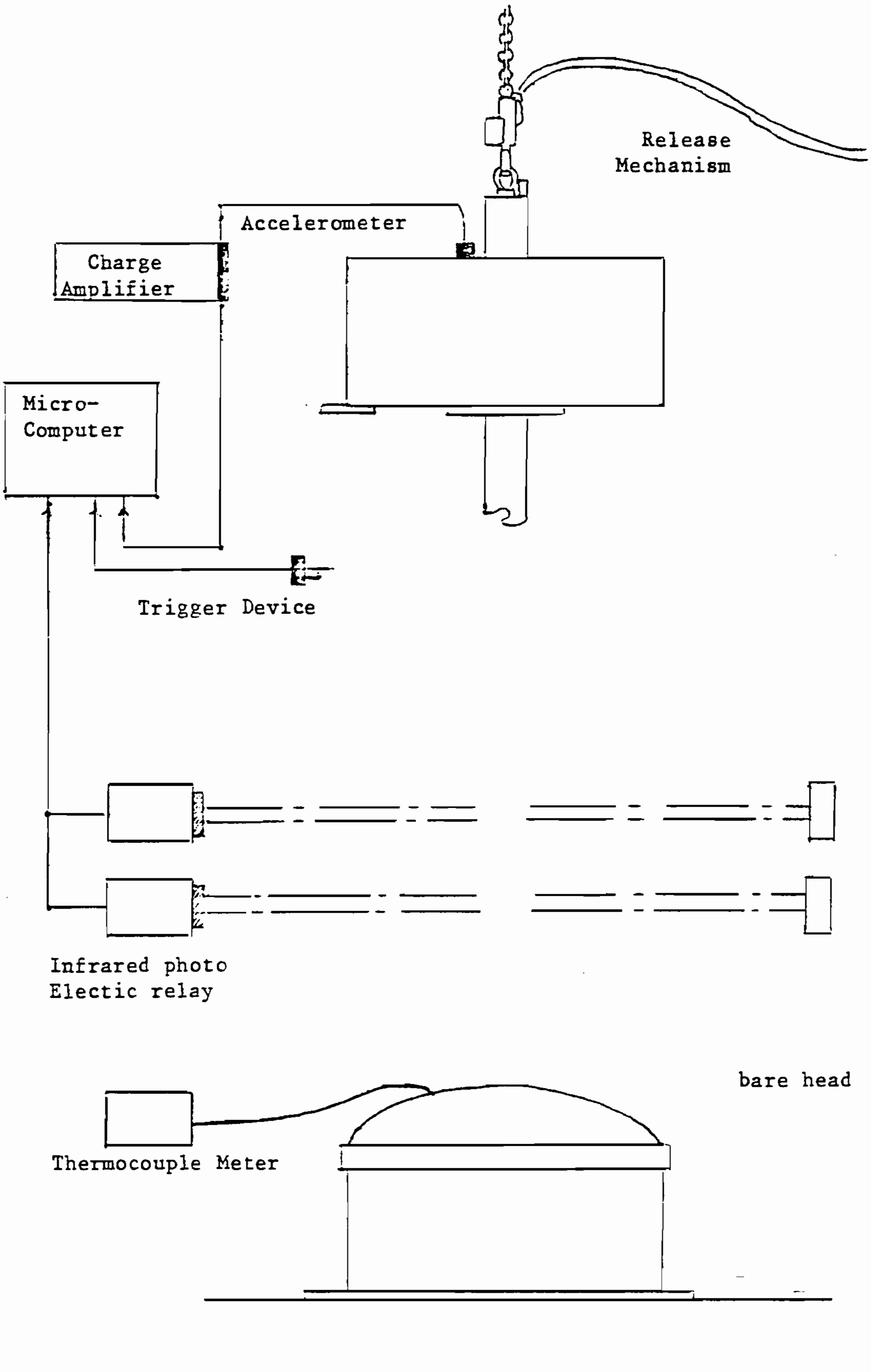

Figure 6a Drop Weight Test Setup
(with bare model tank head)

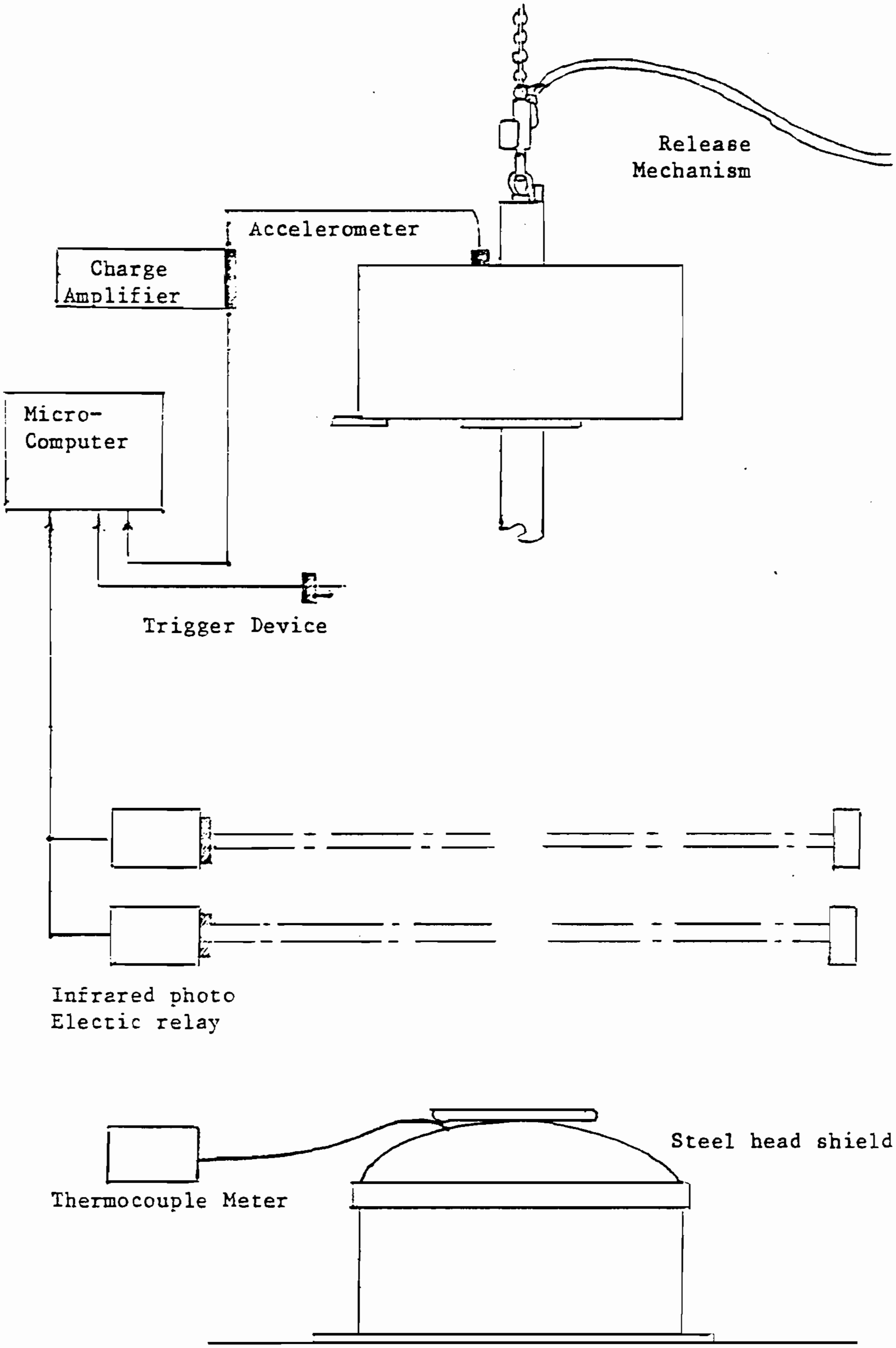

Figure 6b Drop Weight Test Setup
(model tank head with steel plate
head shield)

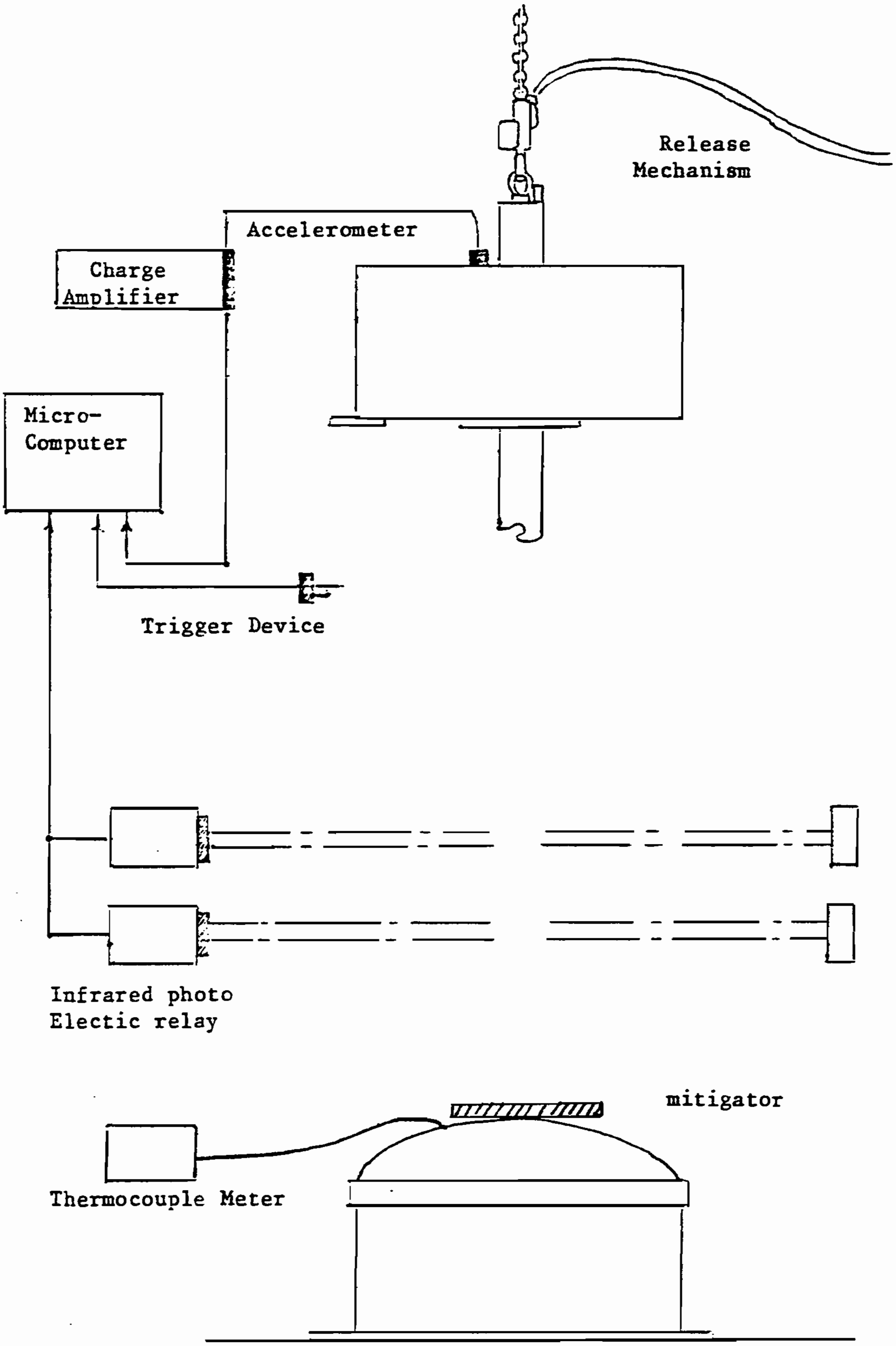

Figure 6c Drop Weight Test Setup
(model tank head with mitigator)

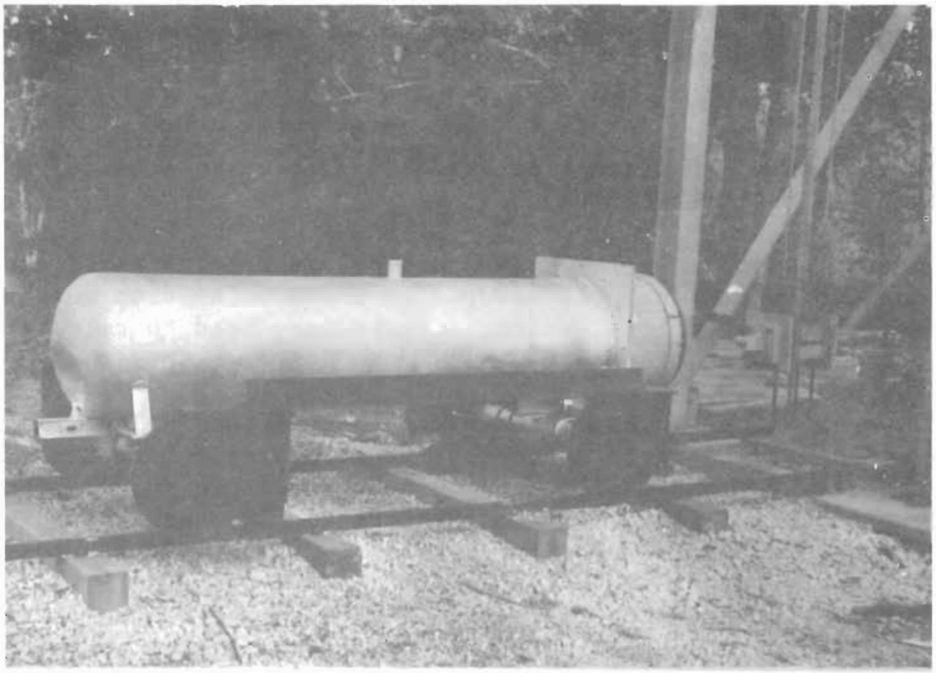

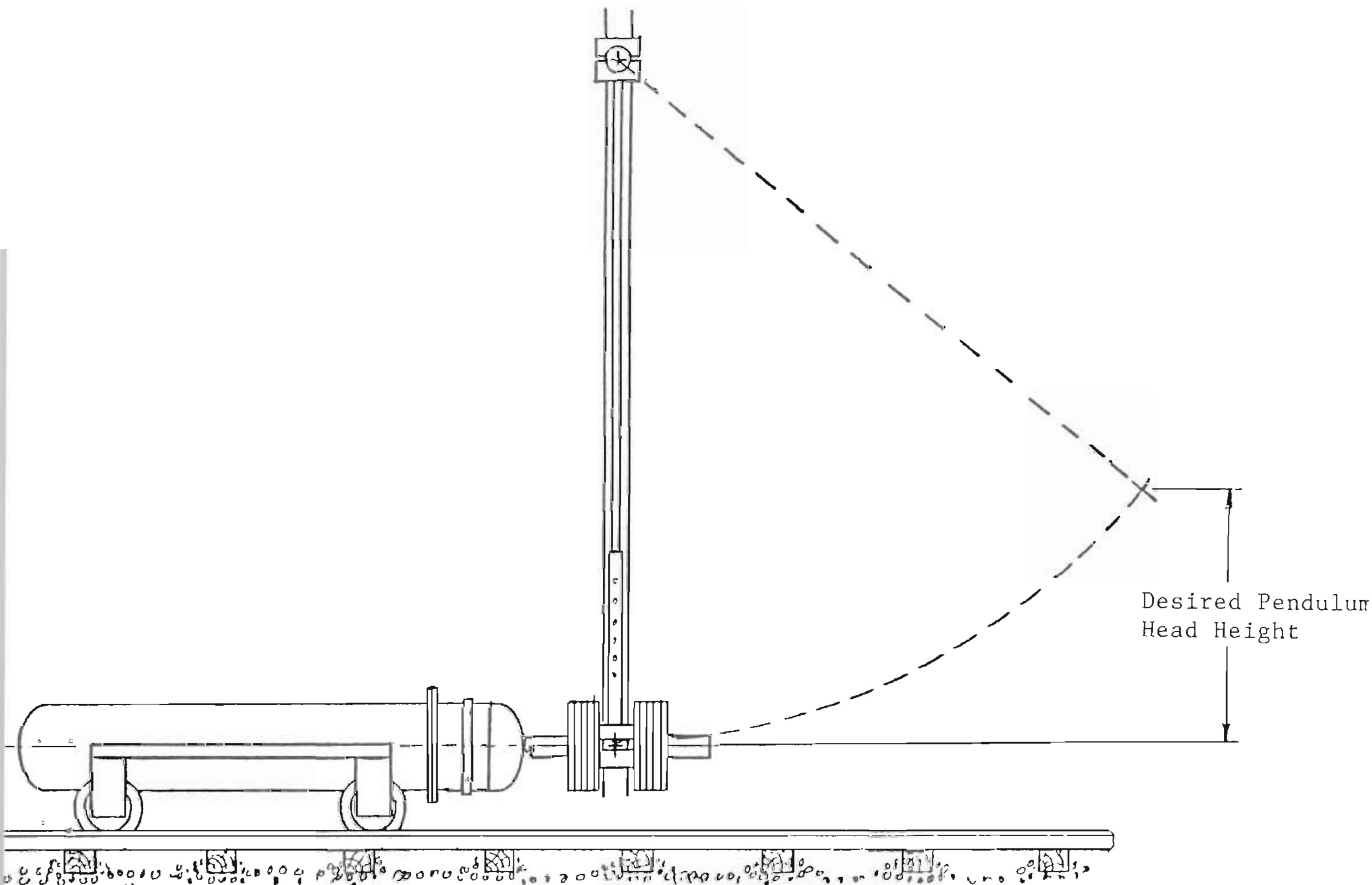

Figure 7 - A Sketch And A Photo Picture of Pendulum Impact Test Setup (Horizontal Impact Test)

b. Triggering system - A triggering system is set up to activate a microcomputer when the test is in progress.

c. Infrared photoelectric relay - Two such relays are installed above the model head tested (see Figures 6a, 6b, and 6c) to measure the drop weight velocities at respective elevations, which, in turn, are used to calculate the drop weight velocity at point of impact.

d. Microcomputer with ADC (Analog to Digital Converter) - The signals from the accelerometer and infrared photoelectric relays are discretized and digitized. These data are then manipulated through a computer program to provide velocity-time and deceleration-time histories. They are then displayed in graphic form on the monitor and/or the printer.

e. Thermocouple and thermocouple meter - When model heads are cooled to $-60^{\circ}F$, thermocouple and thermocouple meter are used to accurately measure their temperature.

3.7 Safety

All the tests were monitored from inside the instrumentation room, and the test area around the tower is cleared before starting a test. All the preparation work preceding a test was done while the ram weight is secured near ground level and not swinging as in the case of the pendulum tests. When lifting the weight, the operator made sure the fast release hook is properly locked. In addition, a sign such as "Test in Progress, Do Not Enter" is posted to caution people from coming too close to the test area.

4. TEST RESULTS AND DISCUSSION

4.1 Evaluation of Mitigating Material Effectiveness.

Before starting the drop weight tests on the 1/10 scale model tank heads, a preliminary static test was conducted on the same model. The load was applied by a hydraulic machine through the coupler at the center of the model tank head. The load-deflection curve for the load up to 5,090 lbs (the corresponding center deflection is 3.7 inches) is given in Fig. 8. The total energy absorbed by the model tank head, which is computed using a trapezoidal rule integration of the area under the load deflection curve, is 792 ft-lbs. As will be illustrated later on in this subsection, the energy required to yield the same amount of deflection at the center of the model tank head in the drop weight impact test is 926 ft-lbs (Model no. BE-2, Table I-A).

A comparison between these two cases shows that more energy is required to yield the same amount of the deflection at the center of the model tank head in case of an impact load than that of a static load. A similar observation was also obtained in Ref. 5 for the energy to initiate a threshold puncture for the coke can lid models. This demonstrates that the loading rate has a profound efect on the response of the tank head.

The test results in the static test also serve to approximately estimate the initial height of the 1/10 scale coupler in the drop weight tests. For example, the total weight attached to the coupler in 1/10 scale case was 247 lbs, and if the test is to find the sitution of threshold puncture, then the drop/weight coupler unit should raise up to a distance higher than the specimen surface center, such that the coupler tip would be at a distance no less than (792/247) and that is 3.2 ft. or 38.5 inches.

As to the mitigating materials, a number of shock mitigating materials were investigated. Various types of aluminum honeycomb, aluminum foams, and corrugated steel plates were compared with a new material, TecsPak, from Du Pont.

The Various types of honeycomb materials considered in the primary tests have the following disadvantages: face plates are needed to spread the impact forces on larger area; a very thick layer of honeycomb materials is required to absorb the available impact energy; some of these materials are easy to split under impact lading; they are weaker in shearing strength; and they are very expensive to form.

On the other hand, TecsPak material showed some advantages: TecsPak plates have the ability to spread the impact forces on a larger area; much better in compression and shearing strength; a reasonable plate thickness is required to absorb the available impact energy; and has a good elastic property. Based on this information, TecsPak material was selected as the mitigating material in this study.

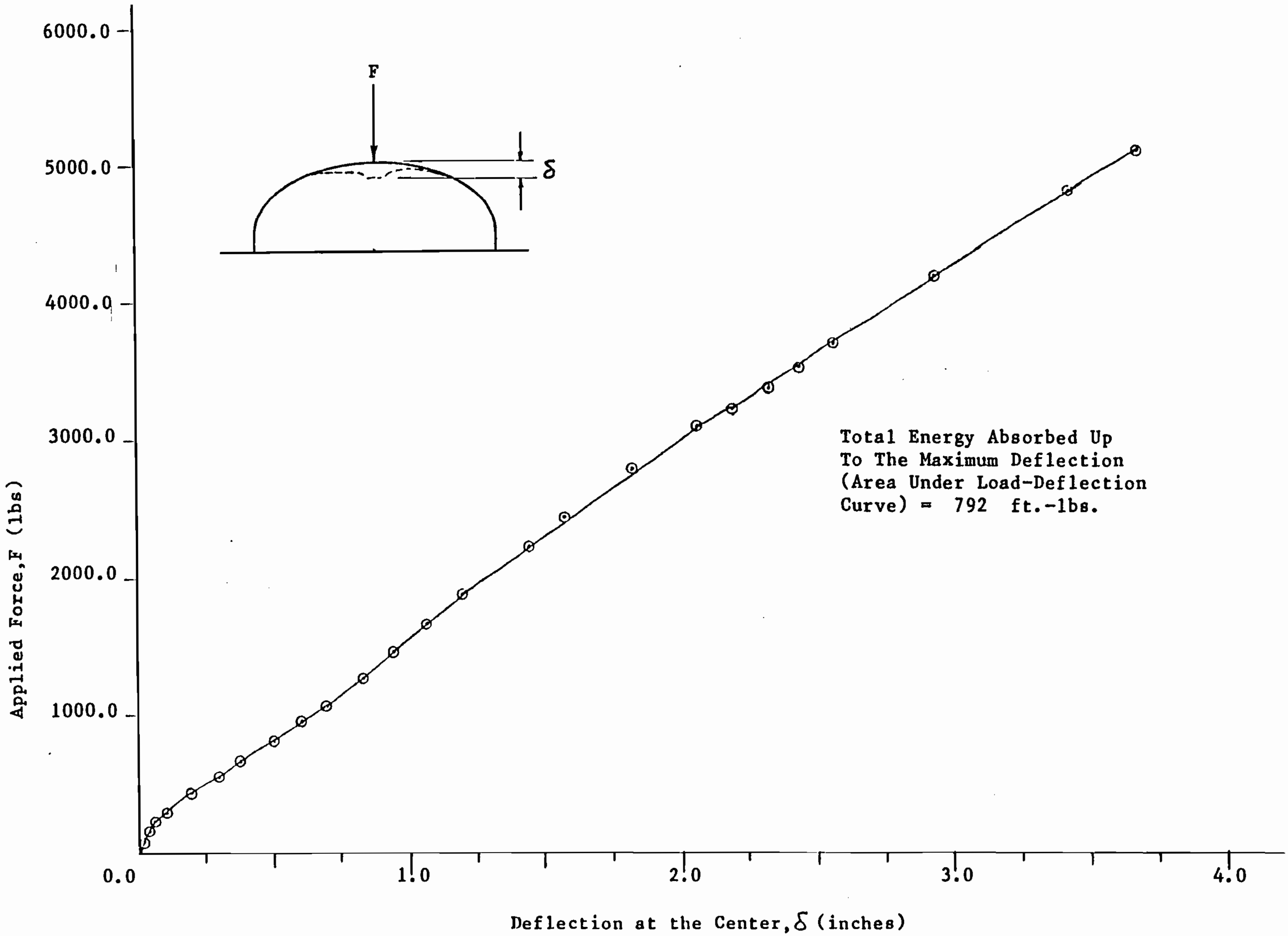

Fig.8 Force vs. Deflection at the center of an 1/10 Scale Model Tank Head in the Static Test.

A total of fifty-one model tank heads of the 1/10 scale model were tested to cover all impact tests needed in the first two series of the drop weight tests. A total of thirty-five impact tests were performed on 1/10 scale model tank heads to investigate the effectiveness of mitigating materials in reducing the vulnerability of head puncture, especially when compared with stainless steel head shields. Since there is a high concern about the weight of the tank head protection devices, an attempt was made in this study to compare the puncture resistance effectiveness vs. weight between the selected mitigating materials and the head shields used in our tests.

For convenience of identifying various situations, two basic conditions imposed on the model tank heads are specified as follows:

(i) Head protective scheme. Three head protetive schemes as shown in figures (6a, 6b, and 6c), are considered in the tests: bare head, head protected with stainless steel head shield, and head protected with TecsPak plate. When either one of the last two protective schemes is adopted in the tests, the protective device is attached to the apex of the model head with a tape.

(ii) Supporting base. Impact tests performed on tank heads without supporting bases (empty base) indicated some large amount of deforrmation to the head without any sign of crack or puncture. To simulate tank cars filled with fluid, some supporting bases were used. Water lading was first used as a supporting base in both the horizontal and drop tests on 1/10 and 1/5 scale model tank car heads. Addtional drop tests were performed on 1/10 scale tank heads using dry sand (uncompacted) as a supporting base. The results were very close to those in the water case. Therefore, sand was selected to be the supporting base material on the remainder of the tests because it was easier to manipulate than water in the vertical position. Three head protective schemes as shown in Figs. (6a, 6b, and 6c), are considered in the tests: bare head, head protected with stainless steel head shield, and head protected with TecsPak plate. When either one of the last two protective schemes is adopted in the tests, the protective device is attached to the apex of the model head with a tape.

Test results obtained were presented and analyzed on the basis of these two model tank head test conditions. The condition of the head protective scheme was first selected as the basis for presentation of test results.

To start off the entire sequence of drop weight tests, six 1/10 scale bare tank head models were experimented, three with water base and the other three with sand base. They are designated as Model no. BW-1, BW-2, BW-3, BS-1, BS-2, and BS-3 in Table I-A. Comparison of their testing data indicates that threshold puncture velocities are 12.48 ft/sec for water base models, and 12.79 ft/sec for sand base models; or in terms of threshold puncture energies, 596.92 ft-lbs for water base models and 627.79 ft/lbs for sand base models. A difference between these types of models is only 2.5% for threshold puncture velocity, or only 5% for threshold puncture energy. Because of this very minor difference as just demonstrated and because of the fact that water, as compared to sand, is much harder to prevent leaking from the model tank head, it was decided that only empty and sand bases should be considered in all other drop weight tests.

Table I-A 1/10 Scale Model Tank Head Drop Weight Tests (with bare head)

Model No.	Test* Condition	Drop Height, in.	Drop Weight, lbs.	Impact Speed, ft/sec.	Kinetic Energy, ft-lbs.	Max. Acceleration G's	Max. Impact Force, lbs.	Depth of Dent, in.	Note**
BE-1	A	40	247	14.65	823	20.40	5,038	3-1/4	D,4AL
BE-2	A	45	247	15.54	926	21.33	5,268	3-3/4	D,4AL
BE-3	A	47.5	247	15.97	978	23.55	5,816	3-15/16	TP,3AL
BE-4	A	50	247	16.38	1,029	22.34	5,517		P,3AL
BE-5	A	51	247	16.54	1,050	26.50	6,545	3-7/8	D,3AL
BE-6	A	53	247	16.87	1,091	26.95	6,657	3-7/8	P,3AL
BE-7	A	60	247	17.94	1,235	***	***	3-13/16	P,4AL
BW-1	C	29	247	12.48	597	26.00	6,422	2-1/4	TP,4AL
BW-2	C	30.5	247	12.80	628	23.55	5,817	3-3/8	P,3AL
BW-3	C	32	247	13.11	659	***	***	2-3/8	P,3AL
BS-1	B	30.5	247	12.79	628	30.91	7,635	2-9/16	TP,4AL
BS-2	B	32	247	13.11	659	***	***	2-1/2	P,3AL
BS-3	B	45	247	15.54	926	***	***	3	P,3AL

* A -Empty base, B - Sand base, C - Water base

** D - Dent, P - Puncture, TP - Threshold puncture, AL - Antinodal lines in head deformation pattern

*** Some of the missing data occurred in situations whenever puncture or measuring difficulties were encountered

For the head protective condition, test results are clasified into three categories: the first one is related to bare head, the second related to stainless steel head shield, and the third related to mitigating materials (TecsPak). Accordingly, results are tabulated and given separately in Tables I-A, I-B and I-C.

The impact velocities contained in these tables are calculated according to the theoretical formula $V = \sqrt{2gs}$ (where V denotes the impact velocity, g the acceleration of gravity, and s the drop weight height). In the experimental tests, velocities were measured by the system described in subsection 3.6. The average velocities of the drop weight at the vicinity of the impact point, can be computed. The following are some examples of measured and calculated velocities:

Drop Weight Height (in.)	Calculated Data (Ft./Sec.)	Measured Data (Ft./Sec.)	Error %
30.5	12.793	12.570	1.70
50.0	16.381	16.286	.58
51.0	16.544	16.300	1.47
65.0	18.677	18.390	1.54
75.0	20.062	19.810	1.25
80.0	20.720	20.600	.58
85.0	21.358	21.110	1.16

Since the measured and calculated velocities are very close with errors varied between .58% to 1.7%, the usage of the calculated velocities in the test data would still give us reliable results.

To assist in visualizing the deformation pattern and magnitude of damage of model tank heads after impact, many of the tested models were photographed and their pictures are displayed in Appendix C. For additional information a number of deceleration vs. time curves covering the entire range of impact duration for some selected models are also given in Appendix D. These curves can be used to obtain the maximum deceleration after impact, and to measure the impact duration for each test.

For easier comparison and interpretation of the test data, results of Table I-A except for those of water base are displayed in Fig. 9-A relating dent depth vs. kinetic energy at impact. As can be seen in this figure, the threshold puncture energies are 978 ft-lbs for the model head of the empty base and 628 ft-lbs for the model head of sand base, with the former being about 56% higher than the latter.

Table I-B comprises of test results with stainless steel plates as head shields which have three different thicknesses: 13 (0.0897 inches), 16 (0.0598 inches) and 24 (0.0239 inches) gages. For the cases of empty model tank heads with steel head shields of 13 and 16 gages, it is found by inspection after the impact, that the deformation in each of the tested models with no crack or puncture was too deep and large. The deformation extends (as shown in Figure C-2a), to the region near the knuckle area where a bend with a very sharp edge was formed at the end of each deformation antinodal line. This type of

Table I-B 1/10 Scale Model Tank Head Drop Weight Tests* (with stainless steel head shields)

Model No.	Test** Condition	Drop Height, in.	Drop Weight, lbs.	Impact Speed, ft/sec.	Kinetic Energy, ft-lbs.	Max. Acceleration G's	Max. Impact Force, lbs.	Depth of Dent, in.	Note***
SE-1	A1	75	247	20.06	1,544	29.93	7,393	4-9/16	D,4AL
SE-2	A2	80	247	20.72	1,647	31.89	7,877	4-5/8	D,4AL
SE-3	A2	120	247	25.38	2,470	41.21	10,179	5-7/8	D,3AL
SE-4	A2	150	247	28.37	3,088	53.97	13,331	5-11/16	D,4AL
SE-5	A	88	247	21.73	1,811	****	****	4-7/8	D,4AL
SE-6	A	98	247	22.93	2,017	****	****	5-1/4	D,4AL
SE-7	A	120	247	25.38	2,470	****	****	5-3/4	P,3AL
SS-1	B	62	247	18.24	1,276	56.42	13,936	3	P,4AL
SS-2	B	65	247	18.68	1,338	55.44	13,694	3-1/8	P,4AL
SS-3	B	75	247	20.06	1,544	56.91	14,057	3-1/4	P,3AL
SS-4	B	85	247	21.36	1,750	56.91	14,057	4	P,3AL

* In tests of condition A and B, threshold puncture energies are estimated at 2,150 ft.-lbs, respectively.
** A1, A2, and A - Empty base, stainless steel head shields of 13, 16, and 24 gages, respectively
*** D - Dent, P - Puncture, TP - Threshold puncture, AL - Antinodal lines in head deformation pattern
**** Some of the missing data occurred in situations when severe puncture or measuring difficulties were encountered

Table I-C 1/10 Scale Model Tank Head Drop Weight Tests* (with mitigating material - tecspac

No.	Test** Condition	Drop Height, in.	Drop Weight, lbs.	Impact Speed, ft/sec.	Kinetic Energy, ft-lbs.	Max. Acceleration G's	Max. Impact Force, lbs.	Depth of Dent, in.	Note***
ME-1	A	75	247	20.6	1,544	28.46	7,030	4-7/8	D,4AL
ME-2	B	98	247	22.93	2,017	****	****	4-7/8	D,3AL
ME-3	B	102	247	23.40	2,100	36.80	9,090	5-7/8	P,3AL
ME-4	B	112	247	24.52	2,305	39.25	9,695	6-1/4	P,3AL
ME-5	B	122	247	25.59	2,517	44.16	10,908	6-5/8	P,4AL
ME-6	B	135	247	26.92	2,779	45.63	11,271	6-1/8	P,4AL
ME-7	B	150	247	28.37	3,088	43.67	10,787	5-7/8	P,4AL
MS-1	C	60	247	17.94	1,235	46.12	11,392	3	D,3AL
MS-2	C	62	247	18.24	1,276	50.05	12,362	3-1/2	P,3AL

* In cases of condition B and C, the threshold puncture energies are estimated at 2,050 and 1,256 ft-lbs, respectively.
** A - Empty base, 7/16" TecsPak plate; B - Empty base, 3/16" TecsPak plate; C - Sand base, 1/4" TecsPak.
*** D - Dent, P - Puncture, TP - Threshold puncture, AL - Antinodal lines in head deformation pattern.
**** Some of the missing data occurred in situations when severe puncture or measuring difficulties were incountered.

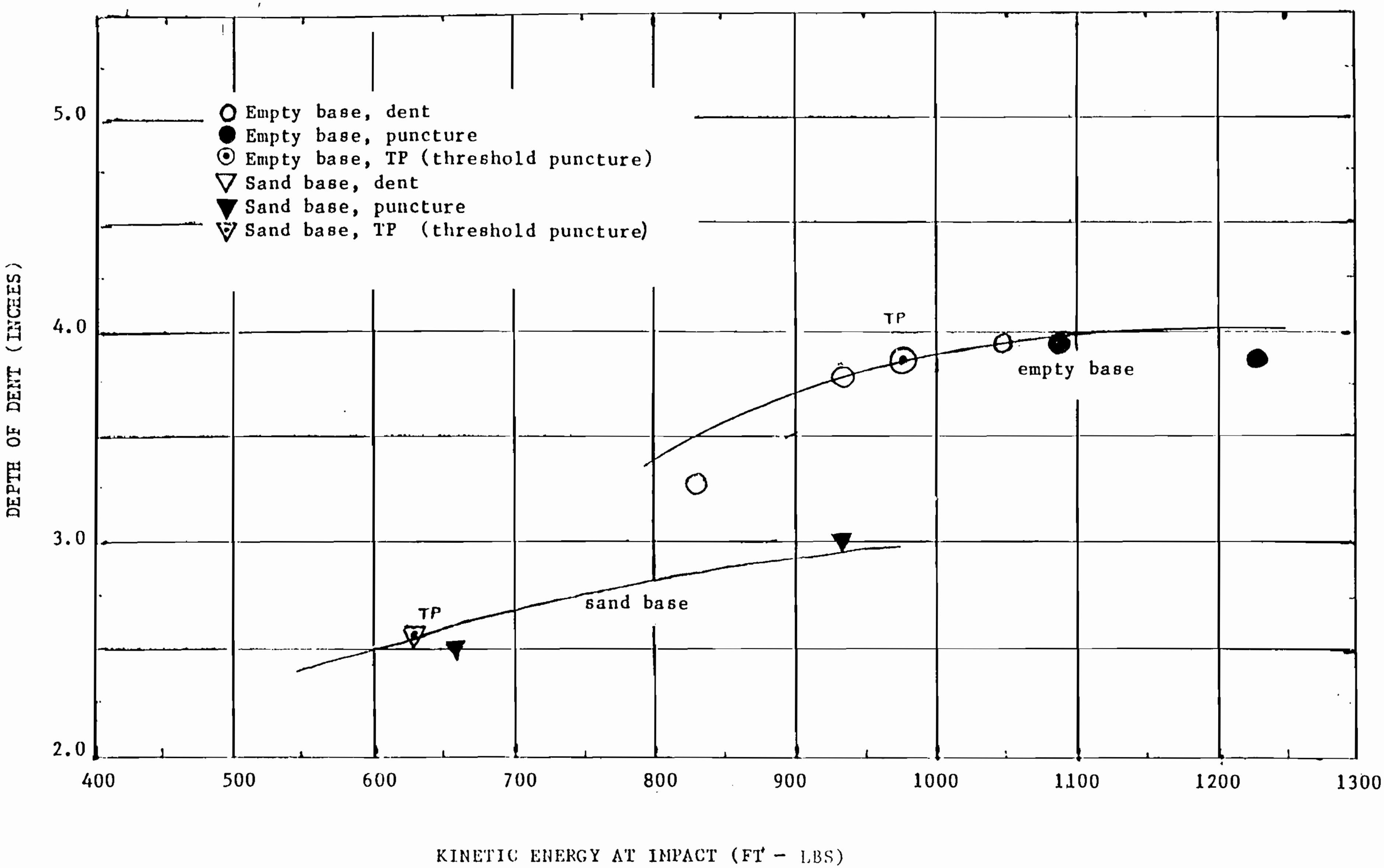

Figure 9-A Kinetic Energy vs. Dent Depth, 1/10 Scale Drop Weight Impact Tests (with bare head)

deformation is quite contrary to what was experienced in prototype tank car head puncture wherein the permanent deformation is confined to a region immediately surrounding the impact point. The drastic departure from usual prototype tank car head deformation pattern may be ascribed to relative greater stiffness of head shield employed and lack of lading backing the model heads. Thus, the test results involving 13 and 16 gages of steel head shields are disregarded, and only those with 24 gage steel plate head shields are shown in Fig. 9-B. Similarly, the data of Table I-C are also presented in curves of Fig. 9-C in the form of dent depth vs. kinetic energy at impact.

A study of Fig. 9-B reveals that, under the condition that stainless steel plates of 24 gage are used as head shields, the threshold puncture energies for 1/10 scale model heads are estimated at 2,150 ft-lbs for the case of empty base, and 1,200 ft-lbs for sand base, with a difference of about 79% between them. Fig. 9-C also indicates that, under the condition of using TecsPak plates as head shields, the threshold puncture energies for the 1/10 scale model heads are estimated at 2,050 ft-lbs for the case of empty base and 1,250 ft-lbs for sand base, with a difference of about 64% between them. A summary of threshold puncture energies for the 1/10 scale models as indicated in Figs. 9A to 9C is given in Table II for easier comparison.

A careful review of these three figures reveals that, with reference to the same head shield condition, the energy absorbed by an empty model tank head up to the point of incipient puncture is more than that by the same scale model tank head backed up by sand, with a difference between them of ranging from 56% to 79%. In other words, an empty model tank head is less susceptible to puncture than a head backed up by sand. The same situation is also observed in Ref. 3 wherein the tests were performed with water backing up the tank heads.

It is also demonstrated from these three figures that, under the same head shield condition, the depth of dent for an empty model head at threshold puncture is greater than that for a model with sand backing up the tank head. In other terms, an empty model tank head is susceptible to deeper dents than one backed up with sand; the same observation was also revealed in Ref. 3.

An examination of the figures in Appendix C indicates that two types of deformation patterns appear in the tested models: three and four equally-spaced antinodal lines. In general, a pattern described by three equally-spaced antinodal lines is a lower energy configuration than a pattern with four such lines. However, an inspection of all impact models does not render a consistent correlation between deformation pattern and corresponding threshold puncture energies. This same observation is also shared in the finding of Ref. 5.

The same examination also reveals that the effect of essentially incompressible sand backing up the model head is to confine permanent deformation to a smaller region surrounding the impact point than that for an empty model head. As a result, a model head with sand base allows a smaller amount of wrinkling and plastic deformation to occur before the material fails, and, consequently, the model absorbs less impact energy. This may serve to explain why the threshold puncture required for a model with sand base or other lading to back up the tank head is less than that for an empty one. In other

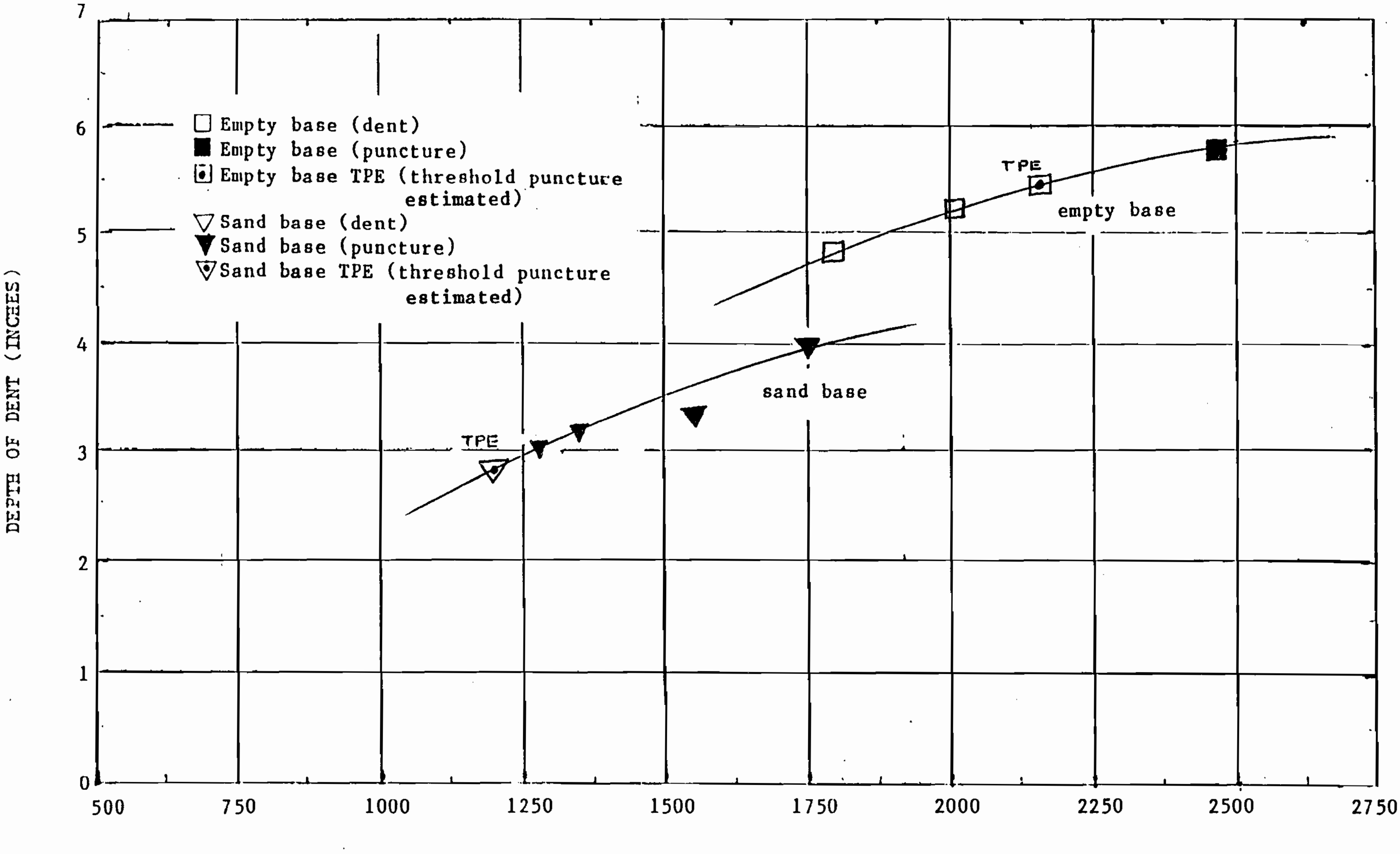

Figure 9-B Kinetic Energy vs. Dent Depth, 1/10 Scale Model Drop Weight Tests.
(with stainless steel head shield of .0239")

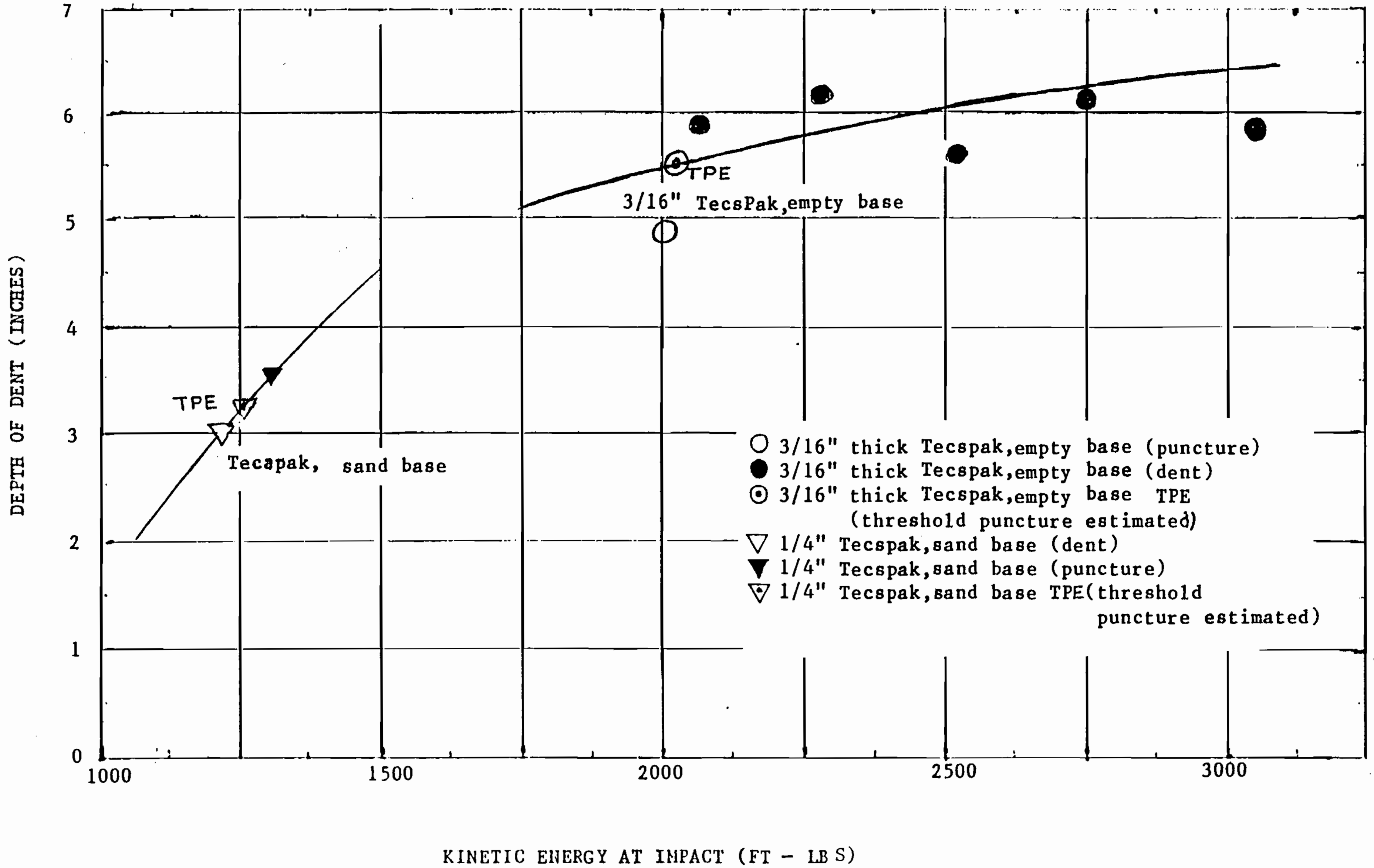

Figure 9-C Kinetic Energy vs. Dent Depth for 1/10 Scale Model Drop Weight Impact Test (with mitigating material - Tecspak)

Table II Threshold Puncture Energies for 1/10 Scale Model Tank Heads in Drop Weight Tests

Base Condition	Threshold Puncture Energy (ft-lbs)		
	bare head	steel head shield	TECSPAK
Empty base	978	2,150	2,050
Sand base	628	1,235	1,256

words, this tends to suggest that lading has the effect of reducing threshold puncture energy for a tank head, and thus increases the vulnerability of tank head to puncture in an impact situation. This same subject will be further discussed in Subsection 4.4 through the use of pendulum tests on the 1/5 scale tank heads.

Figures 10 and 11 show the comparison of the impact test results as described in Figures 9 (A, B, and C) on the basis of supporting base. Figure 10 shows the comparison of the test results when empty base was used in the tests and Figure 11 shows the comparison when the model tank head base was filled with dry sand.

Threshold puncture energies associated with various situations are listed in Table II. It is unfortunate to note that no substantial difference is found in protecting the model tank heads against puncture damage between stainless steel plate and TecsPak proposed in this study. This may be partially ascribed to a smaller size of TecsPak plates employed in the tests than that of steel plates.

An examination of deceleration history after impact for the 1/10 scale models shown in the figures in Appendix D points out that the average impact duration is about 40 m-sec for steel plate and 70 m-sec for TecsPak plate in the case of empty base, and that the average impact duration is about 40 m-sec for steel plate and about 40 m-sec for TecsPak plate in the case of sand base. Therefore, the change in impact duration with respect to TecsPak plate vs. steel plate is inconsistent and inconclusive.

It is of interest to compare the dynamic response between Model S, SE-4 (Table I-B, Fig. D1-c), and ME-7 (Table I-C, Fig. D2-c). Model SE-4 is with empty base and using steel plate of 16 gage as head shield, while Model ME-7 is also with empty base but using TecsPak plate of 3/16 inches in thickness as the head shield.

Both were subjected to the same drop weight (247 lbs) at the same drop height (150 inches), thereby also under the same impact energy. The duration of the impact for Models SE-4 and ME-6 are 33 and 65 m-sec, respectively. But the maximum impact force is 13,330 lbs for SE-4 and 10,786 lbs for ME-6. Therefore, it is concluded that if under the same impact energy, the one with the smaller duration of impact should be subjected to a higher value of the maximum impact force.

An examination of the deceleration history for the models subjected to the same test conditions reveals that the deceleration vs. time curve for the one with a dent after an impact is usually quite smooth, and that the curve for the one with the puncture displays the fluctuation right after the maximum deceleration has been reached. This phenomenon is evidenced by Figs. D7-a (with dent) and D7-b (with puncture).

An obvious question immediately posed here is: can other types of mitigating materials provide better protection against head puncture than TecsPak proposed in this study? This is a research area that needs to be explored further.

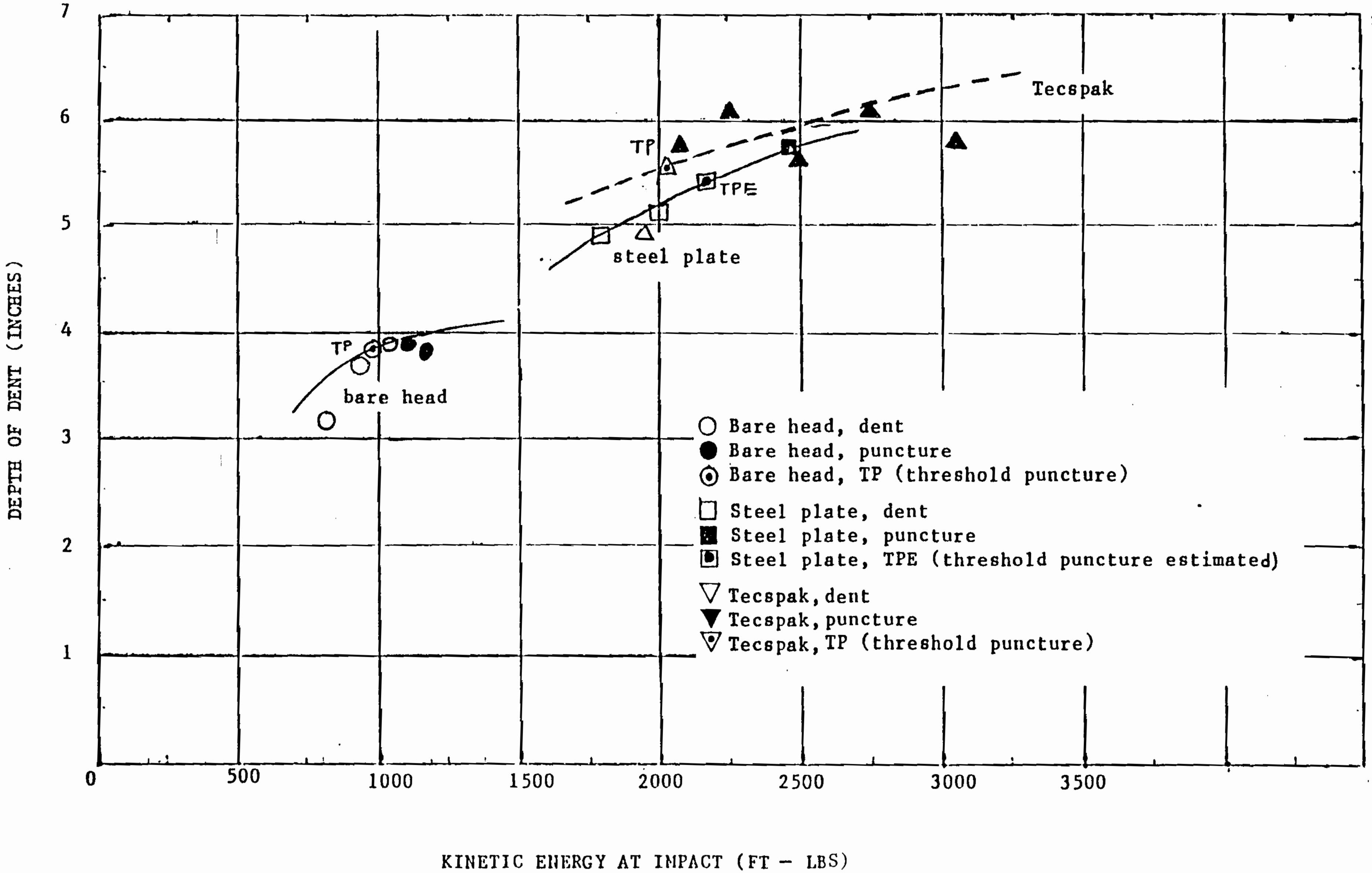

Figure 10 Comparison of Dent Depth vs. Kinetic Energy Between 1/10 Scale Model Heads with Bare Head, Tecspak, and Stainless STeel Plate (Empty Base)

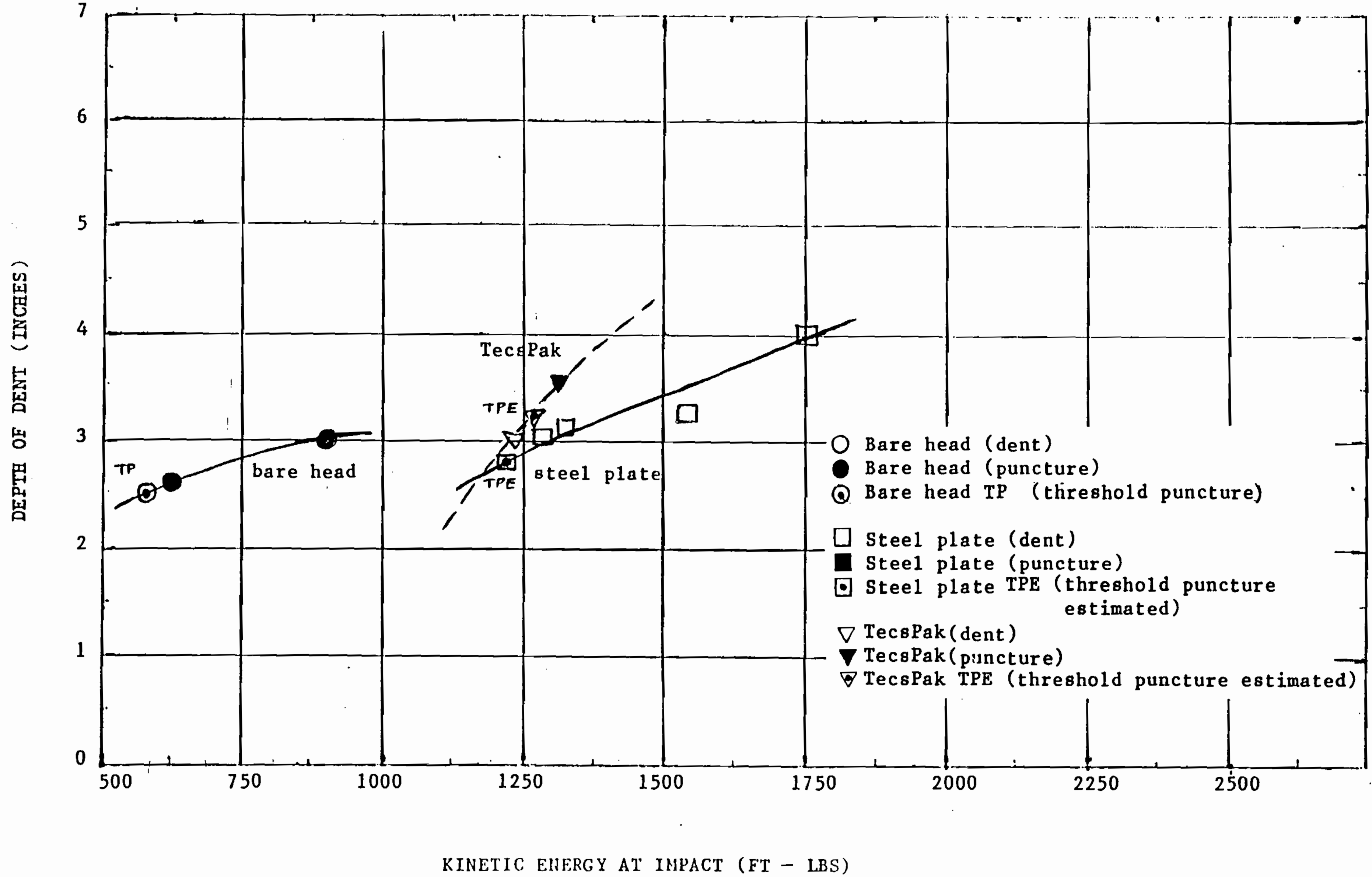

Figure 11 Comparison of Dent Depth vs. Kinetic Energy Between 1/10 Scale Model Head with Bare Head, TecsPak and Stainless Steel Plate (Sand Base)

As expected, both TecsPak and stainless steel plates provided excellent protection against head puncture when compared with bare tank heads. Both have the capability of spreading the impact load to a larger tank head area, and more significantly, both blunted the striking edge of the impacting object.

Because of being able to spread the impact load to a larger tank head area and hence decrease the shear force intensity, both TecsPak and steel plates can reduce the chance of local puncture surrounding the impacting object. As a result, the deformation pattern in a tank head with TecsPak or a steel plate as a protective device tends to extend toward the knuckle region and thus permits a deeper dent than that of a bare tank head.

4.2 Low Temperature Effect

Eleven model tank heads of the 1/10 scale cooled down to -60° F with liquified nitrogen were experimented in a drop weight setup. Test results obtained for all these models with different testing conditions are tabulated and given in Table III.

The drop weight tests were conducted on five of these models at -60° F with bare head and empty base. A fair estimate of threshold puncture energy based on the test data is about 1,156 ft-lbs, which is slightly higher than that (978 ft-lbs) listed in Table II for the identical models under the same testing conditions and tested at room temperature.

Two other models at -60° F were tested under the conditions of using TecsPak as a head shield and sand to back up the model head. The threshold puncture for this case is found to be about 1,255 ft-lbs, which is nearly the same as that (1,256 ft-lbs) listed in Table II for the identical models subjected to the same testing conditions at room temperature.

The last four models at -60° F were tested under the conditions of 24 gage steel plate head shield and a sand base. One model (Model LSS-4) was subjected to kinetic energy of 1,523 ft-lbs, and no puncture was found. It is obvious that threshold puncture energy required for this case is higher than that (1,235 ft-lbs from Table II) for the identical models under the same testing conditions at room temperature.

Based on this information, it may be concluded that low temperature has the effect of slightly increasing the magnitude of threshold puncture energy required for the model tank heads used in this study. This finding is quite interesting. To further verify this finding, more research on the material property of stainless steel at low temperature is recommended.

Table III 1/10 Scale Model Tank Head Drop Weight Tests at -60°F*

Model No.	Test** Condition	Drop Height, in.	Drop Weight, lbs.	Impact Speed, ft/sec.	Kinetic Energy, ft-lbs.	Max. Acceleration G's	Max. Impact Force, lbs.	Depth of Dent, in.	Note***
LBE-1	A	45	247	15.54	926	****	****	3-9/16	D,4AL
LBE-2	A	47.5	247	15.97	329	****	****	3-7/16	D,3AL
LBE-3	A	49	247	16.22	1,009	****	****	3-3/4	D,3AL
LBE-4	A	50	247	16.38	1,029	26.99	6,667	3-3/4	D,3AL
LBE-5	A	53	247	16.87	1,091	26.99	6,667	4-1/8	D,3AL
LMS-1	B	60	247	17.94	1,235	54.95	13,572	3	D,4AL
LMS-2	B	62	247	18.24	1,276	55.93	13,815	3-1/16	P,4AL
LSS-1	C	62	247	18.24	1,276	57.41	14,180	3	D,4AL
LSS-2	C	64	247	18.35	1,317	53.48	13,210	3-1/4	D,3AL
LSS-3	C	67	247	18.96	1,379			3-7/16	D,4AL
LSS-4	C	74	247	19.93	1,523	57.90	14,301	3-7/16	D,3AL

* Threshold puncture energies for cases of condition A, B, and C are estimated at 1,150, 1,255, and 1,523 ft-lbs, respectively.

** A - empty base, bare head; B - Sand base, 1/4" TecsPak plate; C - Sand base, steel plate of 24 gage.

*** D - Dent, P - Puncture, TR - Threshold puncture, AL - Antinodal lines in head deformation pattern.

**** Some of the missing data occurred in situations when severe puncture or measuring difficulties were encountered.

4.3 Validity of Scaling Laws

4.3.1 Scaling Laws

In the development of small scale simulation tests, it is very important to adopt appropriate scaling laws so that model results can be extrapolated to the full scale cases. The scaling laws adopted in this study were developed by Gorman (Ref. 5), using dimensional analysis. Similar dimensional analysis was also done in Refs. 3, 6, 7, 8, 9, and 10.

It was proposed in Ref. 5 that fourteen variables were used to describe the tank car head impact event. These variables are defined as follows:

D	Tank head diameter
h	Tank head thickness
R	Tank head radius of curvature
d	Indenter characteristic dimension
m	Mass of impacting body
m'	Mass of impacted body
V	Initial velocity of impacting body
σ_y	Head material yield stress
E_s	Head material secant modulus
$\dot{\varepsilon}$	Strain rate associated with post impact deformation
ρ_{fl}	Density of fluid
ρ_{hd}	Density of head material
P_o	Internal pressure of impacted tank
K_d	Spring constant of impacting car's draft gear

The Buckingham-π theorem states that, given a list of variables, the total number of independent parameters which can be formed is equal to the total number of variables minus the number of primary units utilized. Since there are three primary units of mass, length, and time involved, eleven independent dimensionless parameters can be obtained from the initial list of fourteen variables. These parameters are defined as:

$$\pi_1 = \frac{\sqrt{m/k_d}}{D\sqrt{\rho_{hd}/E_s}} \qquad \pi_2 = \frac{m}{m'} \qquad \pi_3 = \frac{\sigma_v}{E_s} \qquad \pi_4 = \frac{h}{R}$$

$$\pi_5 = \frac{\sigma_v^2}{E_s\ \rho_{hd}\ \dot{\varepsilon}^2 h^2} \qquad \pi_6 = \frac{mv^2\ E_s}{\sigma_y^2\ d^3} \qquad \pi_7 = \frac{h}{D} \qquad \pi_8 = \frac{P_o R}{\sigma_y h}$$

$$\pi_9 = \frac{\sigma_v^2}{E_s\ \rho_{fl}\ \dot{\varepsilon}^2 h^2} \qquad \pi_{10} = \frac{d}{D} \qquad \pi_{11} = \frac{\rho_{fl}\ D^3}{m}$$

It is noted that these dimensionless parameters are intentionally formed by ratios of physically recognizable quantities such as impact kinetic energy, head deformation kinetic energy, and fluid kinetic energies, strain energy, etc. The definitions of these parameters are given in detail in Appendix E for references.

The scaling laws in this study are formulated by matching each parameter for the scale model and full size case, i.e., $\pi im = \pi if$, for i = 1,2,3,...,11 where the subscripts m and f refer to the model and the full scale, respectively. Moreover, the scaling laws also enforce that the geometric similarity is preserved. According to this argument, it is apparent, after reviewing the matching conditions for $\pi 4$, $\pi 7$, and $\pi 8$, that all of the length variables must be scaled by the same factor S as:

$$\frac{D_m}{D_f} = \frac{h_m}{h_f} = \frac{d_m}{d_f} = \frac{R_m}{R_f} = \frac{1}{S} \qquad (1)$$

The resulting matching relations for π parameters can be simplified greatly if the same material is used for the model and the full scale, and the same fluid is also used to back up the model head and the full size tank head. Under these circumstances, $\sigma_{ym} = \sigma_{yf}$, $E_{sm} = E_{sf}$, $\rho_{hdm} = \rho_{hdf}$, $\rho_{flm} = \rho_{flf}$, and the following scaling relations are obtained:

$$\frac{m_m}{m_f} = \frac{m'_m}{m'_f} = \frac{1}{S^3} \qquad (2)$$

$$\frac{\dot{\varepsilon}_m}{\dot{\varepsilon}_f} = S \qquad (3)$$

$$P_{om} = P_{of} \qquad (4)$$

$$\frac{K_{dm}}{K_{df}} = \frac{1}{S} \qquad (5)$$

$$V_m = V_f \qquad (6)$$

The scale for strain is unity since strain is a nondimensional quantity and thus governed by similarity rules. If the stress-strain relationship is fixed, stress scale should also be unity. Time scale, based on $\dot{\varepsilon} = d\varepsilon/dt$, can be determined as $t_m/t_f = 1/S$. Since acceleration is defined by $a = dV/dt$, this yields acceleration scale as $a_m/a_f = S$. If F, A denote force and area, respectively, force scale can be obtained from $F = \sigma A$ as $F_m/F_f = 1/S^3$. Similarly, energy scale can also be obtained from E(energy) = FxS(distance) as $E_m/E_f = 1/S^3$.

A summary of scaling for important impact parameters is given as follows:

Energy	$E_m/E_f = 1/S^3$	(7)
Force	$F_m/F_f = 1/S^2$	(8)
Acceleration	$a_m/a_f = S$	(9)
Velocity	$V_m/V_f = 1$	(6)
Time	$t_m/t_f = 1/S$	(10)

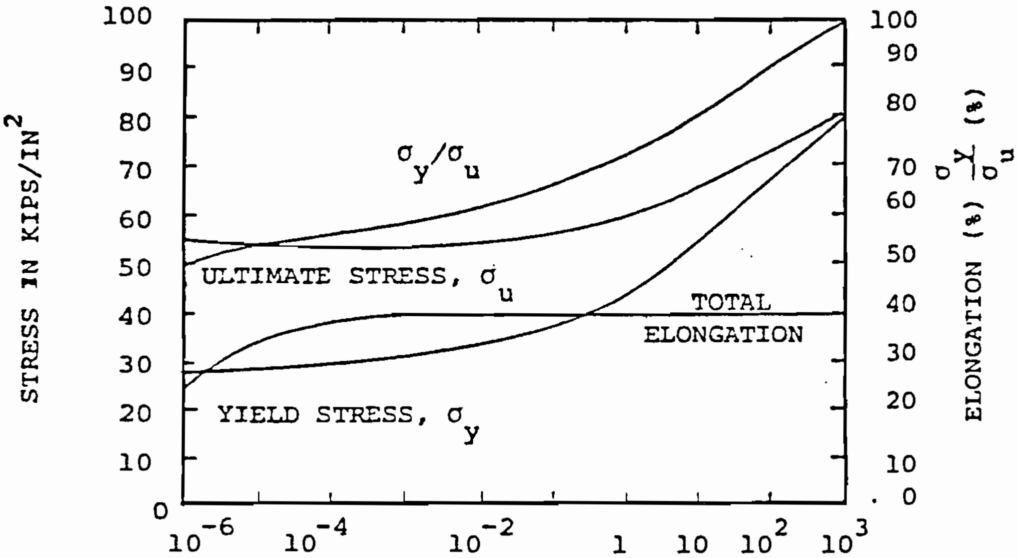

FIG. 12 INFLUENCE OF RATE OF STRAIN ON TENSILE PROPERTIES OF OF MILD STEEL AT ROOM TEMPERATURE

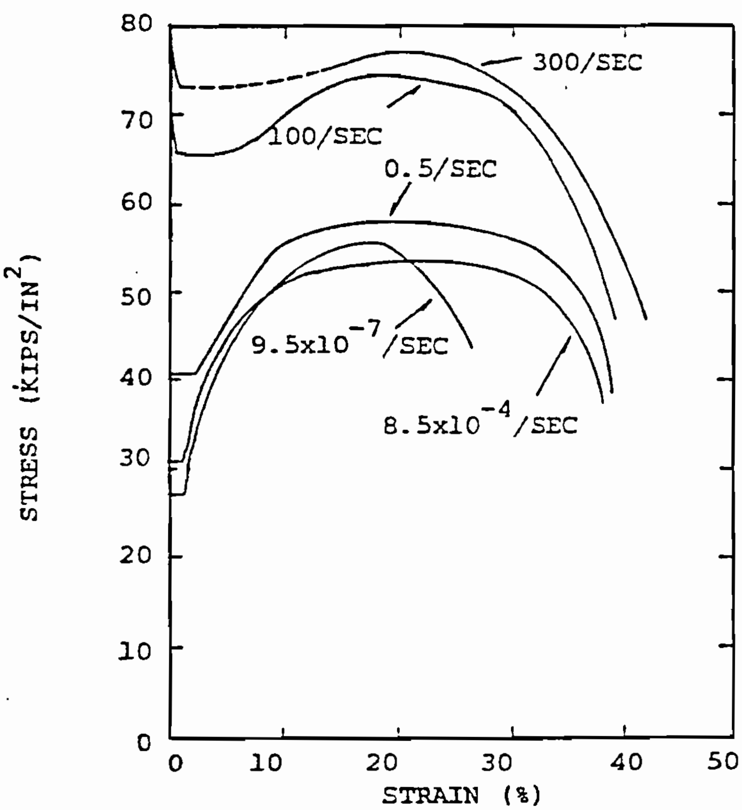

FIG. 13 STRESS-STRAIN CURVES OF MILD STEEL AT ROOM TEMPERATURE FOR VARIOUS RATES OF STRAIN

The scaling laws required for the simulation of full scale behavior as presented above evolve a contradictory point. In the simplification process of matching π-parameters for the model and the full scale, the material properties of both tank heads are assumed to be the same. But the scaling law for strain rate of Eq. (3), $\dot{\varepsilon}m = S\dot{\varepsilon}f$, which was derived based on the same material property assumption, calls for different stress-strain curves for the model and prototype. In other words, eq. (3) asks for different yield stress (σy) and material secant modulus (Es) for the model and prototype. As a result, the requirement from strain rate effect clearly contradicts with the earlier same material property assumption.

Based on this finding, the scaling laws listed above are, from very vigorous viewpoint, not quite valid. The degree of validity certainly depends on the magnitude of error induced by strain rate effect. The magnitude of error. which certainly is also related to the property of material employed, can be reduced by adopting a smaller s value.

To illustrate the effect of strain rate on the validity of scaling laws adopted in this study, mild steel, the material property of which is well known (Refs. 11 and 12), is selected for demonstration. Two figures showing the effect of strain rate for mild steel reproduced from Ref. 11. Fig. 12 displays the variations of ultimate stress, yield stress, and total elongation with increasing strain rate. Fig. 13, on the other hand, shows a series of stress-strain curves for various rates of strain.

It can be seen from Fig. 12 that above a strain rate of 10^{-3}/sec, the total elongation almost stays constant, while the ultimate stress increases with increased strain rate. The rate of increase is about 10% per decade for strain rates between 1/sec. and 10^{3}/sec. These observations along with the estimation of the area between two successive stress-strain curves in Fig. 13 lead to the conclusion that an increase of one decade in strain rate can correspond to an increase of about 10% in the strain energy at failure. According to this argument, the strain rate scaling law, $\dot{\varepsilon}m = S\dot{\varepsilon}f$, demands that the strain energy in a model is proportionately larger than that of a full scale tank car.

Now, we are ready to illustrate the effect of strain rate for mild steel on, for example, the velocity scaling. From the matching condition of $\pi 6$ parameter,

$$\frac{m_m V_m^2 E_{sm}}{\sigma_{ym}^2 d_m^3} = \frac{m_f V_f^2 E_{sf}}{\sigma_{yf}^2 d_f^3}$$

After applying Eqs. (1) and (2), this expression is reduced to

$$\frac{V_m^2}{V_f^2} = \frac{\sigma_{ym}^2/E_{sm}}{\sigma_{yf}^2/E_{sf}}$$

The right hand side of this equation represents the ratio of strain energy of the model to that of the full scale. If S = 10, the above expression may yield V_m/V_f = 1.1 at point of failure; or V_m/V_f = 1.05, which may be translated as threshold puncture velocity for the model is about 5% higher than that for the prototype. This is in a direct contradiction to $V_m/V_f = 1$ of Eq. (6).

When the scaling is applied to the 1/5 and 1/10 scale models, a scaling factor of 2 will yield V_m/V_f = 1.01. With a difference of only 1% in the threshold puncture velocities between these two models, the strain rate effect can be neglected.

It may be concluded that the accuracy of the scaling laws adopted in this study depends on the error introduced by strain rate effect. the error involved is related to the magnitude of scale factor and the property of material used. The smaller the scaling factor and the less sensitive the material to the variation of the strain rate, the better the accuracy of the scaling laws adopted.

4.3.2 Results of 1/5 Scale Drop Weight Tests

A total of eight 1/5 scale tank heads, all with sand bases, were tested in the drop weight setup, three with bare head, two with stainless steel plates of 24 gage, and three with TecsPak of 1/4 inches. It is noted that mitigating material used in this case was comprised of two pieces of 1/4 inch TecsPak. and that the steel head shield used consists of two pieces of 24 gage steel plates.

Tests results of these models are tabulated in Table IV. For better comparison, these results are also displayed in curves relating kinetic energy vs. dent depth in Fig. 14. The estimated threshold puncture energies are about 5,996. 11,579, 10,421 ft-lbs for the models with bare head, steel head shield, and TecsPak, respectively.

4.3.3 Comparison of 1/5 and 1/10 Scale Model Test Results

The threshold puncture velocities and threshold puncture energies for three different cases of the 1/5 scale models as shown in Fig. 14 together with those of the 1/10 scale models are listed in Table V for the purpose of comparison. It can be seen from this table that, in each case of head protection schemes, the threshold puncture velocity for 1/5 scale is higher

Table IV 1/5 Scale Model Tank Head Drop Weight Tests* (with sand base)

Model No.	Test** Condition	Drop Height, in.	Drop Weight, lbs.	Impact Speed, ft/sec.	Kinetic Energy, ft-lbs.	Max. Acceleration G's	Max. Impact Force, lbs.	Depth of Dent, in.	Note***
BS-1A	A	30.5	1,985	12.79	5,045	18.64	37,000	4-1/2	D,3AL
BS-2A	A	35	1,985	13.71	5,790	22.81	45,278	4-1/2	D,3AL
BS-3A	A	37.5	1,985	14.19	6,203	19.38	38,469	5	P,3AL
SS-1A	B	67	1,985	18.96	11,083	32.87	65,246	5-3/8	D,3AL
SS-2A	B	73	1,985	19.79	12,075	26.74	53,079	5-5/8	P,3AL
MS-1A	C	63	1,985	18.39	10,421	31.65	62,825	5	TP,2AL
MS-2A	C	67	1,985	18.96	11,083	31.40	62,329	6-1/4	P,4AL
MS-3A	C	73	1,985	19.79	12,075	29.44	58,438	7	P,3AL

* Threshold puncture energies for cases of conditions A, B, and C are estimated at 5,996, 11,579, and 10,421 ft-lbs., respectively.

** A - Bare head, B - 2x24 gage steel plate head shield, C - 2x1/4" TecsPak plate.

*** D - Dent, P - Puncture, TP - Threshold puncture, AL - Antinodal lines in head deformation pattern.

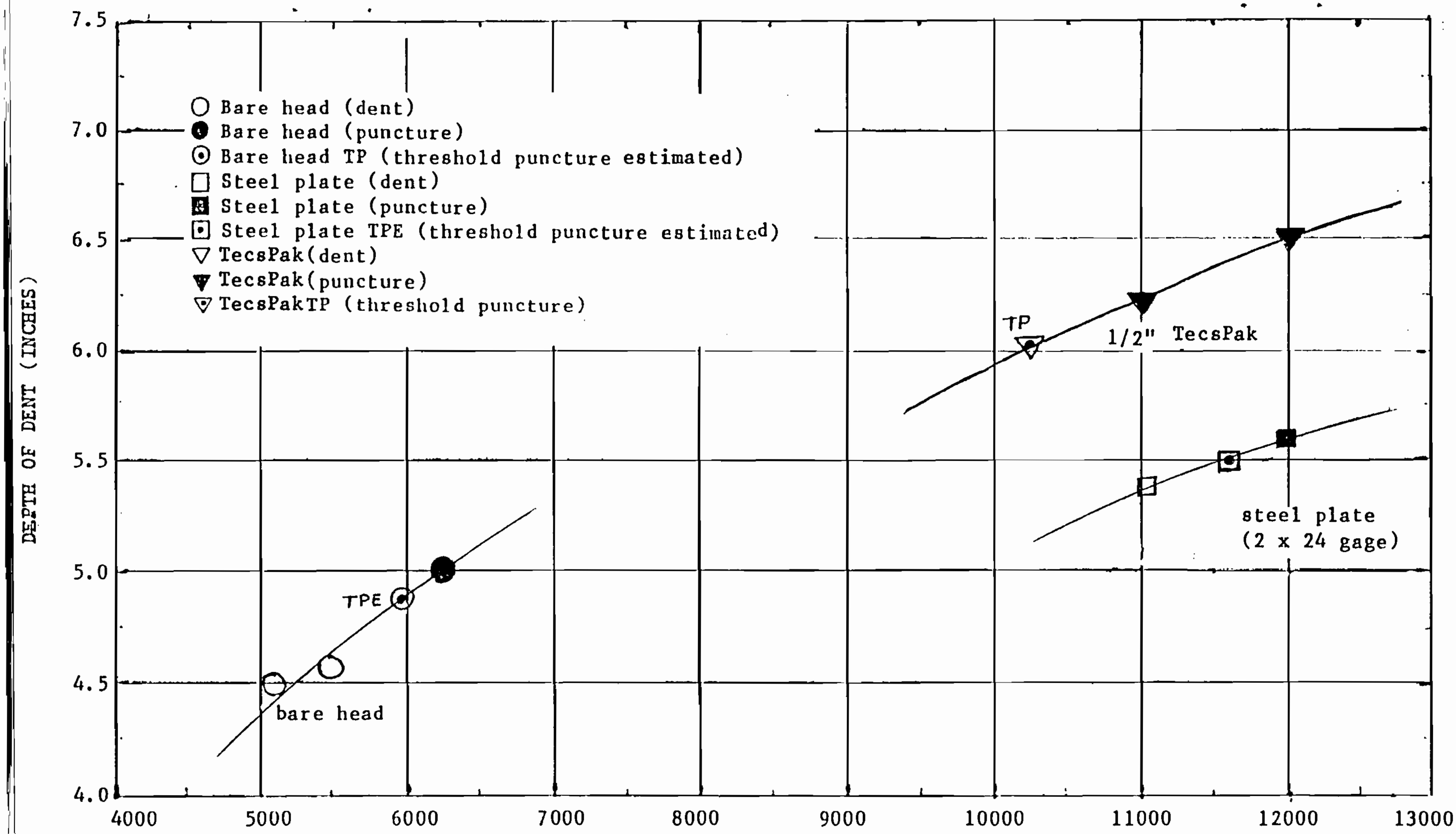

Figure 14 Kinetic Energy vs. Dent Depth For 1/5 Scale Model Drop Weight Impact Tests (with Sand Base)

Table V Comparison of Threshold Puncture Velocities and Energies for 1/5 and 1/10 Scale Model Tank Heads in Drop Weight Tests (with sand base)

	Threshold Puncture Velocity (ft/sec)			Threshold Puncture Energy (ft-lbs.)		
	1/5 scale	1/10 scale	1/5 scale is higher than 1/10 scale by (%)	1/5 scale	1/10 scale*	1/5 scale is higher than 1/10 scale by (%)
bare	13.95	12.79	9.07	5,996	628 X 8 = 5,024	19.35
steel	19.36	17.94	7.92	11,579	1,235 x 8 = 9,880	17.20
Tecspak	18.39	18.09	1.66	10,421	1,256 X 8 = 10.048	3.71

* Threshold puncture energies for 1/10 scale models are shown here as original threshold puncture value x S^3 (S = 2, a scale factor between 1/5 and 1/10) for comparison purposes.

than that of 1/10 scale, with the difference ranging from 1.66% to 9.07%. The same situations also hold when comparison is made on the threshold puncture energies, with a higher degree of difference which ranges from 3.71% to 19.35%.

According to the scaling law adopted in the study, the threshold puncture velocity (Eq. (6)) should be the same for both 1/5 and 1/10 scales. If the effect of strain rate is taken into account, then the previous argument indicates that an error of only 1% in the threshold puncture velocity was involved, and hence the strain rate effect, in this case, can be neglected.

Therefore, the difference in the threshold puncture velocities of less than 10% between these two different scale models may be attributed to the various errors involved in the tests such as inaccurate scaling in the thickness of the model tank heads and mitigating materials, imperfections of the model tank heads, inaccuracy in measurements, etc.

It may be concluded from the test results obtained that good accuracy of the scaling laws is obtained for the models considered in this study. The smaller the scaling factor and the less sensitive the material to the variation of the strain rate, the better the accuracy of the scaling laws adopted.

4.4 Effect of Lading

The effect of lading on the threshold puncture energy of the 1/10 scale tank heads has been examined in great detail in Subsection 4.1 through a series of drop weight tests. To simulate the lading effect, both water and sand were used to back up the model tank heads. Results indicate that, when compared with empty heads, both have about the same effect on reducing model head threshold puncture energies.

Curves relating kinetic energy vs. dent depth for empty tank heads and heads backed up with sand are displayed in Figs. 9A, 9B and 9C for various head protection conditions. From these figures, threshold puncture energies associated with model heads of empty base and sand base for various head protection conditions were obtained and summarized in Table II for the purpose of comparison. Results in Table II show that the energy absorbed by model heads backed up with sand is less than that absorbed by empty heads. This, in turn, indicates that a model tank head backed up with sand is more susceptible to puncture than empty ones.

The effect of lading is reexamined in this section with pendulum impacted tests. Detailed procedure of the test is described in Subsection 3.5.2; a photograph showing testing setup with the pendulum arm lifted up to the desired height is given in Fig. 7.

Four model tank heads of the 1/5 scale, attached on the tank car of the same scale, were impacted with the pendulum. The test results of these models are listed in Table VI. It is noted that all four tests were performed on the model heads with no protection head shields and with the same weight of 1,900 lbs at the coupler. Two models, one empty and one filled with water up to 10% outage, were impacted by the pendulum at a height of 55 inches; no puncture was found in either case.

Table VI 1/5 Scale Model Tank Head Pendulum Impact Tests (with bare head)

Model No.	Test* Condition	Drop Height, in.	Drop Weight, lbs.	Impact Speed, ft/sec.	Kinetic Energy, ft-lbs.	Max. Acceleration G's	Max. Impact Force, lbs.	Depth of Dent, in.	Note**
BE-1A	A	55	1,900	17.18	8,708	7.36	13,984	4-1/8	D,3AL
BE-2A	A	61	1,900	18.09	9,658	***	***	4-1/4	D,4AL
BW-1A	B	55	1,900	17.18	8,708	8.59	16,321	4	D,3AL
BW-2A	B	61	1,900	18.09	9,658	***	***	3-1/4	P,4AL

* A - Empty base, B - Water base
** D - Dent, P - Puncture, TP - Threshold puncture, AL - Antinodal lines in head deformation pattern.
*** Some of the missing data occurred in situations when severe puncture or measuring difficulties were encountered.

The remaining two models, also one empty and one backed up with water up to 10% outage, were impacted by the pendulum head at a height of 61 inches. Test results showed that puncture occurred only for the model backed up with water. Therefore, the pendulum tests conducted here yield the same conclusion regarding the lading effect on tank head puncture phenomenon as that previously obtained from the drop weight tests in Subsection 4.1

5. CONCLUSIONS

1. No substantial difference between stainless steel plates and TecsPak proposed in this study is found in protecting the model tank heads against puncture damage. This may be, in part, attributed to a smaller size of TecsPak used in the tests than that of steel head shields.

2. Both TecsPak and stainless steel plates provide good protection against head puncture when compared with bare tank heads.

3. Both TecsPak and stainless steel head shields have the capability of spreading impact load to a larger tank area, and thereby reducing load intensity. More significantly, both also are capable of blunting the striking edge of the impacting object.

4. Effect of low temperature on vulnerability of the stainless steel model tank heads used is negligible.

5. The test results obtained show only a difference of less than 10% in the threshold puncture velocities between the 1/5 and 1/10 scale model tank head. This may be attributed to various errors introduced in the tests. Therefore, it is concluded that good accuracy of scaling laws is obtained for the models considered in this study.

6. For mild steel, an increase of one decade in strain rate can correspond to an increase of about 10% in strain energy at failure. For the 1/5 and 1/10 scale models, a scaling factor of 2 can create a difference of only about 2% in strain energy between these two models. Hence, strain effect on the accuracy of the scaling laws adopted, when applied to 1/5 and 1/10 scale models, is of minor importance.

7. An empty model tank head is susceptible to deeper dents than one backed up with water or sand.

8. An empty tank head is less susceptible to puncture than one backed up with water or sand.

9. Lading has the effect of increasing vulnerability to puncture for tank heads.

10. No significant difference between water and sand is found in terms of protecting model tank heads against puncture.

6. RECOMMENDATIONS

1. A theoretical analysis including geometric and material nonlinearities should be performed for tank heads under axisymmetric impact loading. It may be assumed that the tank head deforms axisymmetrically until a critical impact is reached. At this impact, bifurcation of the solution occurs: an axisymmetric branch of solution, which in general represents unstable states of configuration beyond the point of bifurcation, and a nonsymmetric branch of solutions representing adjacent stable states of configuration. Nonsymmetric branches of solutions are introduced by assuming a number of wavy deformation patterns along circumferential direction. Mathematically, this leads to an eigenvalue problem.

2. Research is recommended on how to apply the scaling laws to extrapolate the model tank head test results to the prototype cases in an impact situation, when the effect of strain rate is taken into consideration. In this connection, a preliminary test program is suggested in order to evaluate the sensitivity of the threshold puncture energy to strain rate and specimen dimensions.

3. A study is also recommended on the effect of initial imperfections in increasing the vulnerability of tank heads in an impact situation.

7. REFERENCES

1. Peters, D.A., B.A. Szabo and W.B. Diboll, "Tank Car Head Puncture Mechanisms," Washington University, St. Louis, Missouri, FRA-OR & D-76-269, April 1980.

2. Orringer, O. and P. Tong, "Results and Analysis of the Switchyard Impact Tests," DOT Transportation Systems Center, FRA-OR & D-80-6, January 1980.

3. Philips, E. and L. Olson, "Final Phase 05 Report on Tank Car Head Study," RPI-AAR Tank Car Safety Research Project, RA-05-1-17, July 14, 1972.

4. Shang, J.C. and J.E. Everett, "Impact Vulnerability of Tank Car Head," The Shock and Vibration Bulletin, No. 42, Part 1, Naval Research Laboratory, January 1972, pp. 197-210.

5. Gorman, J.J., "Applicability of Scale Model Testing to Rail Tank Car Head Impact Phenomena," Aeroelastic and Structures Research Laboratory, MIT, Interim Report for Contract DOT/TSC-1143, December 1976.

6. Baker, W.E., et al., Similarity Methods in Engineering Dynamics, Hyaden Book Co., Inc., Rochelle Park, New Jersey, 1971.

7. Langhaar, H.L., Dimensional Analysis and Theory of Methods, John Wiley and Son, Inc., 1951.

8. Murphy, G., Similitude in Engineering, Press Co., New York, 1950.

9. Goodier, J.N. and Thomson, W.T., "Applicability of Similarity Principles to Structural Models," NACA TN-933, July 1944.

10. Haerta, M., "Analysis; Scale Modeling, and Full Scale Tests of a Truck Spent-Nuclear-Fuel Shipping System in High Velocity Impacts Against a Rigid Barrier," Report no. SAND77-0270, Sandia Laboratories, Albuquerque, New Mexico, April 1978.

11. Monjoine, M.J., "Influence of Rate of Strain and Temperature on Yield Stresses of Mild Steel," Transaction of the ASME, Journal of Applied Mechanics, Vol. 66, December 1944, pp. A-211 - A-218.

12. Baron, H.C., "Stress-Strain Curves of Some Metal and Alloys at Low Temperatures and High Rates of Strain," Journal of the Iron and Steel Institute, Vol. 182, April 1956.

Appendix A

Tank Head Specimen Preparation

a. Drop Test Specimen Preparation

1. Prepare the tank head model with strain gages, thermocouples, etc., as needed.
2. Locate and mark the tank head surface center.
3. Place and fasten the tank car head model on its head holder.
4. Fill up the holder with a clean dry sand from the opposite side and then secure it with a flat wooden plate specially made for this purpose.
5. Place the holder with the head model head up, on the drop tower base, adjust its position such that the coupler points to the center of the head, and fasten the holder to its support.
6. In the test whenever the head shield and/or a mitigating material are used they can be placed directly on the head surface and secured with tape.
7. For tests that require low temperature specimens, some coolant, such as liquid nitrogen, should be applied on the head surface until the temperature goes down to the required degree, and thermocouple system can be used to monitor the temperature.

b. Pendulum Test Specimen Preparation

1. Prepare the tank head model with strain gages, thermocouples, etc., as needed.
2. Locate and mark the tank head surface center.
3. Place and fasten the tank car head model on its head holder.
4. Place the head-holder unit on the tank car model, adjust and fasten it.
5. For tests that require the tank to be filled with water, a rubber gasket and special sealer can be used to prevent water leaks.
6. Adjust the tank car and the pendulum positions such that the coupler points to the center of the tank car head model by adjusting pendulum arm length and/or the tank body position.

Appendix B

Weight Preparation

a. Drop Weight

Before the drop weight can be prepared, the separation of the guide cables should be adjusted so that the test specimen with its holder can be installed and fixed at the tower base (see Figure B1).

1. Place the drop weight shaft vertically on the base with the flanged end down (see Figure B2).
2. Place the assembled bottom guide plate on the shaft with the guide arms on the bottom side (see Figure B3).
3. Hoist the weight shaft above the ground and place the wright stand underneath the bottom guide plate (see Figure B4).
4. Adjust the length of the guide arms to fit the guide cables and install guide bushings and guide arm ends in place to provide sliding bearing on each side (see Figure B3).
5. Mount the coupler to the shaft flange from below and fasten it with bolts (see Figure B4).
6. Lower the assembly on the stand and unhook the shaft.
7. Add weight plates as needed (big or small plates) (see Figure B4).
8. Add the assembled upper guide plate and the clamp and tighten it (see Figure B4).
9. Adjust the length of the upper guide arms to fit the guide cables and install guide bushings and guide arm ends on each side.
10. Insert the threaded bars in position through the steel plates and tighten the plates together with nuts and lock washers (see Figure B4).

b. Pendulum Head Preparation

Depending on the total number of the weight plates needed for the test, one can divide it into two groups to make a weight balance on both sides of the pendulum head.

1. Place the weight plates (two groups) vertically on the pendulum tower base and place the pendulum head sleeve between the two weight groups (see Figure B5).
2. Insert the weight shaft horizontally through the central holes of the weight plates and the sleeve, such that the shaft flange will be toward the tank car and the tank head (see Figure B6).
3. Fasten the coupler onto the shaft flange and place the small plates, the rear plates, and the clamp on the other side (see Figure B7).
4. Align the pendulum head-holder (upper and lower jaws) with the head sleeve and tighten them together (see Figure B7).
5. Insert the threaded bars through the weight plates, tighten them together with nuts and lock washers, and tighten the clamp (see Figure B7).

6. Jack up the pendulum head to the desired height by using a proper hydraulic jack.
7. Fix the head on the pendulum arm at this position by fastening the head holder and arm rods together with nuts an lock washers (see Figure B7).
8. To prevent the pendulum arm from twisting, align the adjustment holes in the central pipes of the pendulum arm, insert the available pins into the holes, and secure it with cotter pins (see Figure B7).

DROP TOWER

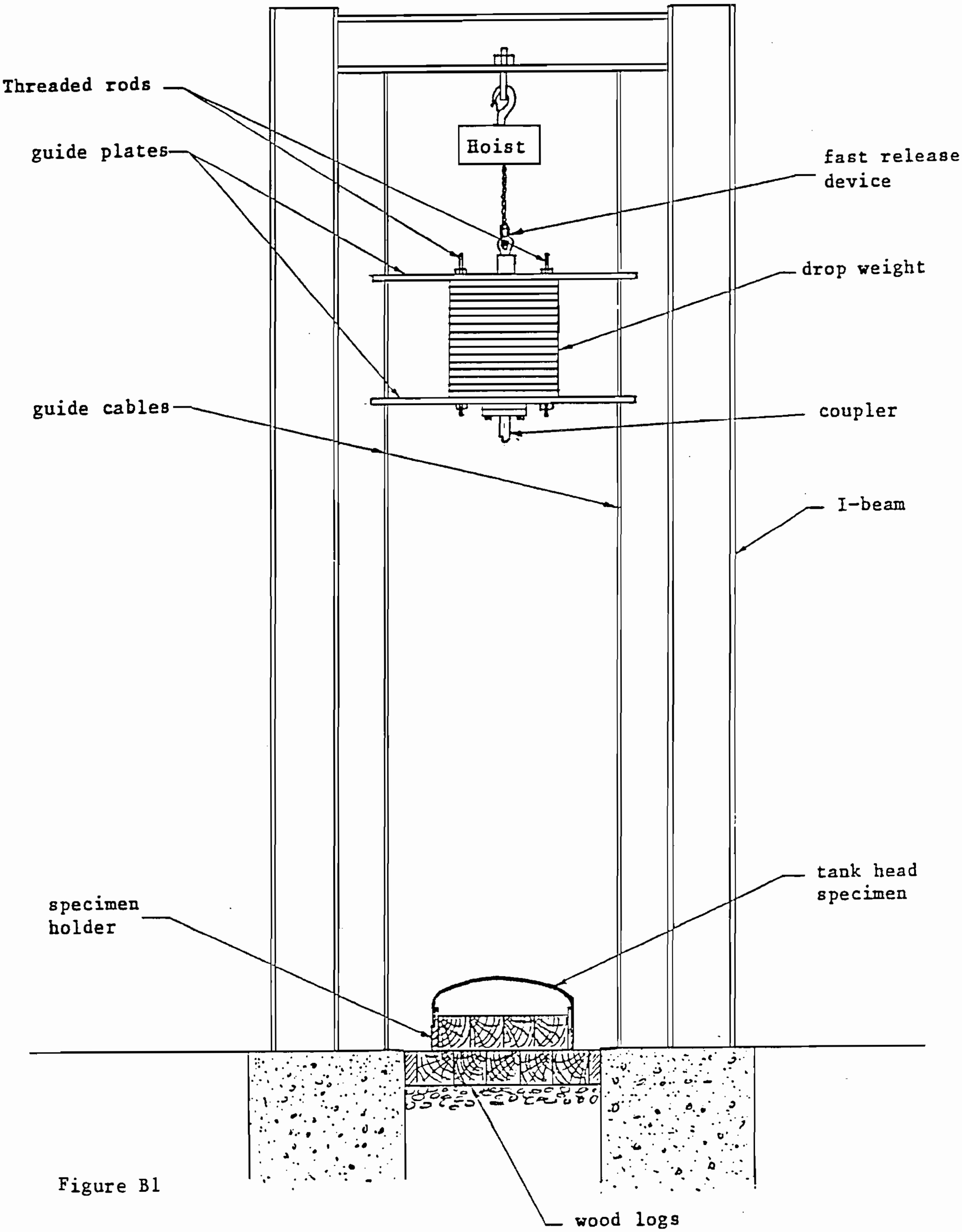

Figure B1

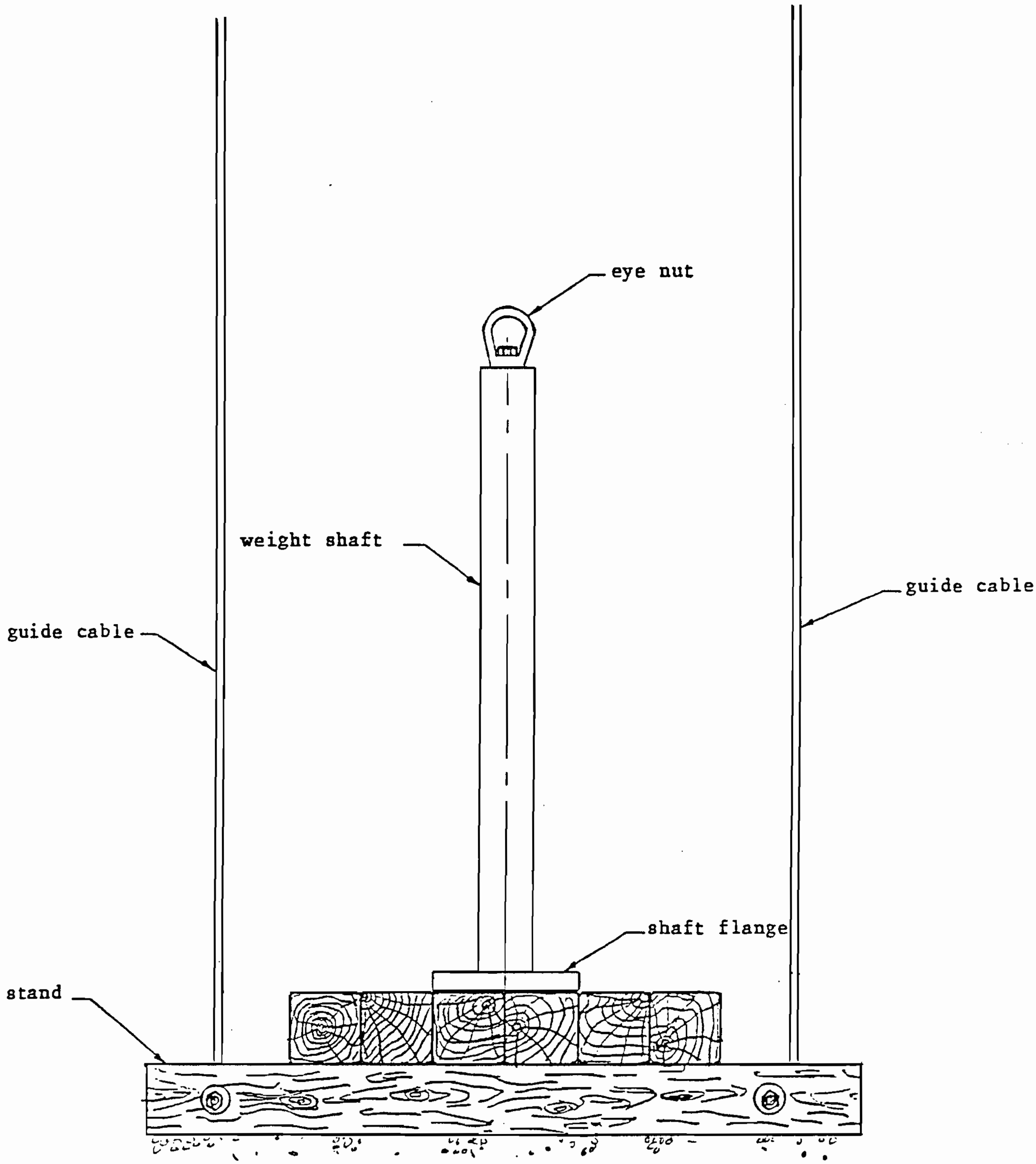
eye nut
weight shaft
guide cable
guide cable
shaft flange
stand

Figure B2

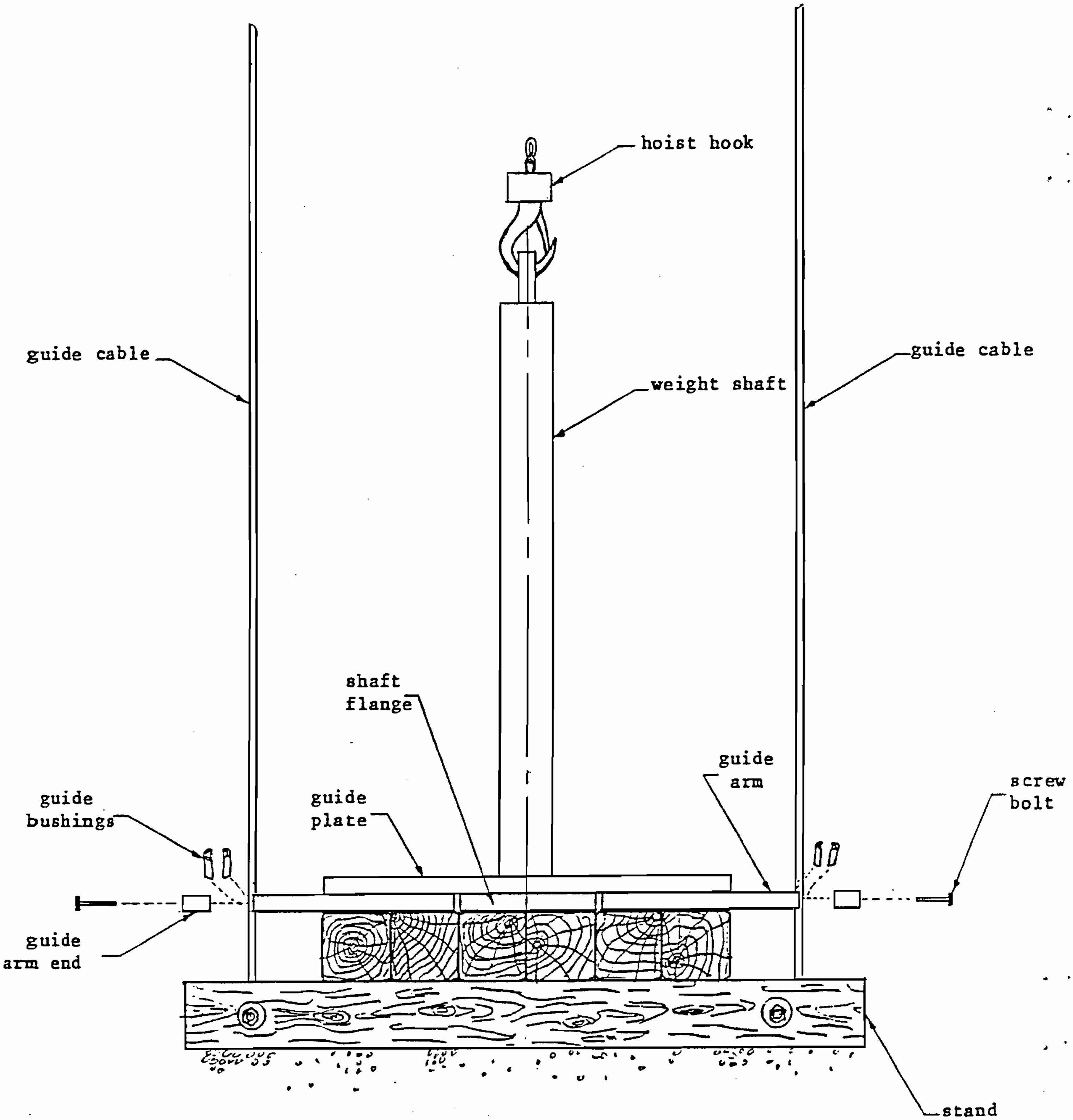
hoist hook
guide cable
guide cable
weight shaft
shaft flange
guide arm
screw bolt
guide bushings
guide plate
guide arm end
stand

Figure B3

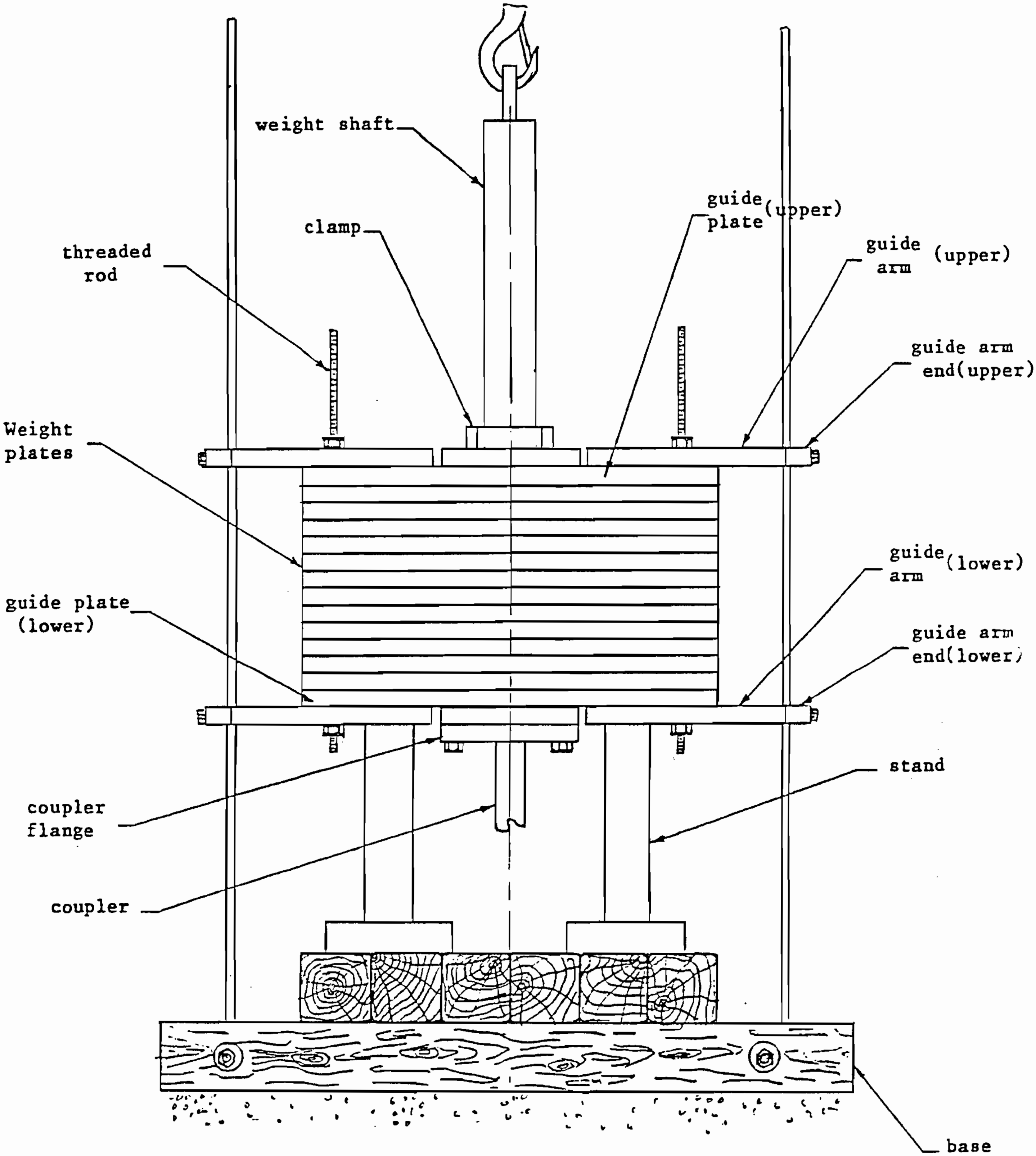
weight shaft
clamp
guide (upper)
plate
guide (upper)
arm
threaded
rod
guide arm
end(upper)
Weight
plates
guide (lower)
arm
guide plate
(lower)
guide arm
end(lower)
stand
coupler
flange
coupler
base

Figure B4

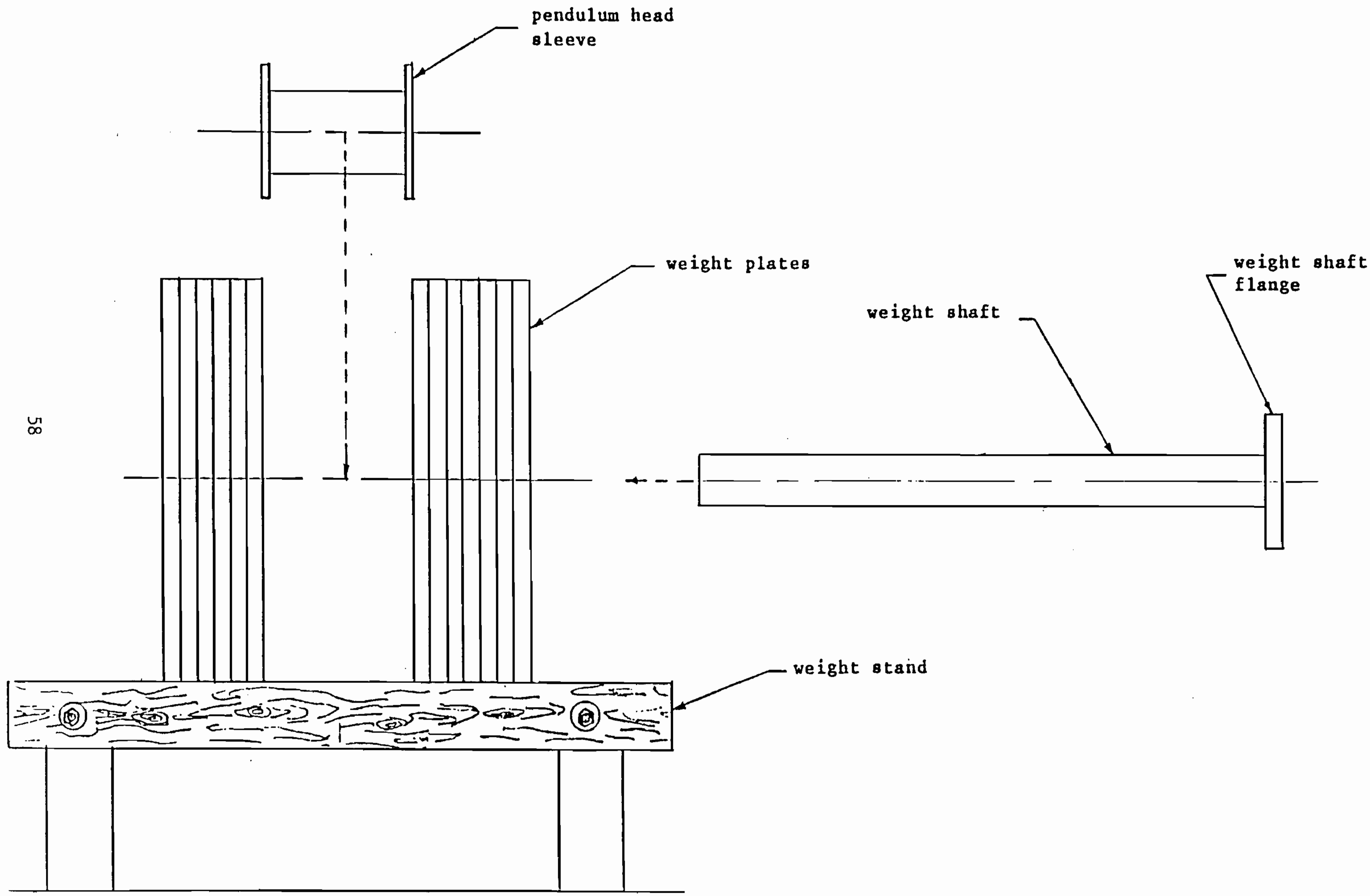
pendulum head
sleeve
weight plates
weight shaft
weight shaft
flange
weight stand

Figure B5

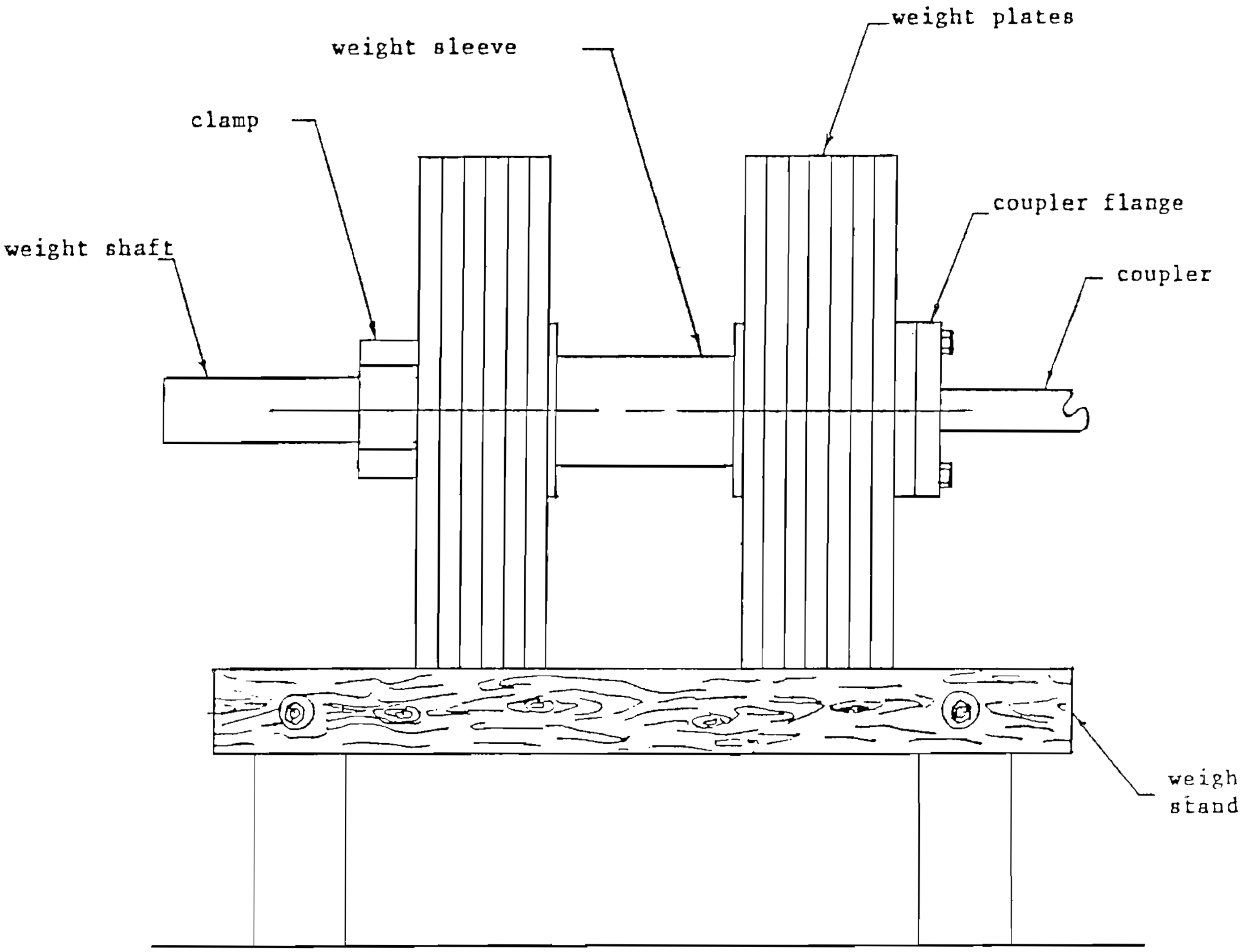
weight plates
weight sleeve
clamp
coupler flange
weight shaft
coupler
weight
stand

Figure B6

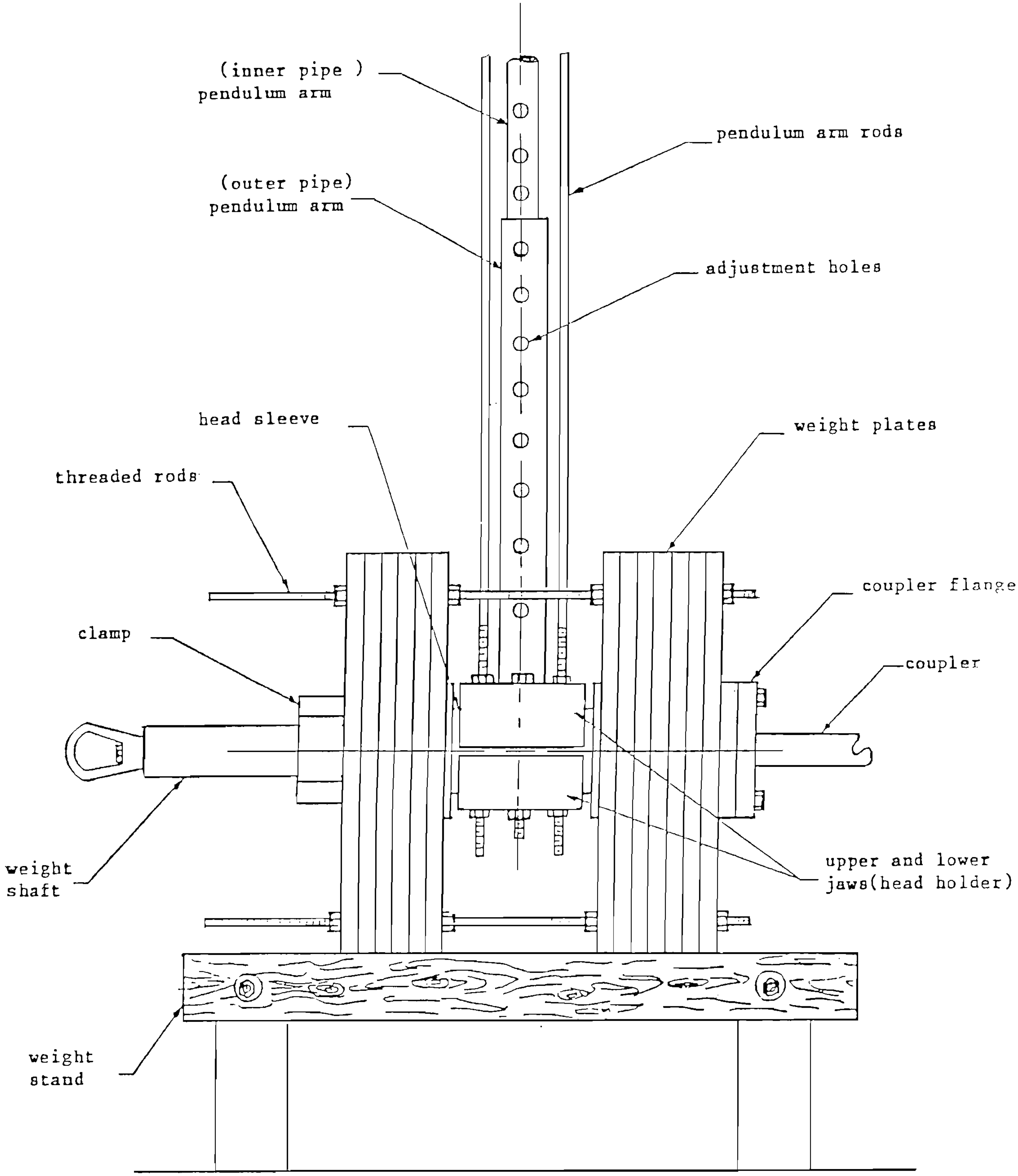
(inner pipe)
pendulum arm
pendulum arm rods
(outer pipe)
pendulum arm
adjustment holes
head sleeve
weight plates
threaded rods
coupler flange
clamp
coupler
weight
shaft
upper and lower
jaws(head holder)
weight
stand

Figure B7

APPENDIX C

Models shown in this appendix are either deformed or punctured.

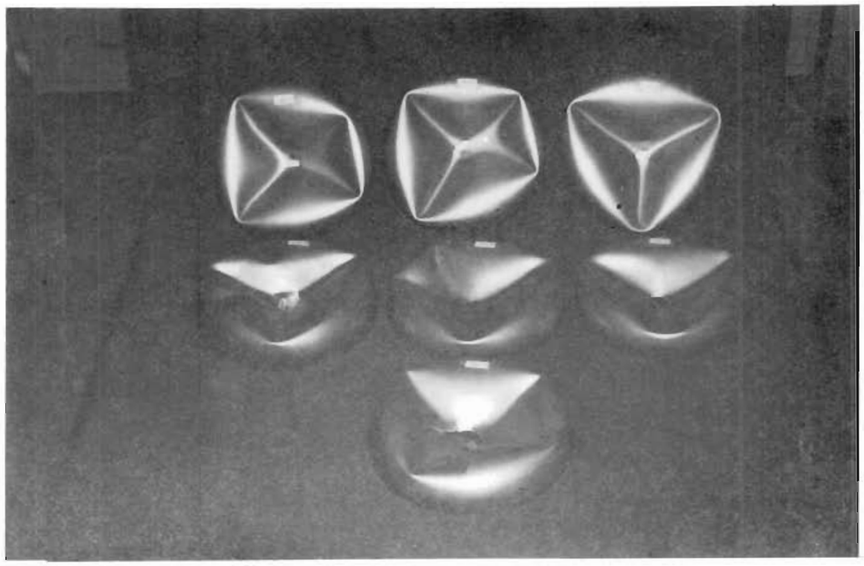

Fig. C-1a (From left to right) 1/10 Scale Test Models, BE-1 to BE-7

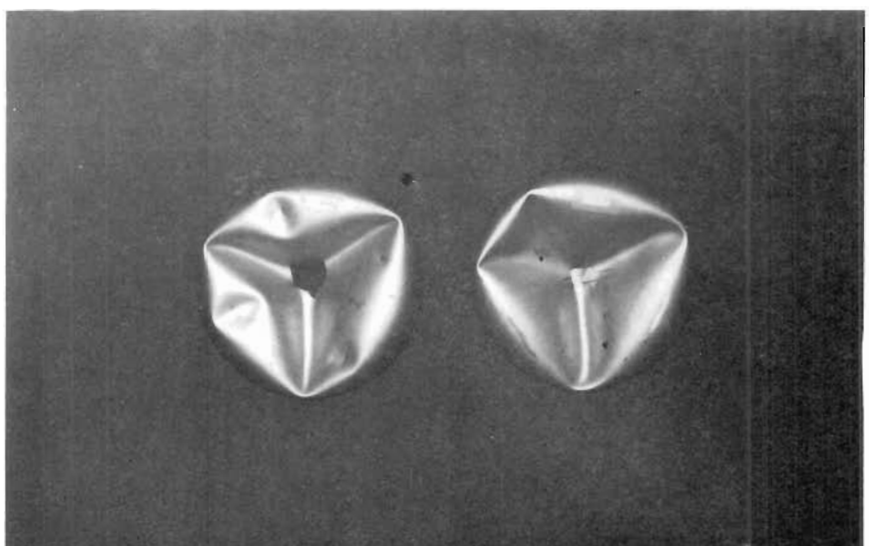

Fig. C-1b 1/10 Scale Test Models, BE-4 (L) and BE-5 (R)

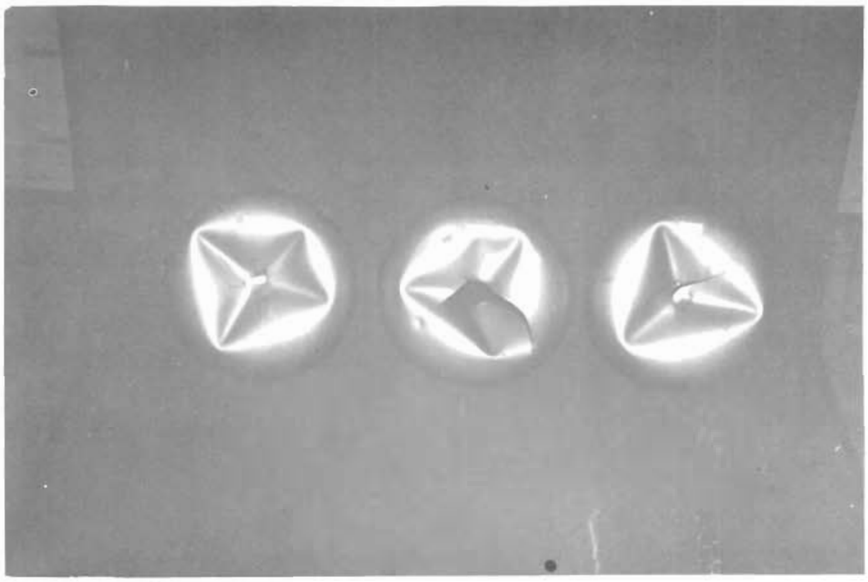

Fig. C-1c (From left to right) 1/10 Scale Test Models, BW-1, BW-2 and BW-3

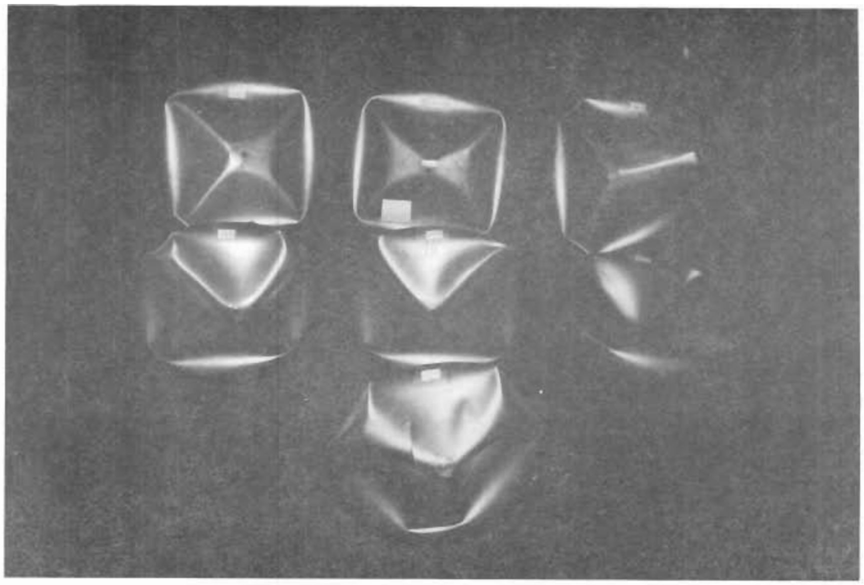

Fig. C-2a (From right to left) 1/10 Scale Test Models, SE-1 to SE-7

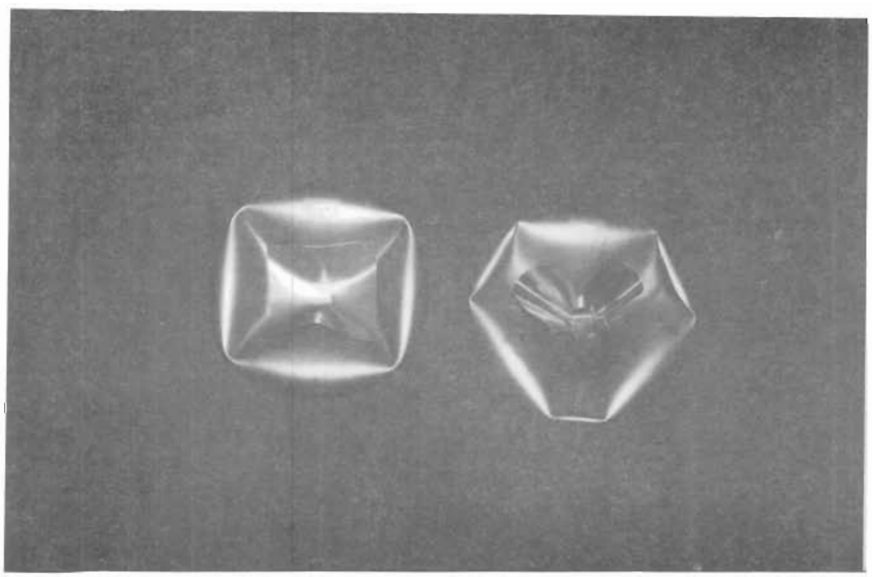

Fig. C-2b 1/10 Scale Test Models, SE-2 (L) and SE-7 (R)

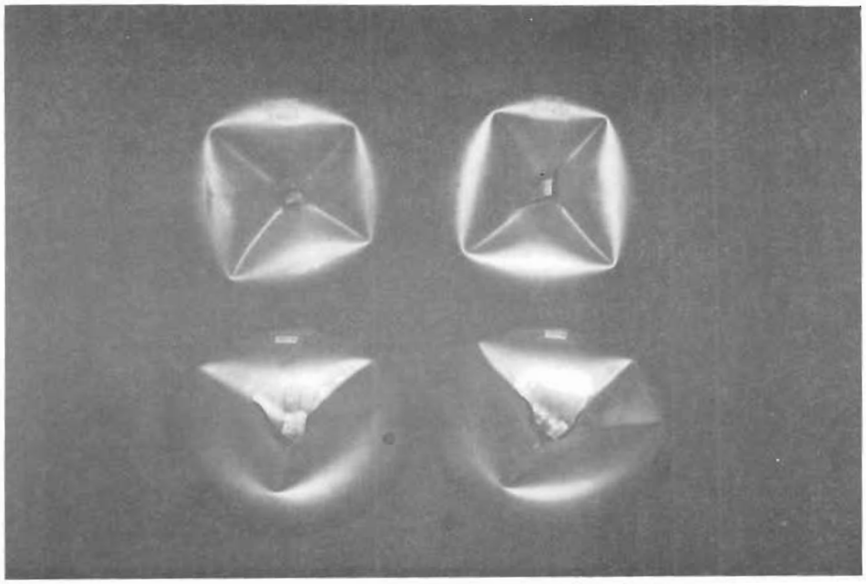

Fig. C-2c (From left to right) 1/10 Scale Test Models, SS-1 to SS-4

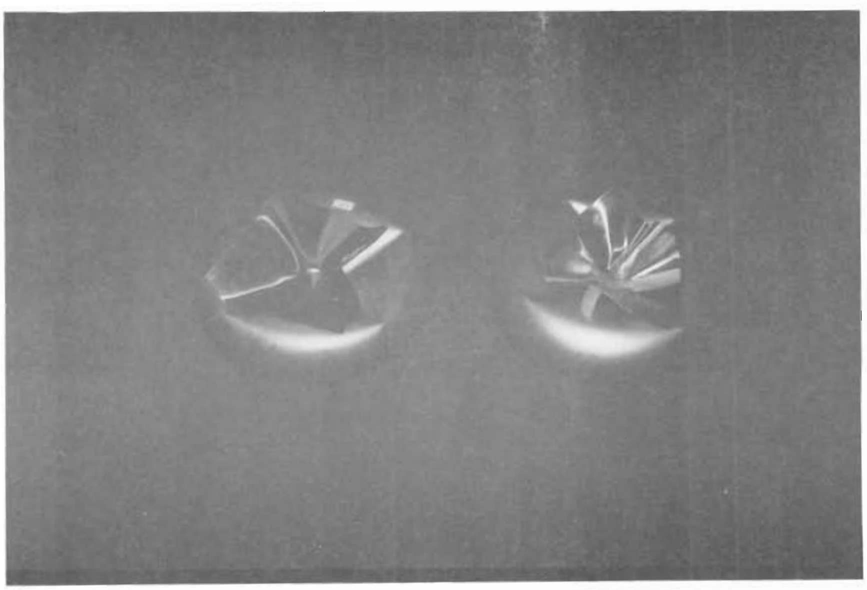

Fig. C-2d 1/10 Scale Test Models, SS-1 (L) and SS-2 (R)

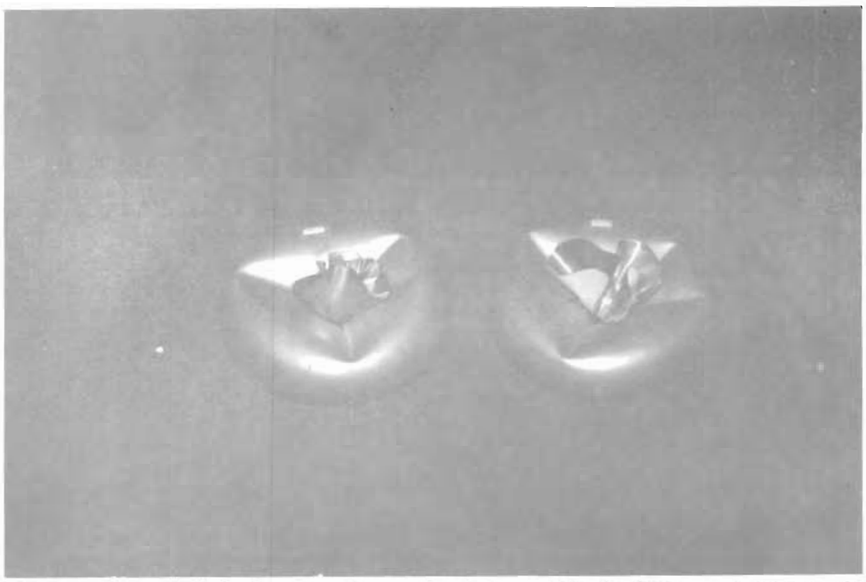

Fig. C-2e 1/10 Scale Test Models, SS-3 (L) and SS-4 (R)

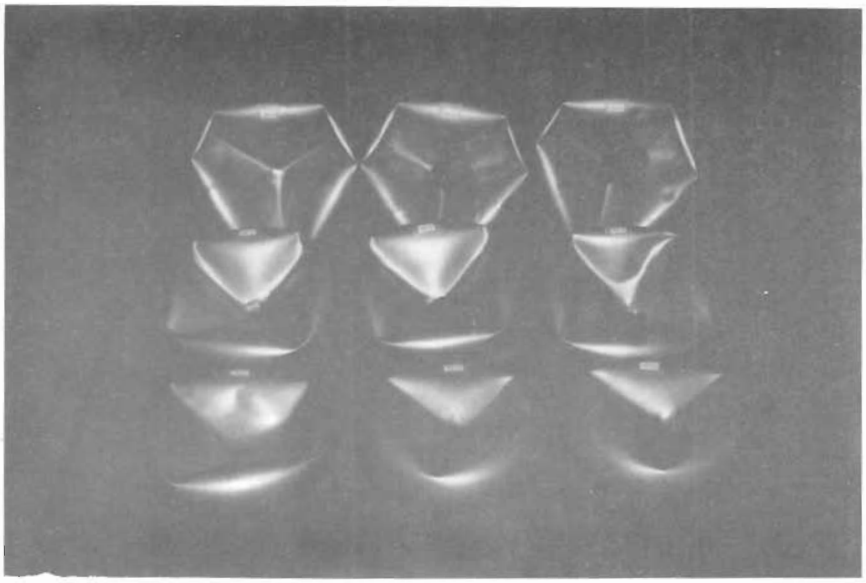

Fig. C-3a (From left to right) 1/10 Scale 1st and 2nd rows
Test Models, ME-1 to ME-6, 3rd row
Test Models, MS-1 to MS-3

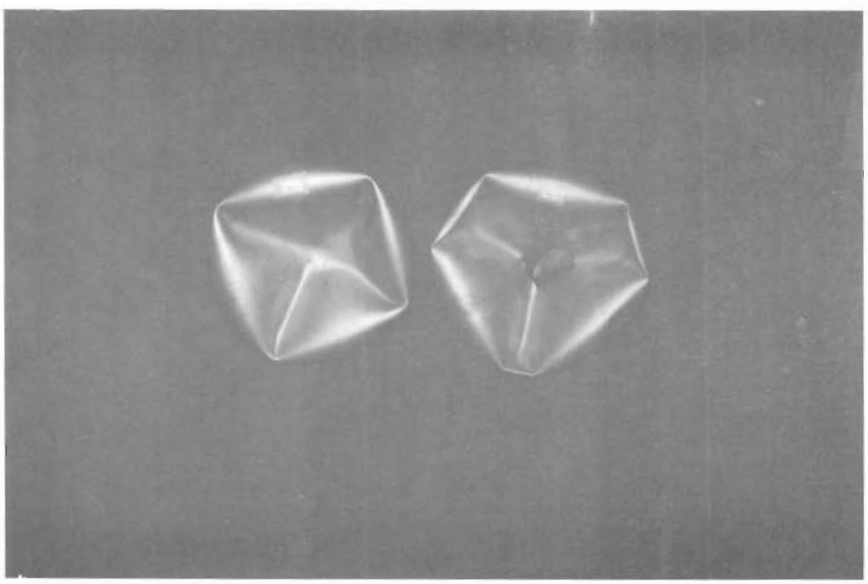

Fig. C-3b 1/10 Scale Test Model, MS-1 (L) and ME-2 (R)

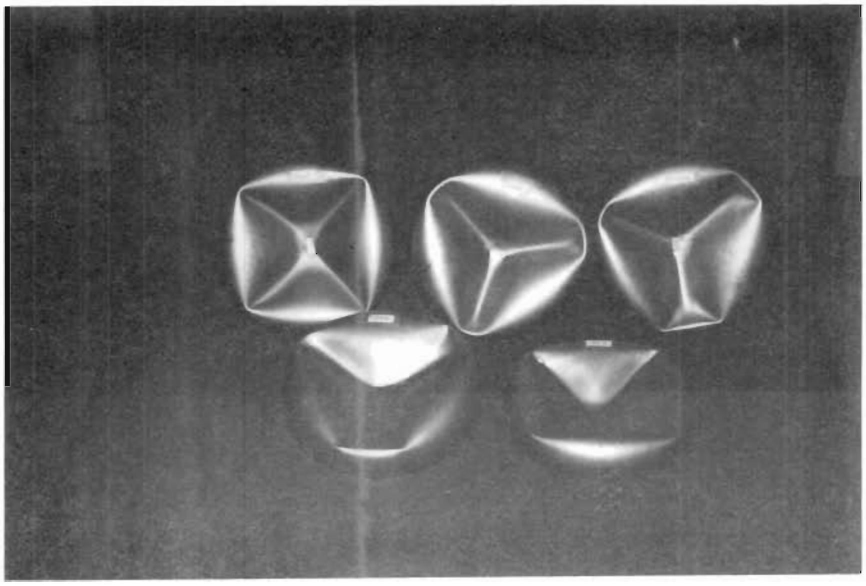

Fig. C-4a (From left to right) 1/10 Scale Test Models, LBE-1 to LBE-5

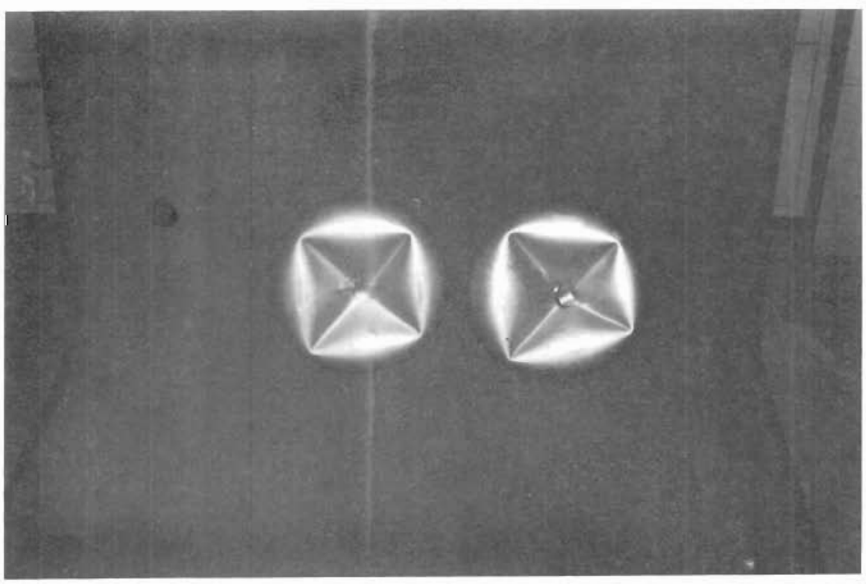

Fig. C-4b 1/10 Scale Test Model, LMS-1 (L) and LMS-2 (R)

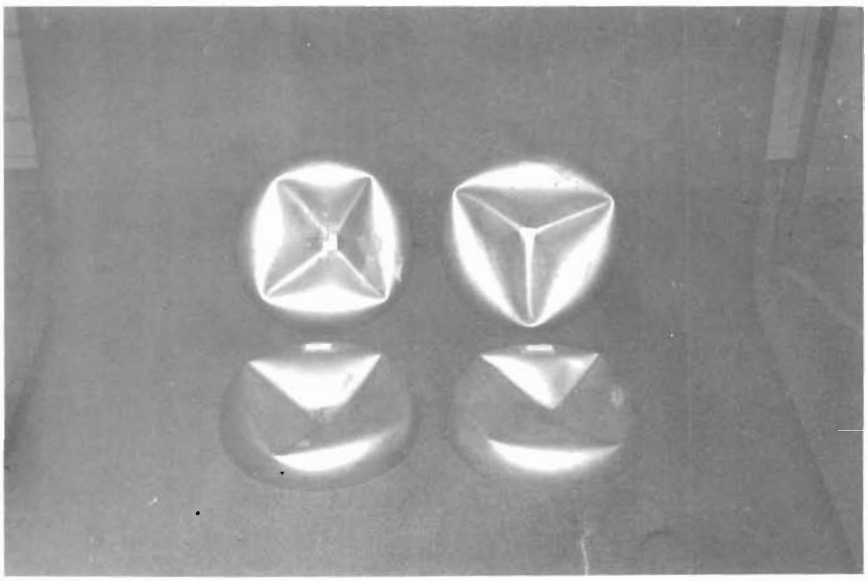

Fig. C-4c (From left to right) 1/10 Scale Test Models, LSS-1 to LSS-4

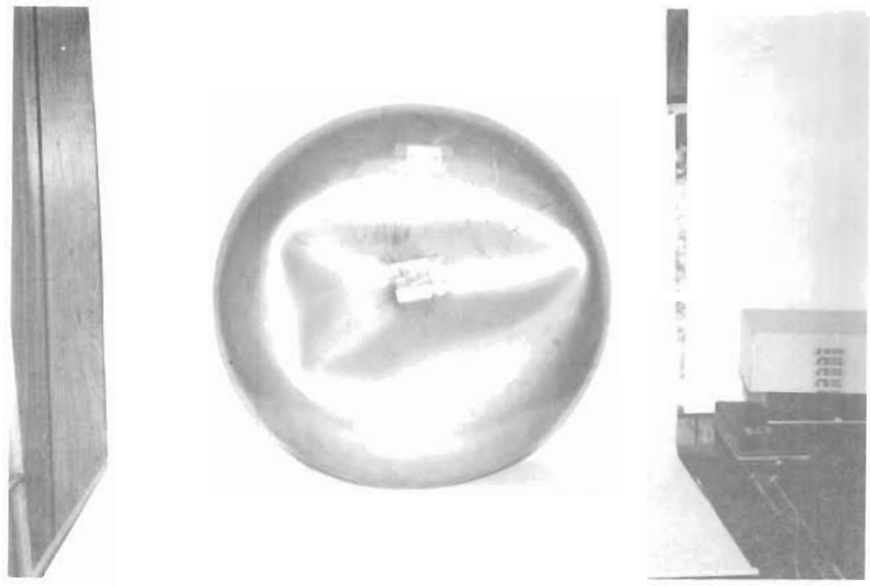

Fig. C-5a 1/5 Scale Test Model, BS-2A

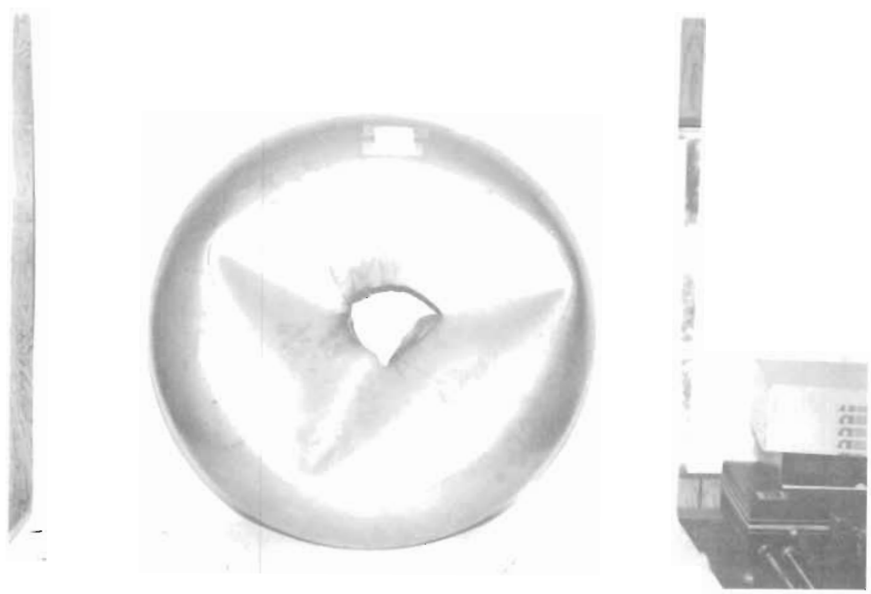

Fig. C-5b 1/5 Scale Test Model, BS-3A

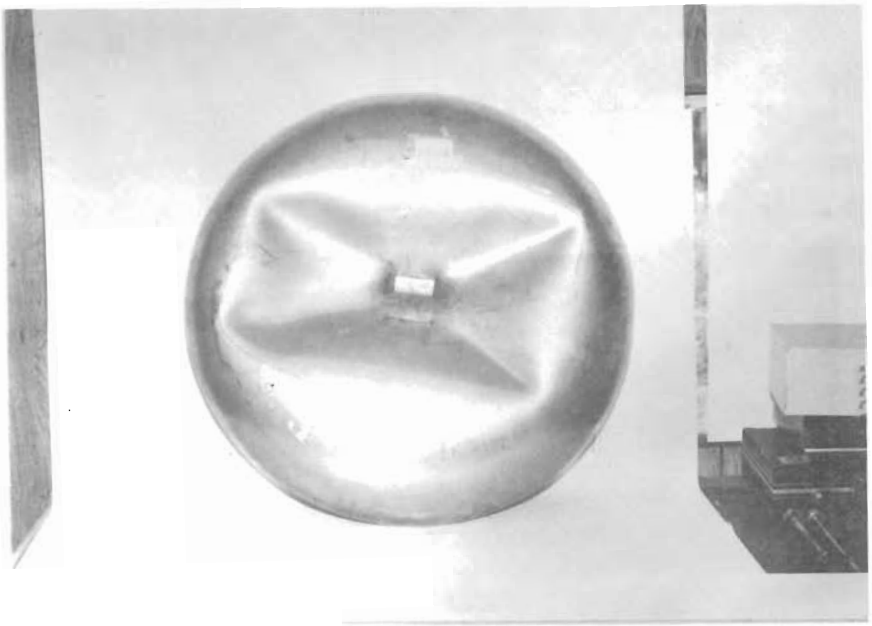

Fig. C-5c 1/5 Scale Test Model, SS-1A

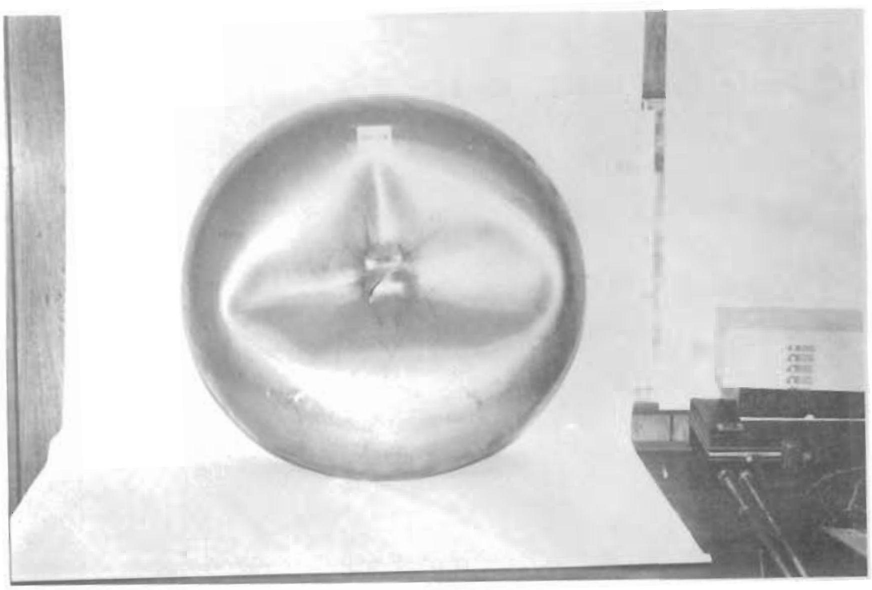

Fig. C-5d 1/5 Scale Test Model, MS-1A

Fig. C-5e 1/5 Scale Test Model, MS-3A

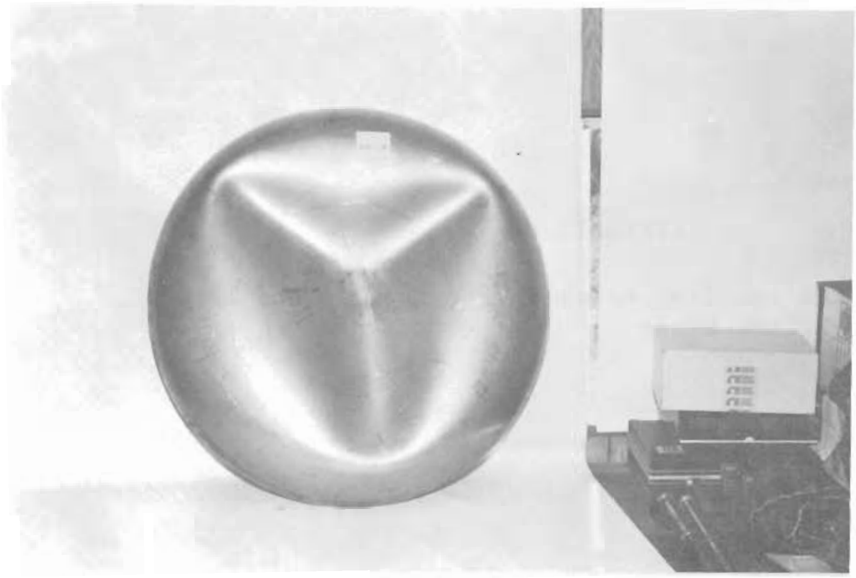

Fig. C-6a 1/5 Scale Test Model, BW-1A

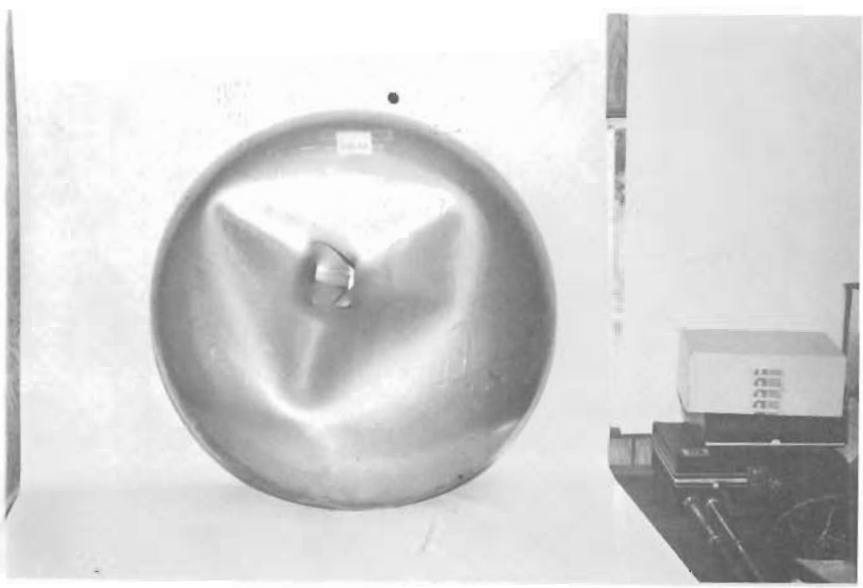

Fig. C-6b 1/5 Scale Test Model, BW-2A

APPENDIX D

Deceleration vs. Time Relation For the 1/5 and 1/10 Scale Model Tank Heads

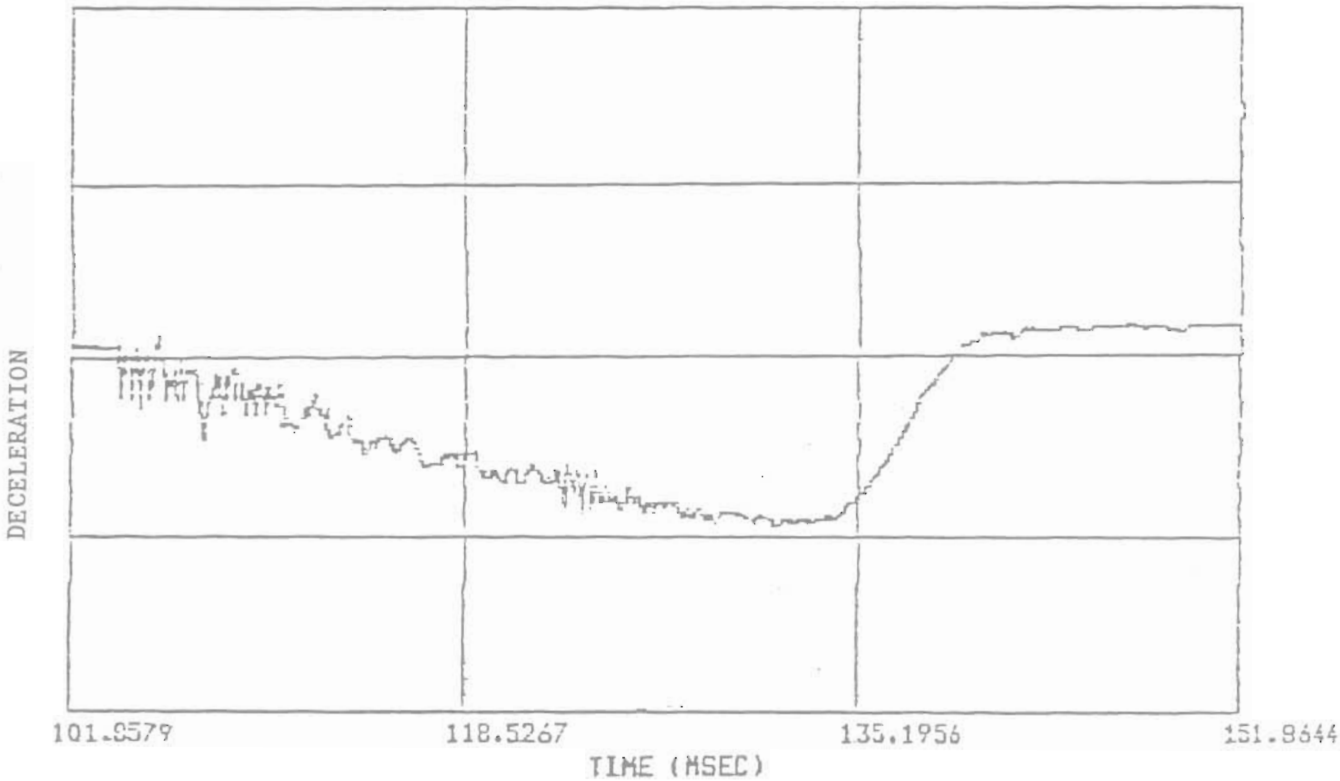

Fig. D1-a Deceleration-Time Relation For Model SE-2

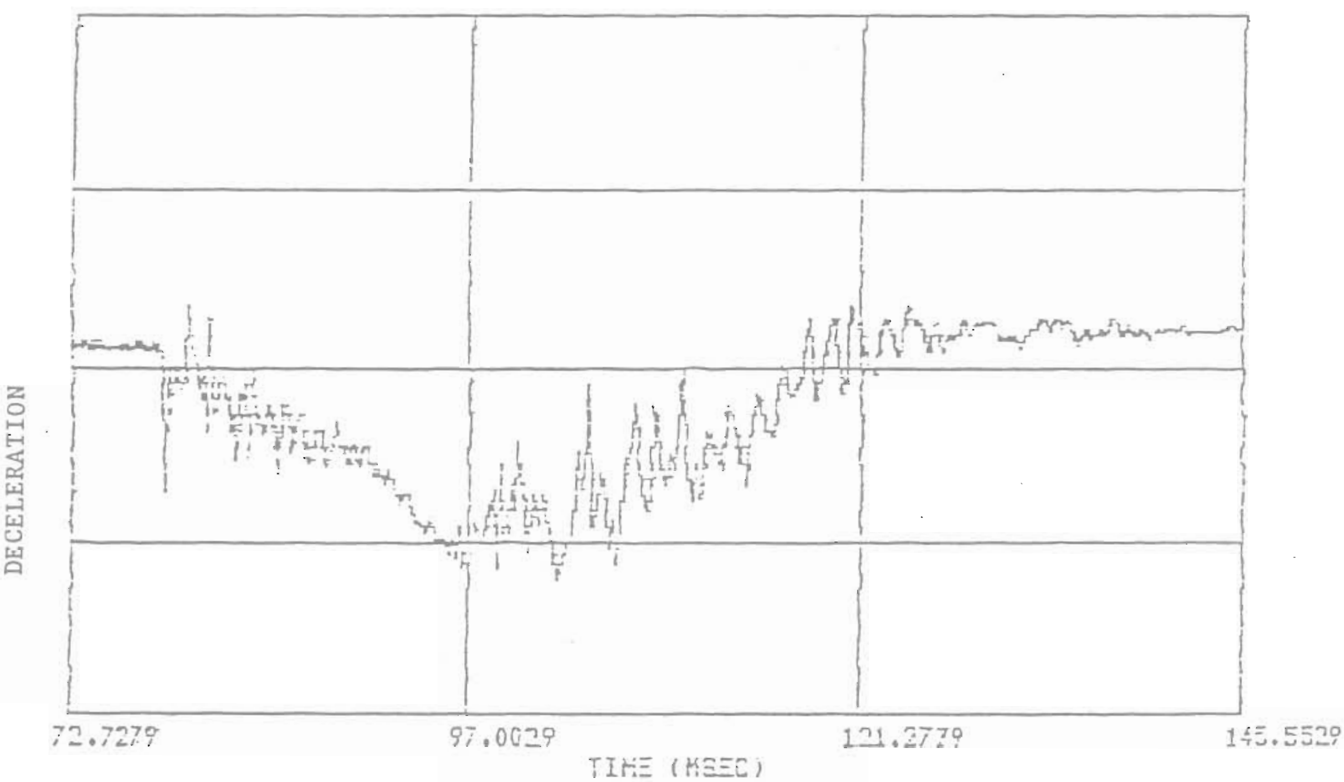

Fig. D1-b Deceleration-Time Relation For Model SE-3

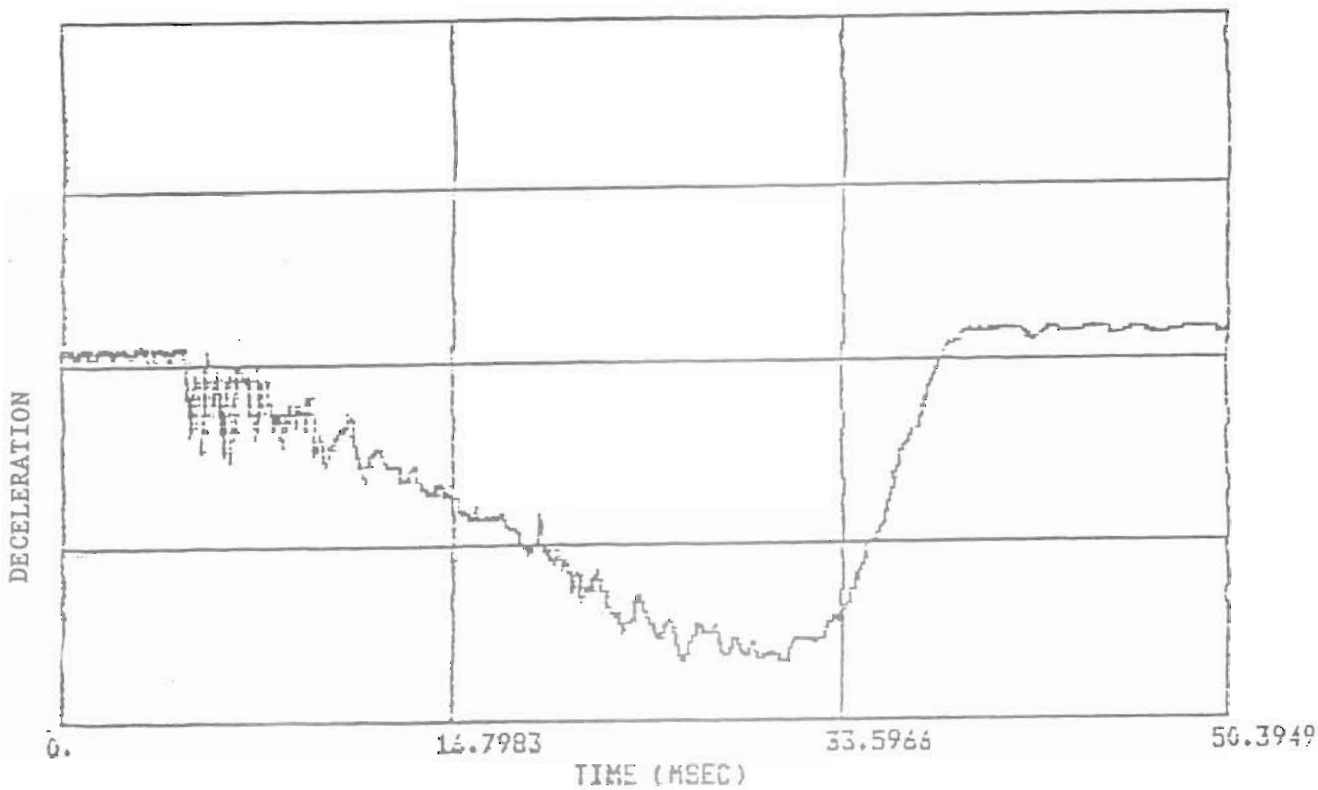

Fig. D1-c Deceleration-Time Relation For Model SE-4

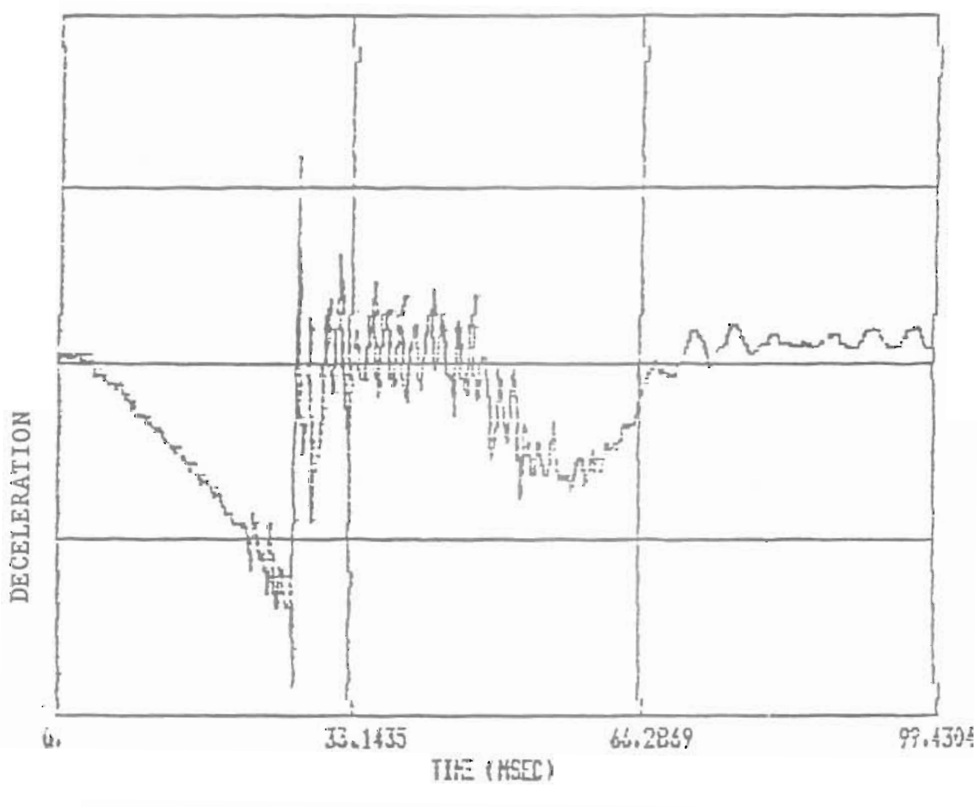

Fig. D2-a Deceleration-Time Relation For Model ME-5

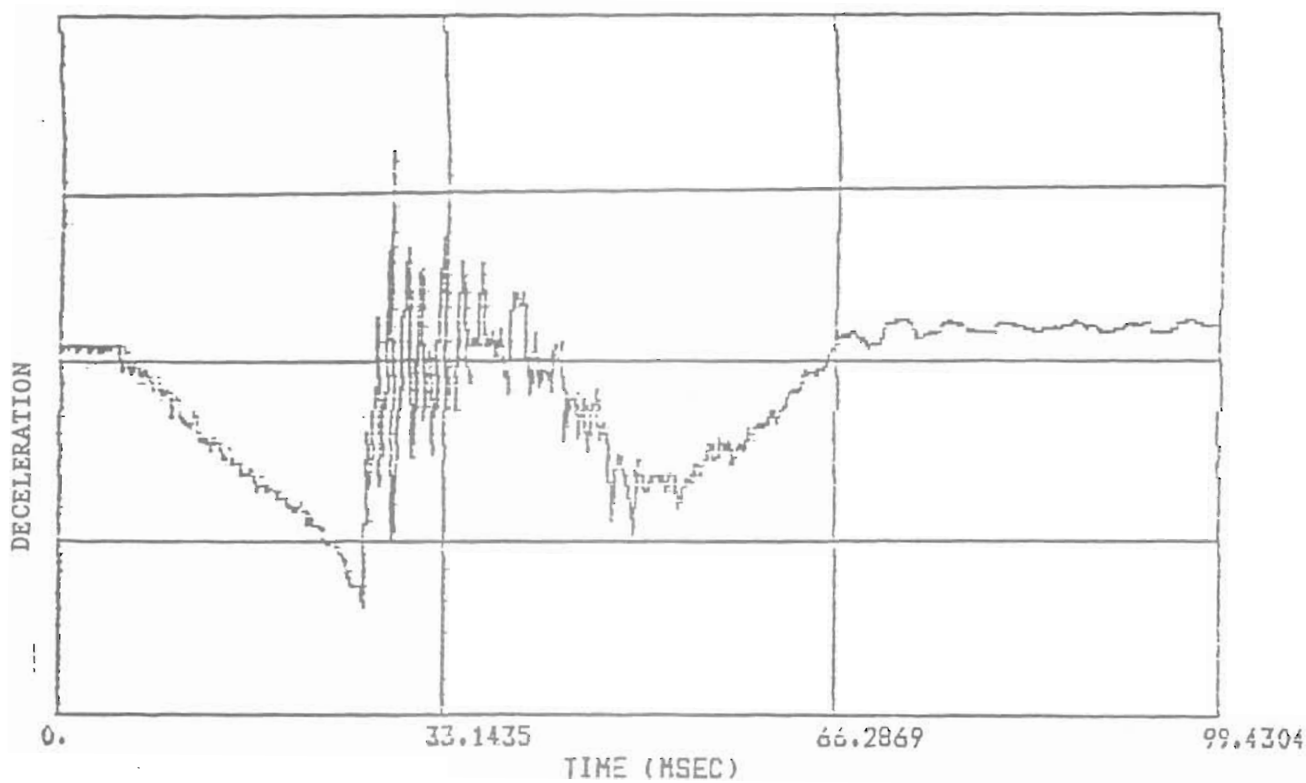

Fig. D2-b Deceleration-Time Relation For Model ME-6

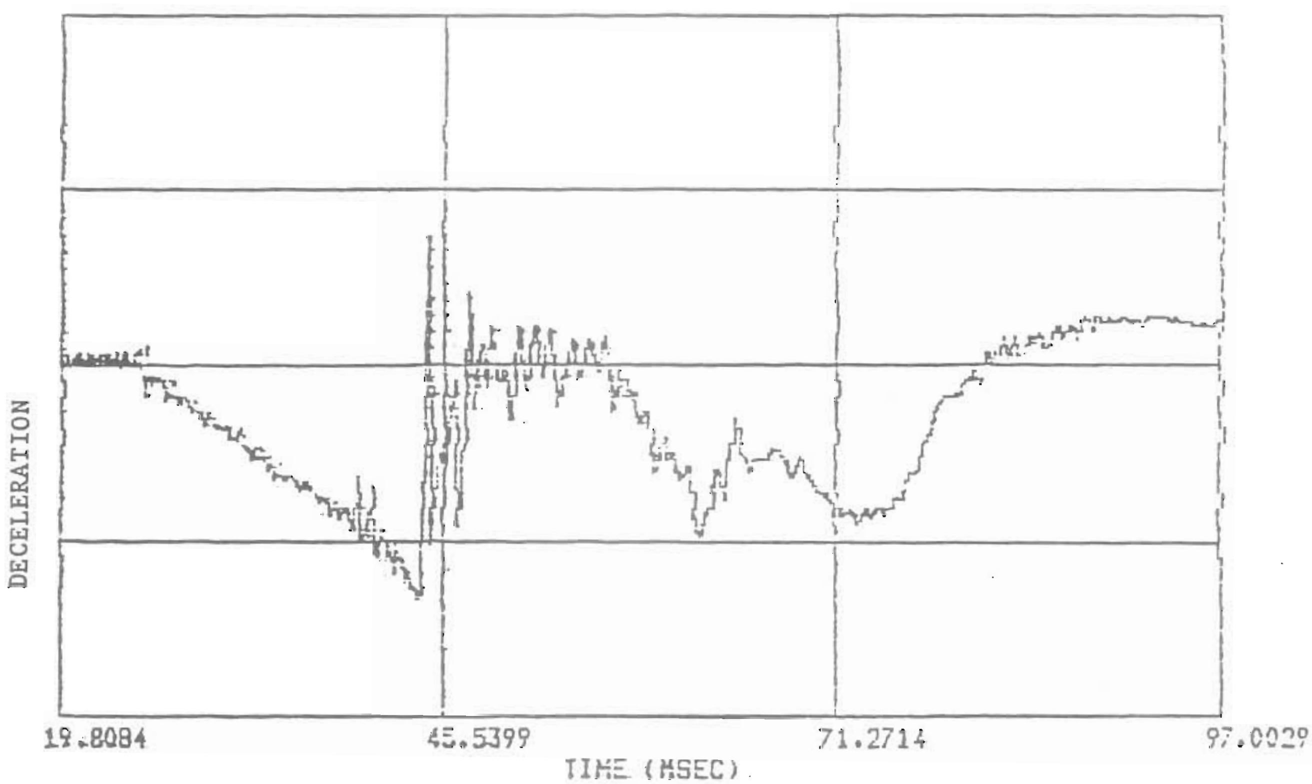

Fig. D2-c Deceleration-Time Relation For Model ME-7

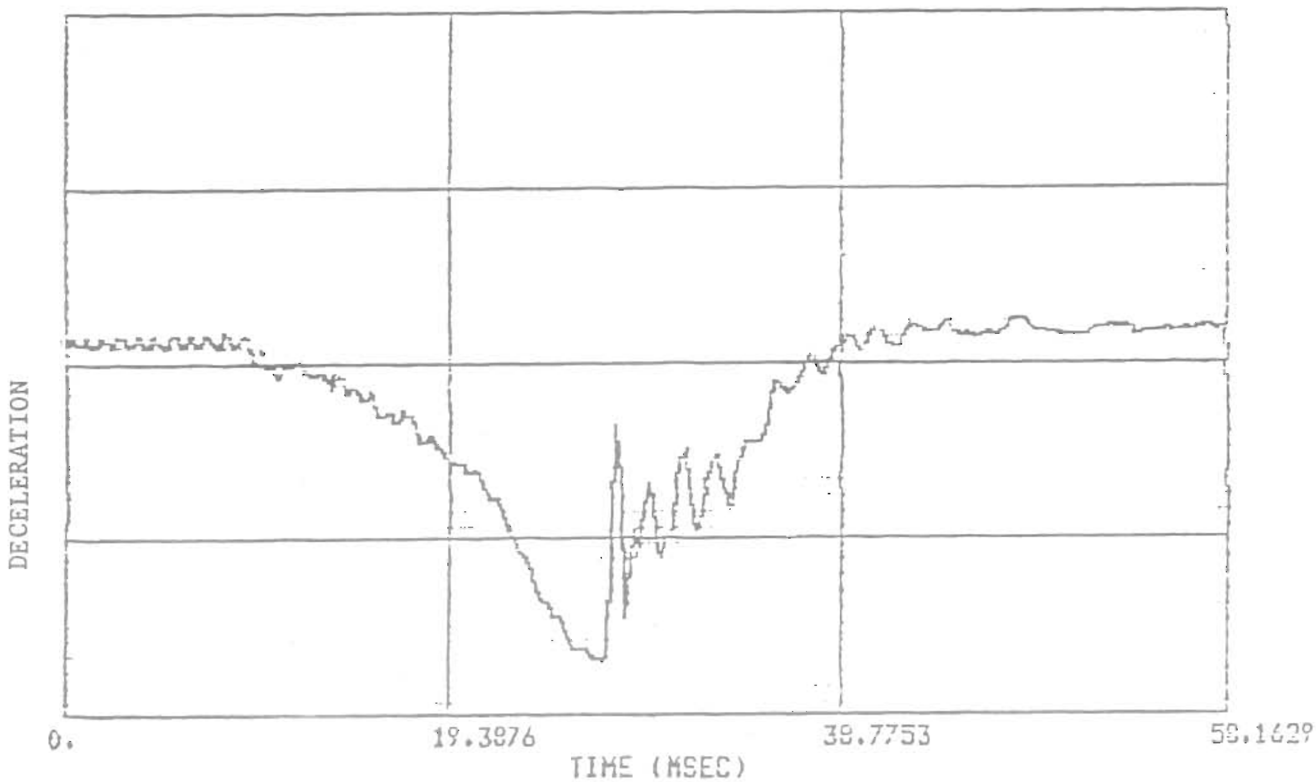

Fig. D3-a Deceleration-Time Relation For Model SS-1

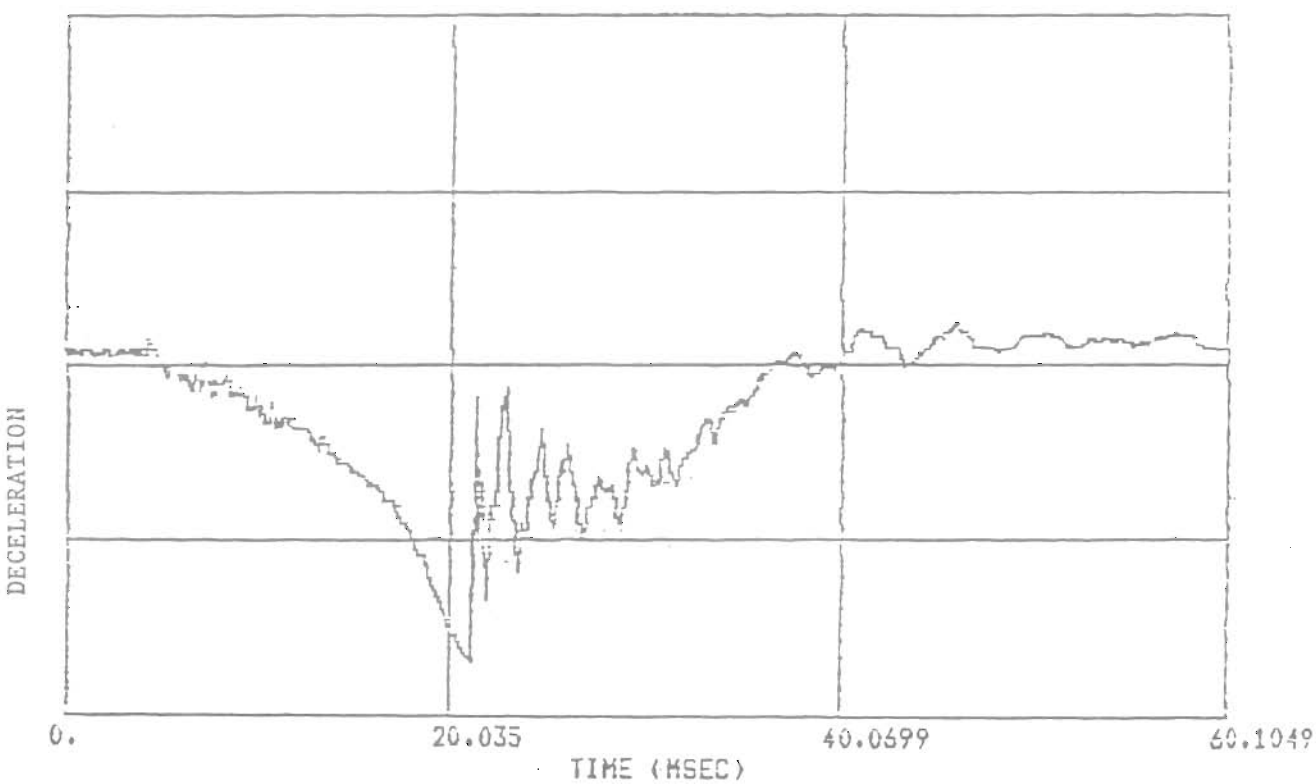

Fig. D3-b Deceleration-Time Relation For Model SS-2

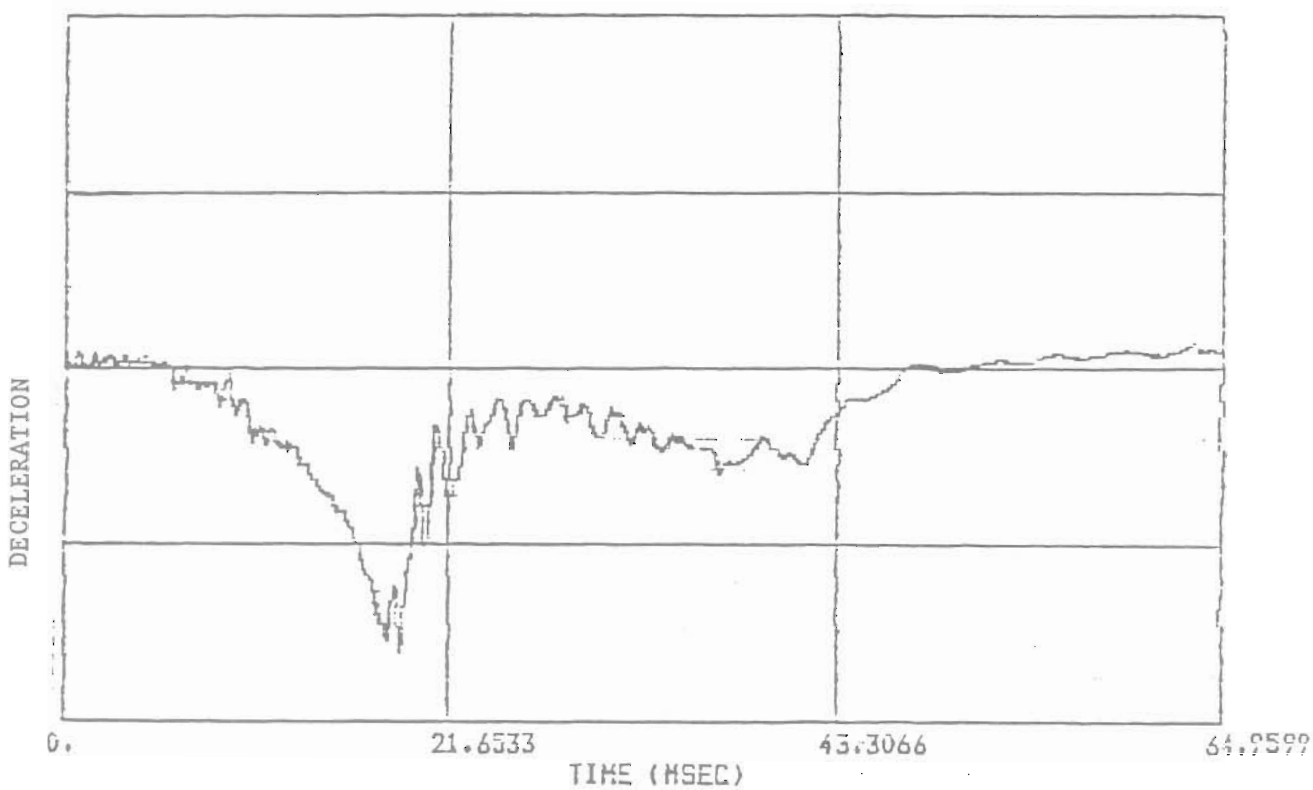

Fig. D3-c Deceleration-Time Relation For Model SS-3

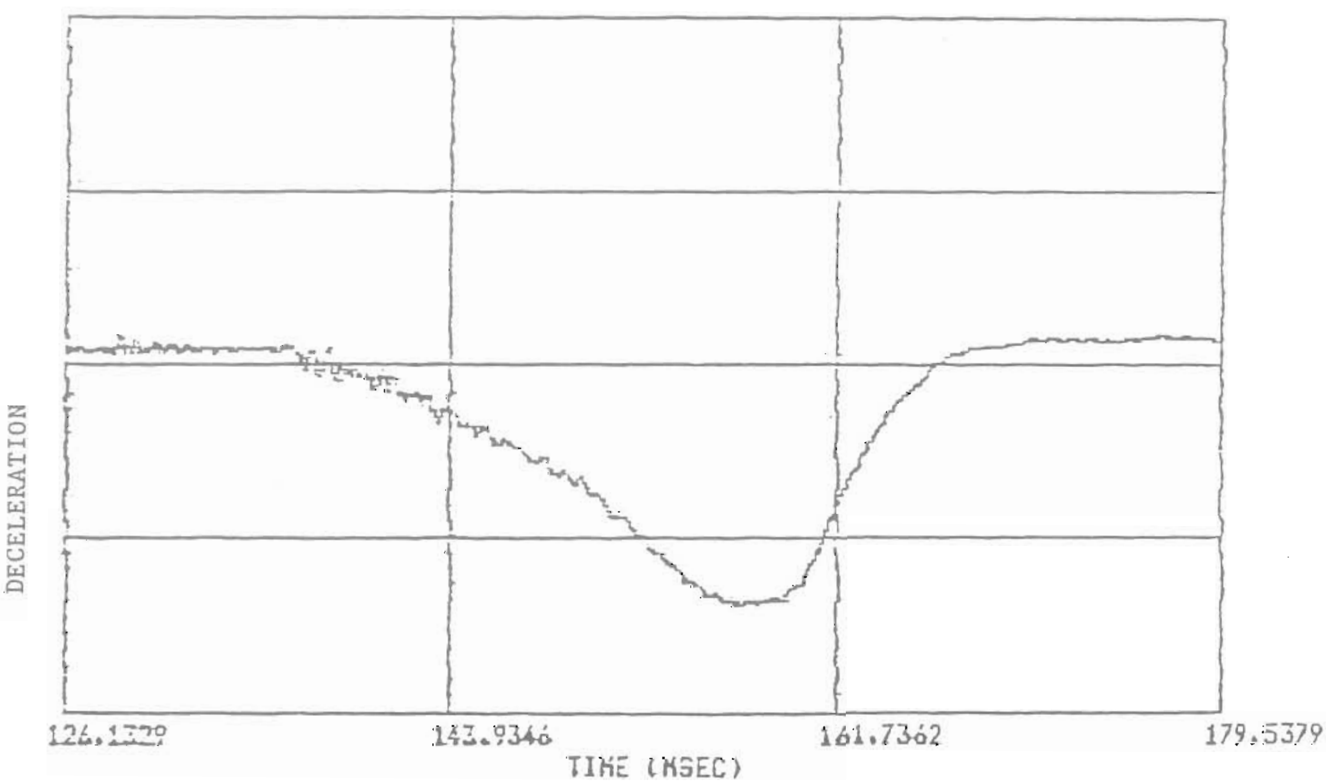

Fig. D4-a Deceleration-Time Relation For Model MS-2

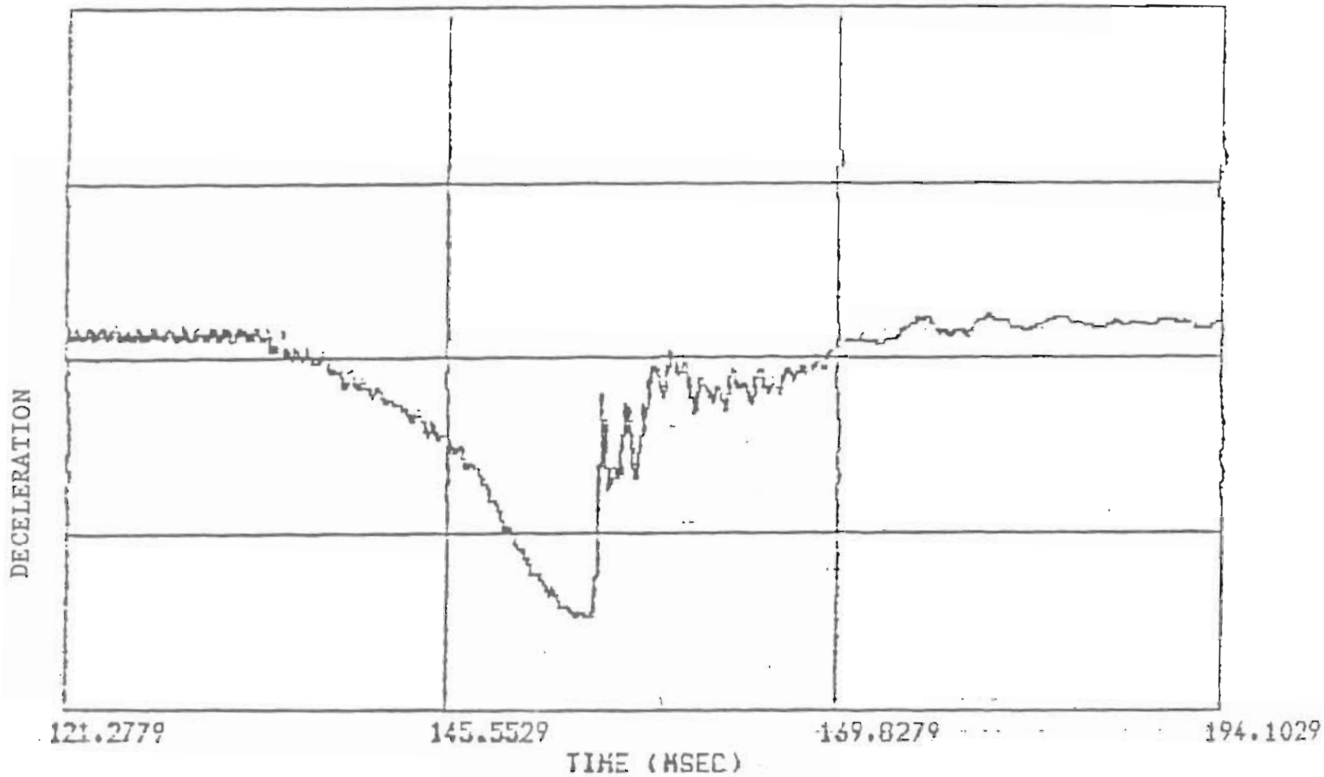

Fig. D4-b Deceleration-Time Relation For Model MS-3

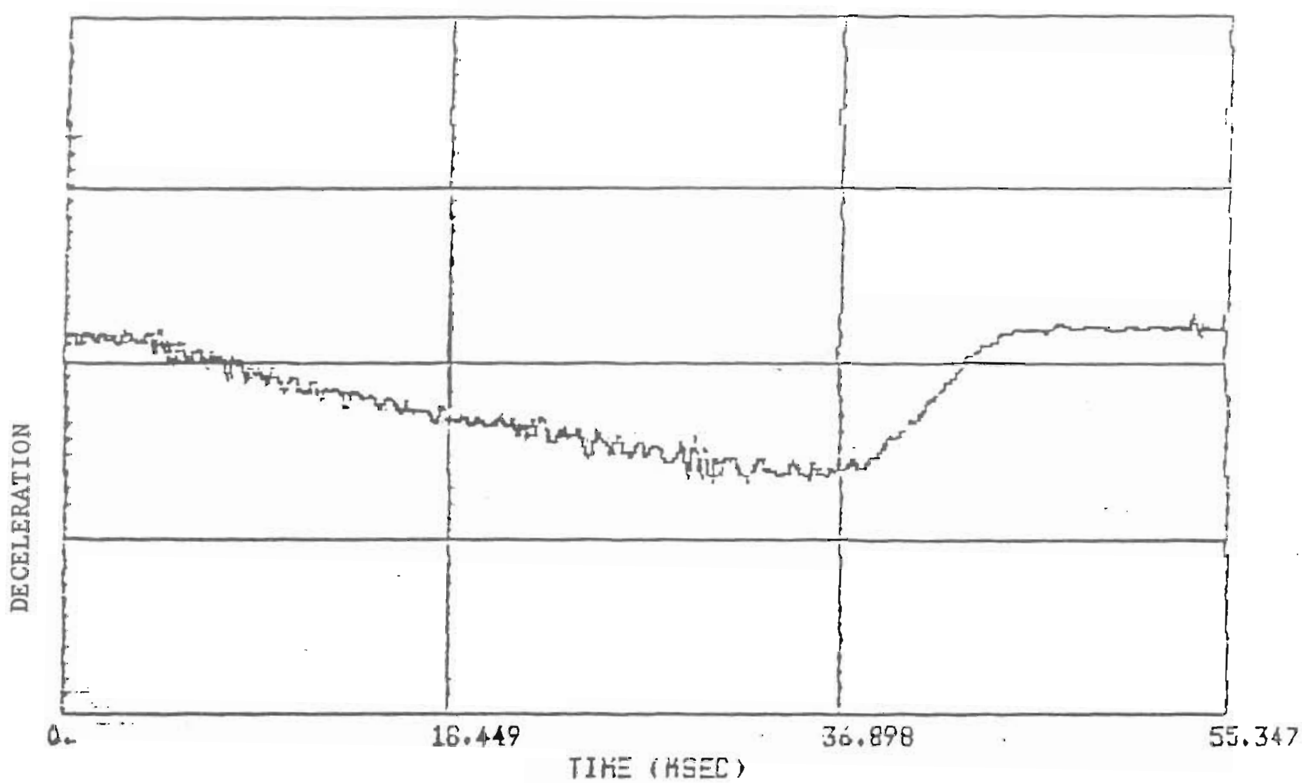

Fig. D5-a Deceleration-Time Relation For Model BE-3

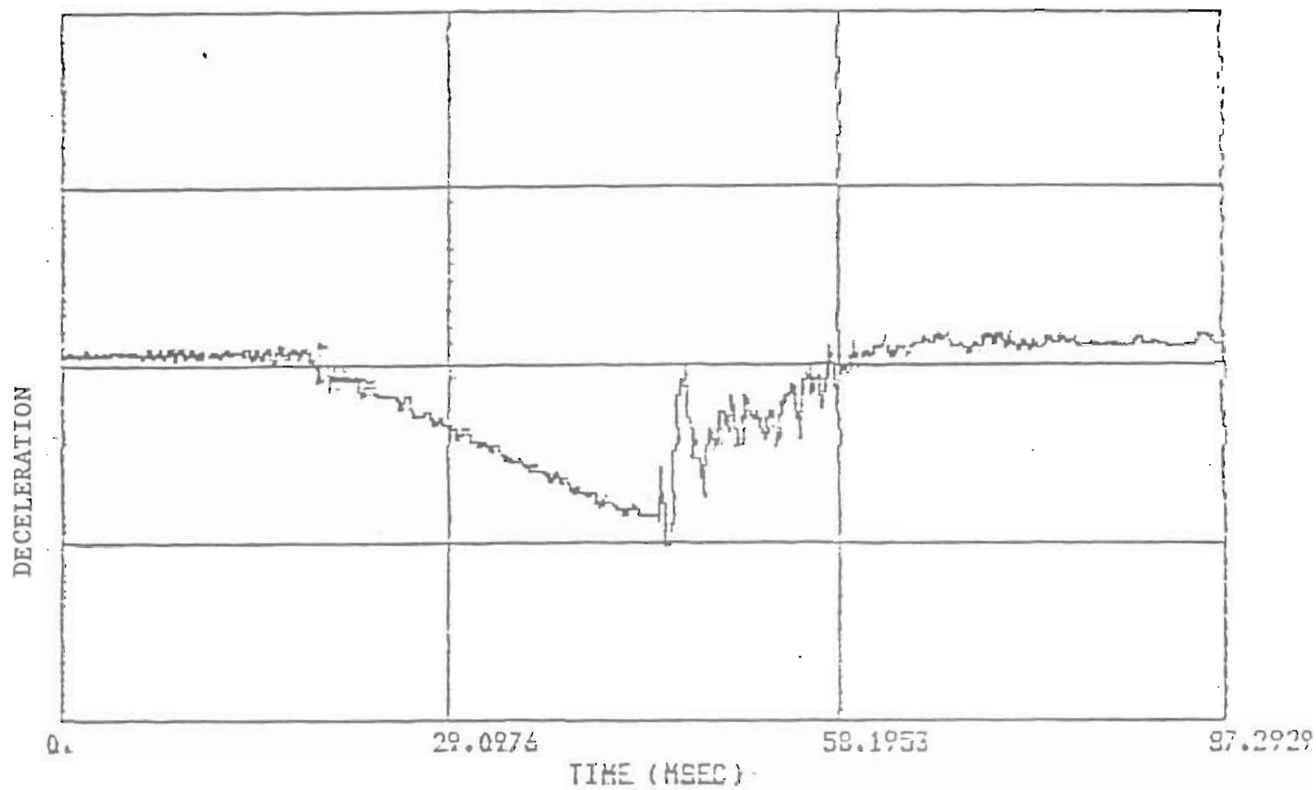

Fig. D5-b Deceleration-Time Relation For Model BE-6

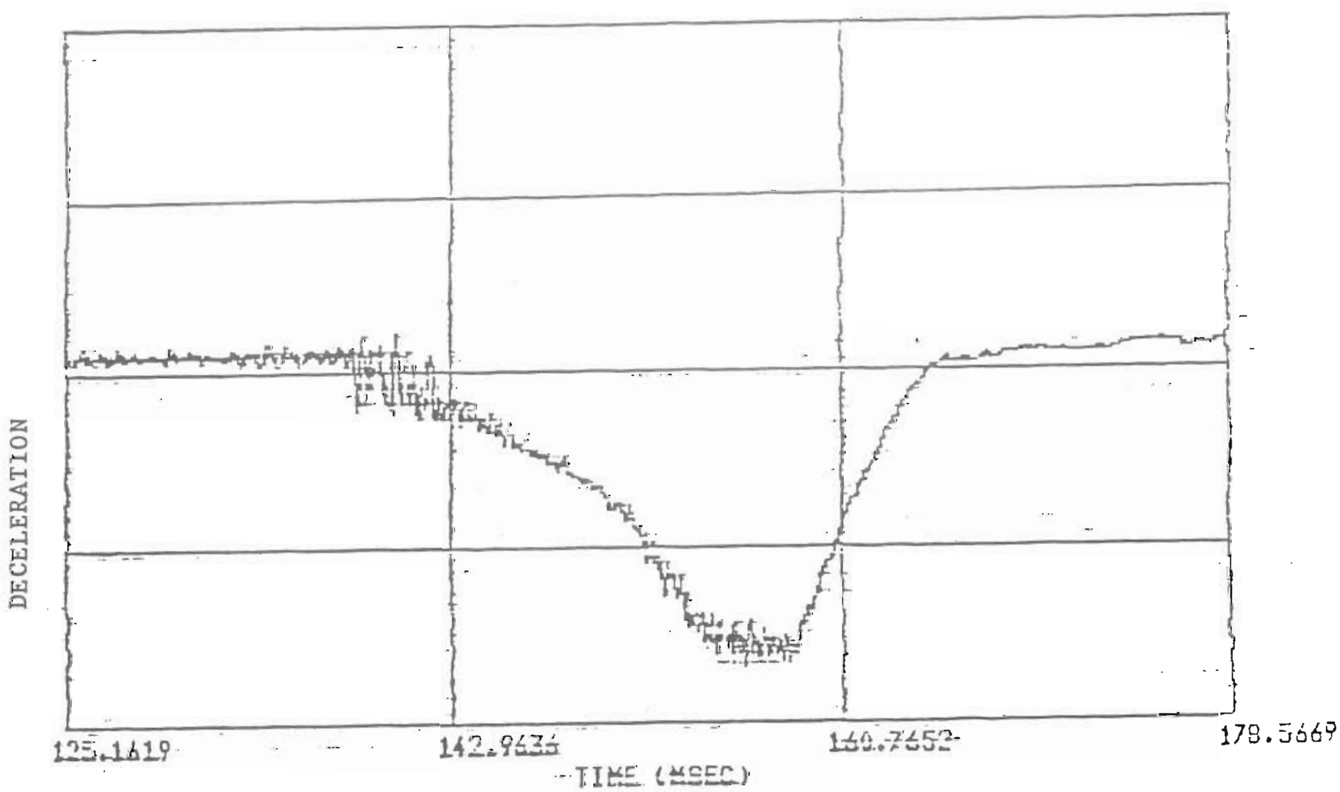

Fig. D6-a Deceleration-Time Relation For Model LMS-1

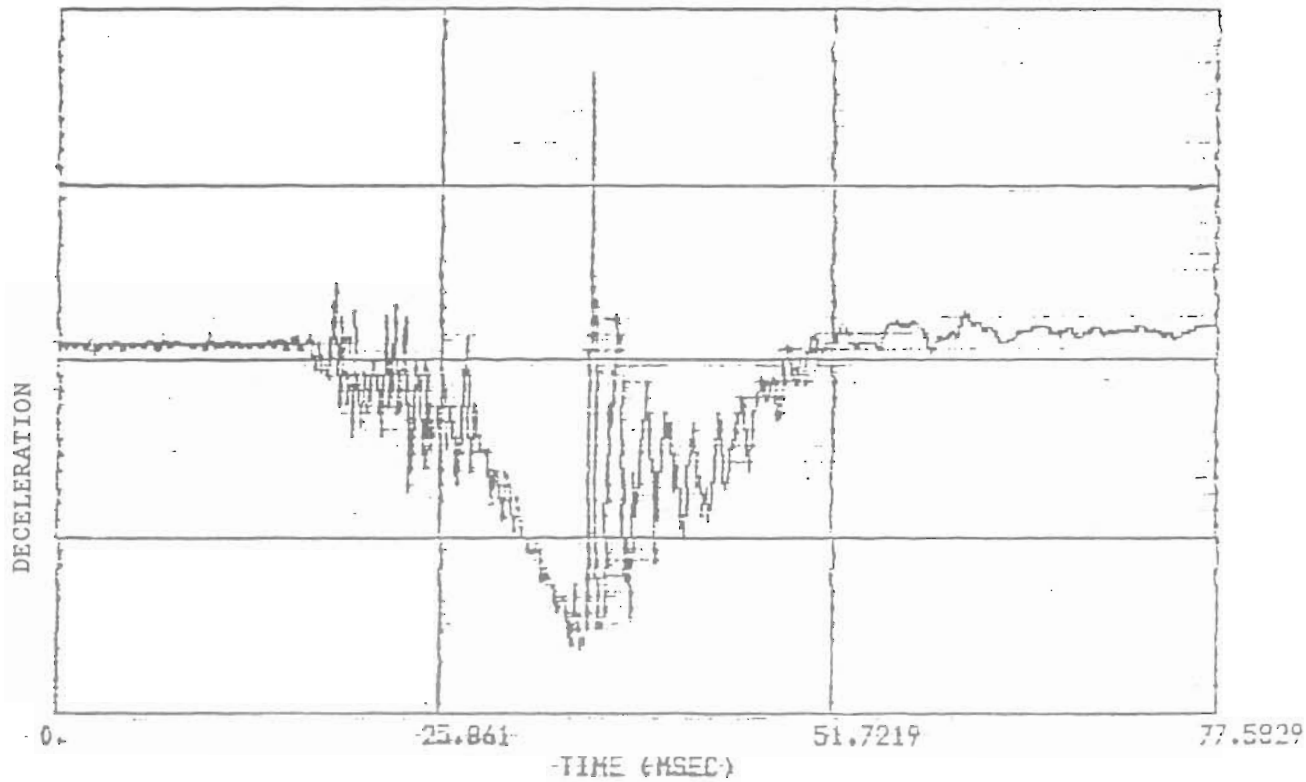

Fig. D6-b Deceleration-Time Relation For Model LMS-2

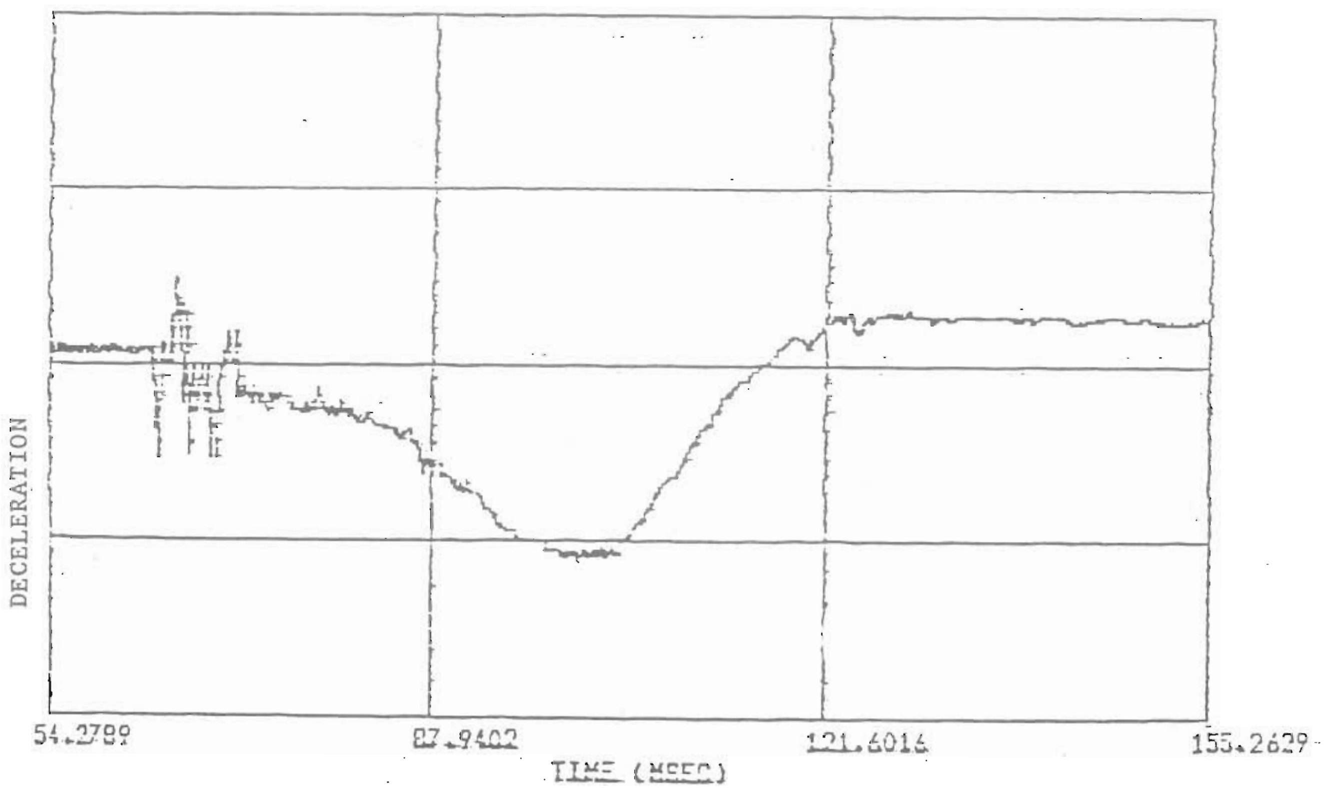

Fig. D7-a Deceleration-Time Relation For Model BS-1A

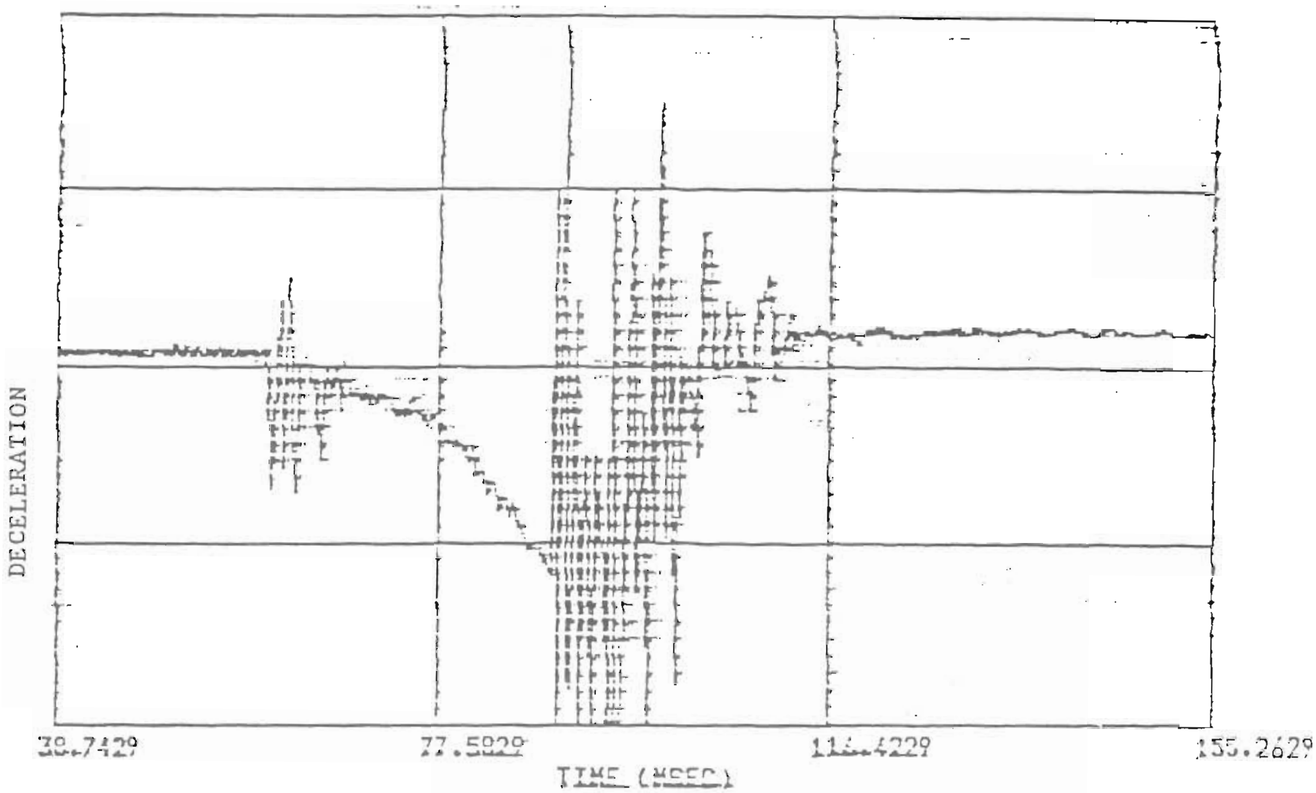

Fig. D7-b Deceleration-Time Relation For Model BS-3A

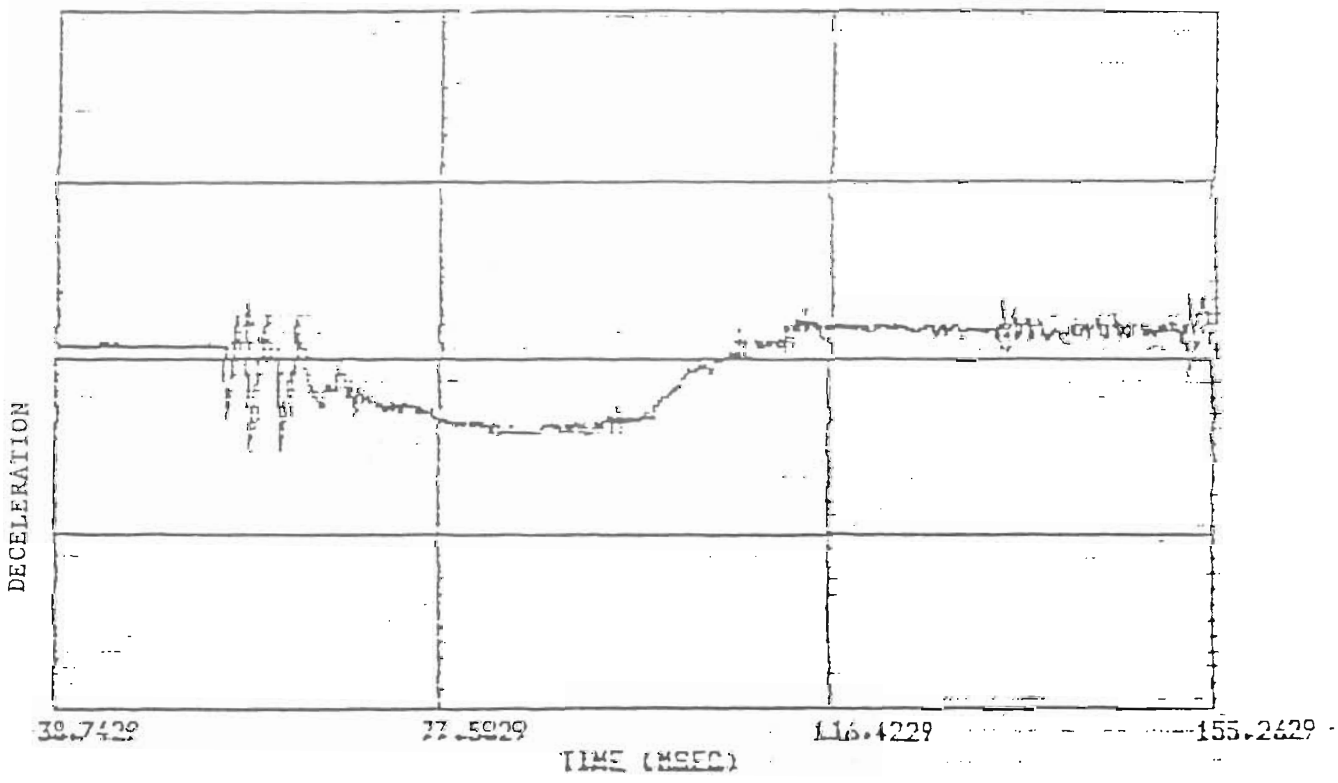

Fig. D8-a Deceleration-Time Relation For Model BE-1A

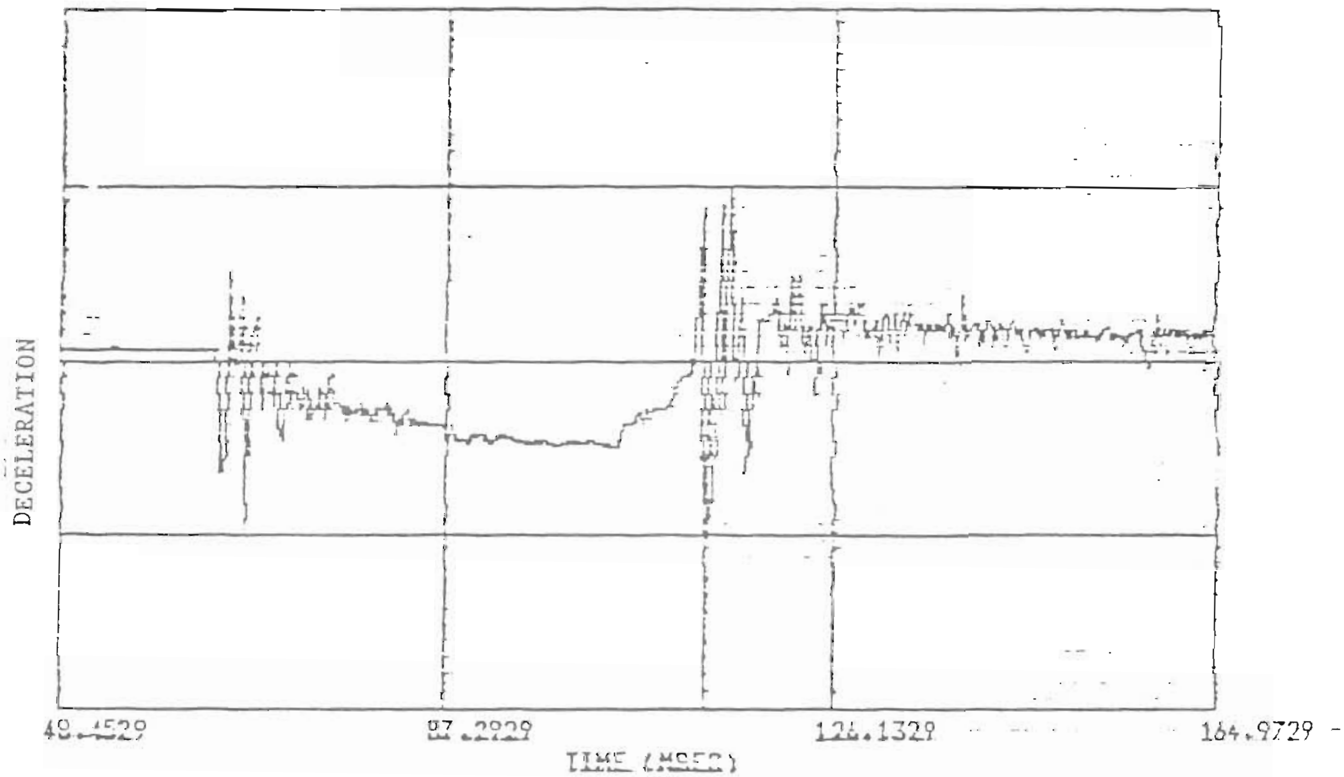

Fig. D8-b Deceleration-Time Relation For Model BW-1A

APPENDIX E

ELEVEN INDEPENDENT DIMENSIONLESS PARAMETERS

$$\pi_1 = \frac{\sqrt{m/k_d}}{D\sqrt{\rho_{hd}/E_s}}$$

The ratio of the time required for the impact force to reach a maximum to the time required for plastic waves to reach the edge of the head.

This ratio will indicate what volume (area) is important in the problem.

$$\pi_2 = \frac{m}{m'}$$

The mass ratio of impacting body to impacted body.

$$\pi_3 = \frac{\sigma_y}{E_s}$$

Ratio of yield stress to secant modulus.

$$\pi_4 = \frac{h}{R}$$

Ratio of head thickness to radius of curvature.

$$\pi_5 = \frac{\sigma_y^2}{E_s\, \rho_{hd}\, \dot{\varepsilon}^2\, h^2}$$

Ratio of strain energy to head kinetic energy of deformation.

$$\pi_6 = \frac{m v^2\, E_s}{\sigma_y^2\, d^3}$$

Ratio of impact kinetic energy to strain energy.

$$\pi_7 = \frac{h}{D}$$

Ratio of head thickness to diameter.

$$\pi_8 = \frac{P_o R}{\sigma_y h}$$

Ratio of pressure induced stress to material yield stress.

$$\pi_9 = \frac{\sigma_y^2}{E_s\, \rho_{fl}\, \dot{\varepsilon}^2\, h^2}$$

Ratio of strain energy to energy absorbed by fluid.

$$\pi_{10} = \frac{d}{D}$$

Ratio of indenter characteristic length to head diameter.

$$\pi_{11} = \frac{\rho_{fl}\, D^3}{m}$$

Ratio of characteristic mass of fluid to mass of impacting body.